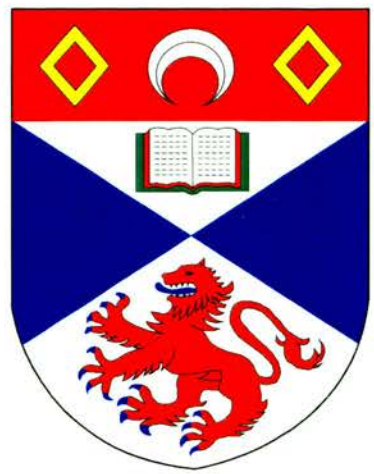

Syntheses and Properties of Liquid Crystalline Macrocyclic Complexes

A thesis presented by Alan M^{c}Gregor, B.Sc., to the University of St. Andrews in application for the degree of Doctor of Philosophy

1996

Declaration.

In submitting this thesis to the University of St. Andrews, I understand that I am giving permission for it to be made available for its use in accordance with the regulations of the University library for the time being in force, subject to any copyright vested in the work not being affected thereby. I also understand that the title and abstract will be published, and that a copy of the work may also be made and supplied to any *bona fide* library or research worker.

Date 10/3/97 Signature of candidate

Declaration.

I, Alan M^{c}Gregor, hereby certify that this thesis, which is approximately 42,000 words in length, has been written by me, that it is the record of work carried out by me and that it has not been submitted in any previous application for a higher degree

Signature of candidate Date 10/3/97

I was admitted as a research student in October 1990 and as a candidate for the degree of Ph.D. in October 1990; the higher study for which this is a record was carried out in the University of St. Andrews between 1990 and 1996

Signature of candidate Date 10/3/97

I hereby certify that the candidate has fulfilled the conditions of the Resolution and Regulations appropriate for the degree of Ph.D. in the University of St. Andrews and that the candidate is qualified to submit this thesis in application for that degree

Signature of supervisor Date 10/3/97

'They are ill discoverers that think there is no land, when they can see nothing but sea.'

Francis Bacon, *Advancement of Learning*, 1605.

CONTENTS

CHAPTER 4

Benzoylation of Tetraazaannulenes

CHAPTER 5

Solid State NMR Of Tetraazaannulenes

Acknowledgements

I would like to thank my supervisor, Dr. Joe A. Crayston, for all the help, guidance and patience he has donated during my time at St Andrews. The bountiful supply of ideas and enthusiasm mark him out amongst supervisors.

All the academic staff and the technical staff have all been exceptionally kind and helpful making the atmosphere in this department very special. Thanks are due in particular to Dr. Frank Riddell (SSNMR), Sylvia Smith (elemental analysis) and Melania Smith (NMR). Prof. John Goodby at Hull also provided invaluable assistance in the examination of my compounds by optical microscopy.

I am indebted to the University of St Andrews for financial support throughout my course.

Thanks must go to the members of lab 248 past and present for all the clean glassware, may all their crystals be large and colourful.

Most of all, I would like to thank my Mum and Dad for their understanding, tolerance and support, without which this work could not have been completed.

Postgraduate Courses.

The Department of Chemistry requires that a number of courses are attended, these courses were ;

"Advanced NMR" Dr. R. K. Mackie
"Advanced Spectroscopic Methods in Inorganic Chemistry" Dr. J. Crayston
"Aspects of Materials Chemistry" Dr. J. Crayston
"Bio-inorganic Chemistry" Dr. D. Richens
"Electochemistry" Dr. P. Bruce
"Heterogeneous Catalysis" Prof. D. J. Cole-Hamilton, Dr J. A. Crayston and Dr. K. D. M. Harris.
"Industrial Chemistry" Dr. C. Glidewell and Dr. D. M. Smith.
"Solid State NMR" Dr. K. D. M. Harris.

List of Abbreviations

δ	Relative to TMS
γ	Magnetogyric Ratios
ν_l	Larmor Frequency
ν_{spin}	Spinning frequency
AEH	7-amino-4-methyl-5-aza-3-hepten-2-one
ar	Aromatic group
Bo	Static Magnetic Field
bs	Broad singlet
C*	Smectic C*
CP	Cross Polarization
CV	Cyclic Voltammetry
d	Doublet
DMF	Dimethylformamide
DMSO	Dimethyl Sulphoxide
DMTAA	Dimethyl tetraazaannulene
DSC	Differential Scanning Calorimeter
EtOH	Ethanol
FAB-MS	Fast Atom Bombardment Mass Spectrometry
FTIR	Fourier transform infrared spectroscopy
HCl	Hydrochloric acid
HPLC	High pressure liquid chromatography
Hz	Hertz
IR	Infra-Red
K	Equilibrium constant
K	Kelvin
kHz	Kilohertz
LB	Langmuir Blodgett
LC	Liquid Crystalline
LCD	Liquid Crystal Displays
LMCT	Ligand to metal charge transfer
M.p.	Melting point
mac	Macrocycle
MAS	Magic Angle Spinning
MBBA	p-Methoxybenzylidene-p-n-butylaniline
MeOH	Methanol
MS	Mass spectrometry
mVs	Millivolts
n	Director
NMR	Nuclear Magnetic Resonance
NQS	Non Quaternary Suppression
PAA	P-azoxyanisole
PHB	Photochemical Hole Burning
rf	Radio frequency

SSB	Spinning Side Bands
SSNMR	Solid State Nuclear Magnetic Resonance
TAA	Tetraazaannulene
ter	Terminal group
TMS	Trimethylsilane
TMTAA	Tetramethyltetraazaannulene
UV-Vis	Ultraviolet and Visible Spectra

Abstract

Investigations are conducted into substituted tetraazaannulenes with the objective of forming novel liquid crystalline compounds. Various synthetic strategies are devised and the compounds tested by differential scanning calorimetry and heated-stage polarised optical microscopy. The electrochemistry and variable temperature solid state NMR properties of certain of these compounds were also investigated.

A series of novel compounds was prepared utilising the active β-methine site of the 7,16-dihydro-6,8,15,17-tetramethyldibenzo[*b,i*]-[1,4,8,11]tetraazacyclotetradecinato(2-) Ni(II)) complex starting material, commonly known as nickel tetramethyltetraazaannulene. Long aliphatic chains were joined to this macrocycle in an attempt to induce mesogenic properties in the crystals. Diazo functional groups were utilised as the link. However, the bulky nature of the benzene side groups on the macrocycle prevented liquid crystalline behaviour. The ability to replace the nickel centre in these macrocycles was demonstrated. The electrochemistry of the cobalt rod shaped complex was investigated on gold electrodes.

A further series of compounds based on a macrocycle with less bulky side groups was prepared. The dibenzo groups were replaced by ethylenediamine groups. Diazo linked compounds exhibited mesogenic behaviour for the longer chain length, the molecules displaying smectic A mesophases at high temperatures.

Once liquid crystalline properties had been established by reducing the bulk of the molecules the effect of the linkage was examined. The diazo linkage was replaced with a dibenzoyl linkage while keeping all other factors constant. However, this small alteration was sufficient to destroy the mesogenic properties for the entire range of chain lengths. In

addition to the liquid crystal transitions several solid state crystalline transitions were observed for these compounds.

The effect of making the inner core of the molecules more planar by removing the peripheral methyl groups was investigated. Results suggested that the methyl groups have opposing roles, i.e. they increase the steric bulk of the molecules, but at the same time prevent strong interactions between molecules. Unfortunately, the best synthetic route to such molecules also left the unsymmetrical mono substituted complex as an impurity which could not be easily removed. This impurity was likely to be liquid crystalline in its own right.

Variable temperature solid state NMR studies of these compounds were begun by investigating the metal-free parent macrocycles and the intramolecular proton transfer which takes place between the four inner nitrogen atoms. Comparison with X-ray data and ^{15}N isotope enriched studies revealed that the αC ^{13}C CP / MAS spectra was a valid probe for this tautomerism. This was then extended to TAA which had not been studied by solid state NMR. The results were consistent with an equal population of both tautomers, apparently in conflict with the evidence from the original crystal structure. Later crystallographic work by revealed that the packing in the crystal structure is dependent on the method of formation (recrystallisation or vacuum sublimation).

CHAPTER 1

Introduction

The aim of this work was to prepare novel liquid crystalline compounds based on a family of macrocyclic tetraazaannulenes. This introduction will describe the nature of liquid crystalline compounds, tetraazaannulenes and metallomesogens, giving a brief history of the subject and a review of current research. It will also provide an introduction to the theory of solid state NMR which was used to investigate thermally-induced motion in the crystalline state.

1.1 Liquid crystals

There are states of matter which exist between solid and liquid for certain materials. These intermediate states, collectively known as liquid crystalline (LC) phases, have properties of both solids and liquids. They can flow like a liquid yet retain a degree of long-range orientational order present in solids. The unusual properties exhibited by this select group of materials already have a wide range of practical applications from liquid crystal displays to thermometers.

The discovery of LC phases is generally credited to Friedrich Reinitzer in 1888[1]. He was investigating the role of cholesterol in plants when he noted that solid cholesteryl benzoate possessed two melting points. At 145.5 °C it melted into a cloudy liquid and at 178.5 °C the cloudy liquid turned clear. He sent a sample of cholesteryl

benzoate to Otto Lehmann who observed that when placed between crossed polarisers and heated above first melting point the sample allowed light to pass through. Anisotropic crystalline solids had been routinely examined in this way in geology and petrology; however, non-chiral liquids were known not to allow any light to pass through.

Liquid crystals can be divided into two broad families:[2,3] thermotropic and lyotropic. Thermotropic compounds exhibit the liquid crystal phases in certain temperature ranges while lyotropic compounds exhibit these properties depending on their concentration in solution. An example of lyotropic LC phases (mesophases) can be found in mixtures of soap and water. Soap consists of sodium stearate, a salt with an amphiphilic (hydrophilic head, hydrophobic tail) anion.[4] They are generally composed of one or more aliphatic chains and a polar head group. With low concentrations of soap, micelles are formed in which the molecules cluster together into spheres with the hydrophobic hydrocarbon chain in the centre as far away from the water as possible and the hydrophilic polar head facing outwards. As concentrations increase the spherical micelles form cylinders with the same principle as before. At yet higher concentrations a hexagonal array of columns is achieved in which the viscosity can become so high that the mixture will not flow. If the concentration is increased beyond this point a further phase is reached, the lamellar phase, in which sheets of soap form tail to tail and the viscosity reduces as the new orientation allows the sheets to flow over each other.

Thermotropic liquid crystals are materials which form LC phases on heating or cooling between solid and liquid. Enantiotropic materials show a thermodynamically stable mesophase (present on both heating and cooling) while monotropic mesophases are not thermodynamically stable and are present only on cooling. These phases can be

detected because they are accompanied by changes in volume and absorption or emission of heat (depending if the sample is being heated or cooled).[5]

Thermotropic mesophases are the ones we were most interested in. The compounds which exhibit thermotropic mesophases have several physical characteristics in common: they are generally elongated, *i.e.* significantly longer than they are wide, possess a certain amount of rigidity in the central part of the molecule and have flexible groups at either end.[4] The rod-like nature of these molecules means that they can align with each other in the liquid phase to maximise intermolecular attractions and form stable mesophases. The mesophases that this type of molecule forms can be subdivided into categories depending on how much long range orientational order is retained. If the centres of the molecules are distributed in a totally random fashion in three dimensions (as would be found in a liquid) but each individual molecule has the tendency to point in the same direction the mesophase formed is called nematic (Figure 1.1).

Figure 1.1 *Nematic phase; molecules with random distribution aligned parallel to the director n.*

If the molecule has a chiral centre in addition to all the other factors necessary to form a liquid crystal phase it may form a cholesteric phase which is a special type of nematic.[6] The cholesteric phase can be thought of as many nematic phases, one

molecule thick, placed on top of each other with the director (n) rotated by a small amount from each layer to the next (Figure 1.2).

The pitch of a cholesteric is the distance it takes for the director to make one full turn. The structure is actually periodic over half the pitch as n and -n are equivalent. The pitch is highly sensitive to temperature.

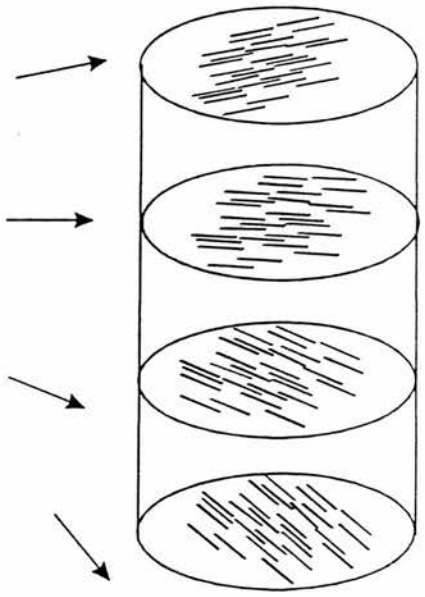

Figure 1.2 *Cholesteric phase; the director changes by a small angle in each layer.*

Smectic A is a phase in which the molecules are arranged in layers perpendicular to the director. When viewed from above the molecules in each layer appear to be randomly distributed.

The smectic C phase is similar to a smectic A phase, however, the molecules are tilted slightly in each layer. In both smectic A and smectic C phases the molecules randomly diffuse within each plane.

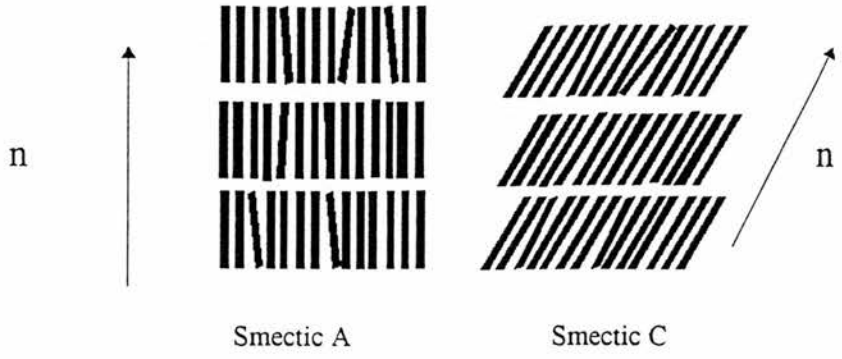

Figure 1.3 Smectic phases; Smectic A director is perpendicular to plane of the layer, Smectic C n is at an angle(other than 90°) to the plane of the layers

A smectic B phase is similar to a smectic C phase but has much greater order within the layer, indeed the centres of mass of the molecules in a layer appear to form a two dimensional solid. Other smectic phases have been discovered, each with varying degrees of conformational order within and between the layers. The smectic C* phase is one which deserves special mention as it has certain features in common with the cholesteric mesophase. In each layer the director is at an angle to the plane of the layer. The angle does not change but the direction of the director changes slightly in each successive layer (Figure 1.4)

The word smectic is derived from the Greek word, smektikos, for soap and indeed these thermotropic mesophases are similar to the lamellar mesophases found with lyotropic compounds.

In 1977 a further class of thermotropic LC phases were discovered which occur in molecules of a completely different shape.[7] These discotic mesophases occur in compounds which have a disc like shape (Figure 1.6). Typically they have a rigid planar centre with hydrocarbon chains emanating outwards in a plane. The simplest discotic phase is called nematic because in common with the nematic phase of rod like molecules it has orientational order but no positional order (Figure 1.5).

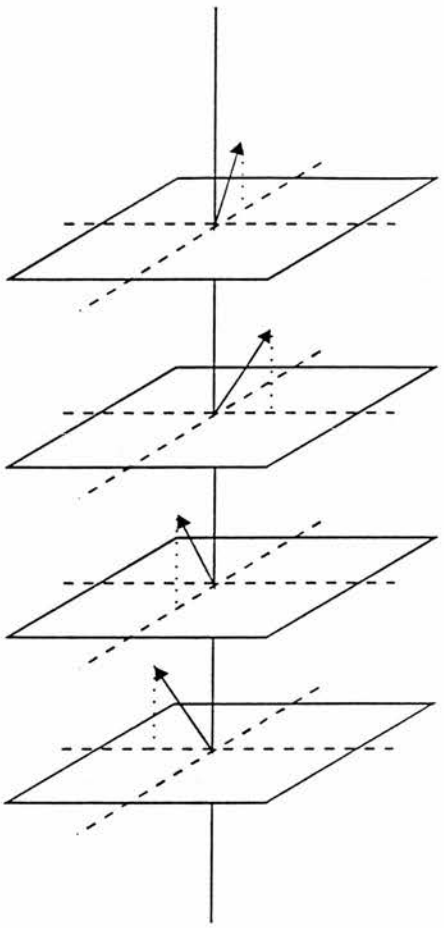

Figure 1.4 *Smectic C*, the director remains at the same angle to the plane yet rotates slightly in each successive layer.*

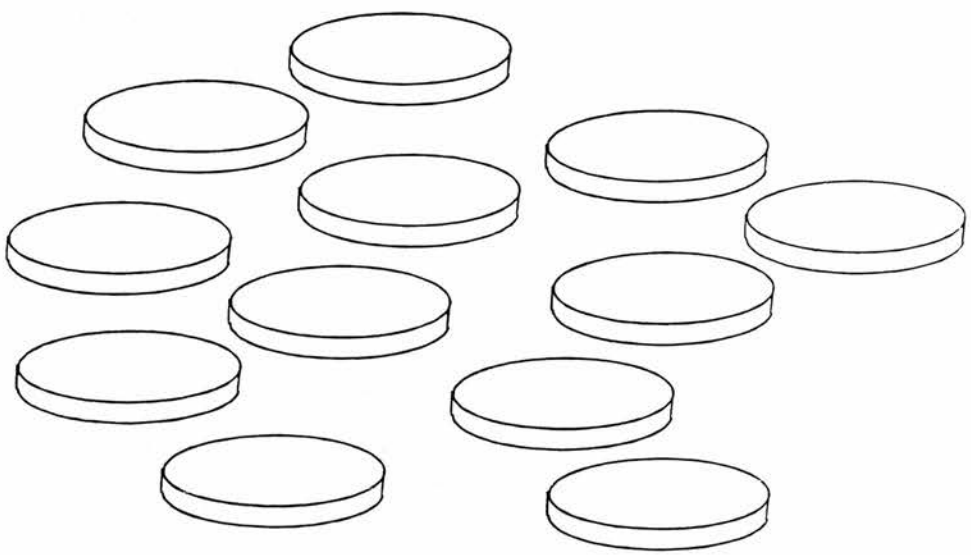

Figure 1.5 *Nematic discotic phase, disk like molecules all aligned in the same direction but with no positional order.*

The smectic analogue for discotic compounds is where the disk-like molecules are stacked in columns arranged in a hexagonal lattice.

One of the unusual properties of these compounds when in the LC state is their effect on plane-polarised light. When placed between crossed polarisers they allow the transmission of light. Isotropic (equal in all directions) liquids do not allow the transmission of light. Electromagnetic waves (light waves) are composed of electric and magnetic fields perpendicular to each other and the direction of propagation of the wave. The strength of both the electric and magnetic fields oscillate in phase as the wave propagates. The direction of the electric field is considered the polarisation of the light wave. A polarising filter allows light only of a particular orientation to pass through while absorbing all other incoming waves. If a second polarising filter is placed above the first but with its polarisation axis rotated by 90°, no light can pass through because the orientation is not correct for the second filter. When isotropic liquids are placed between the polarisers no light can pass through because no change to the direction of polarisation has occurred. In anisotropic crystals the plane polarised light is changed as it passes through the crystal and so light can be seen.

Plane polarised light can be considered as two electromagnetic waves at right angles to each other and in phase. When these two waves encounter an anisotropic medium one will travel through it at a higher velocity than the other. When they emerge from the material they are no longer in phase.

The combination of two out-of-phase plane polarised beams of light at right angles to each other do not form a single plane polarised beam of light as is the case with beams which are in-phase. Instead they combine to form elliptically polarised light.

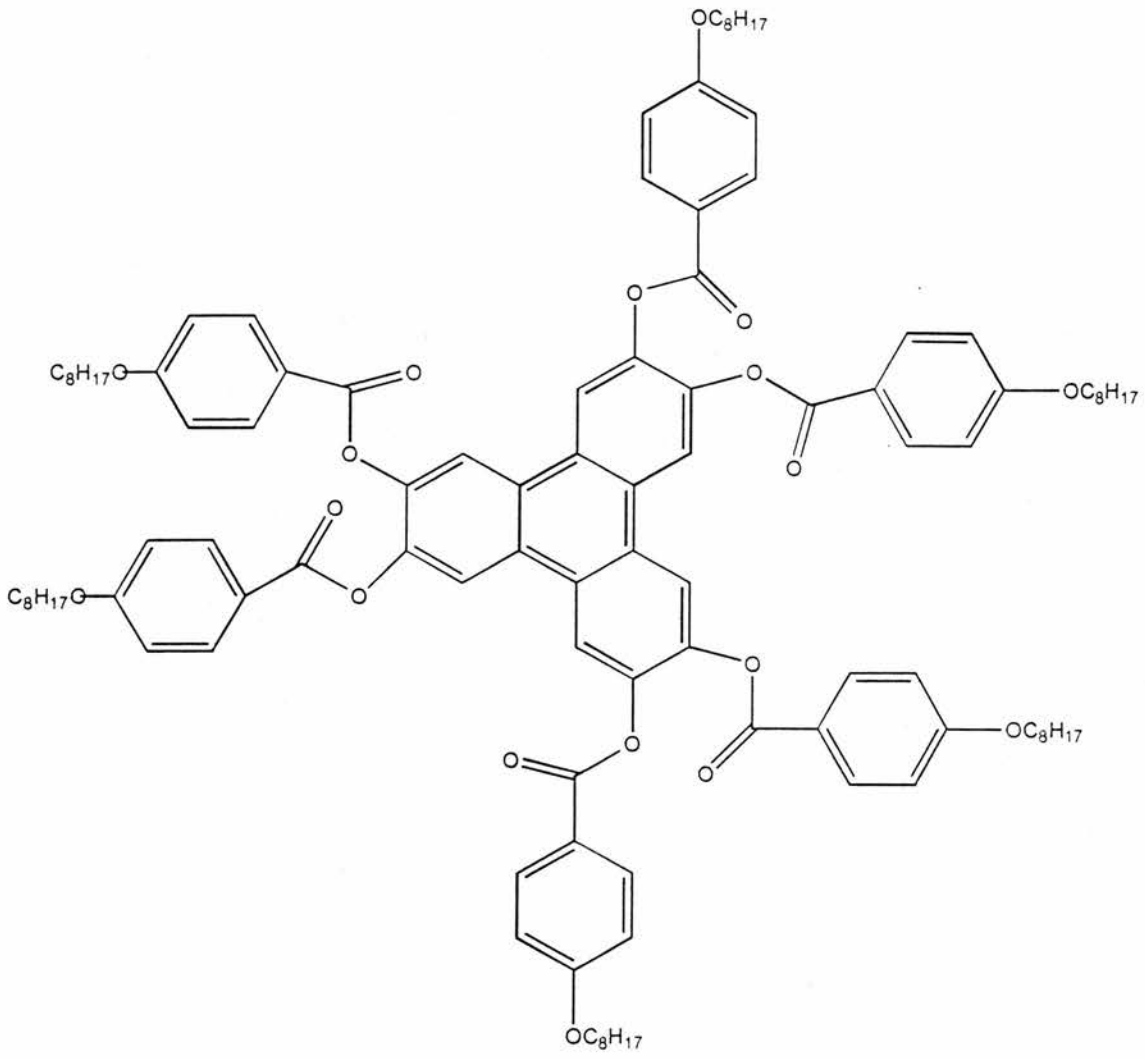

Figure 1.6 *Triphenylen-2,3,6,7,10,11-hexaylhexakis(4-octyloxybenzoate), a compound which displays discotic mesophases.*

As the electric field of elliptically polarised light is constantly rotating it is parallel to the polarisation axis of the second filter twice in each cycle. This allows light to pass through both filters.[2]

Liquid crystals are anisotropic because of their elongated shape and orientational order. They have different properties in different directions and so also allow light to pass through cross polarisers. Nematic liquid crystals show defects as curved lines when viewed through cross polarisers; this is the origin of the name for this phase, nematic, which is derived from the Greek word for thread.

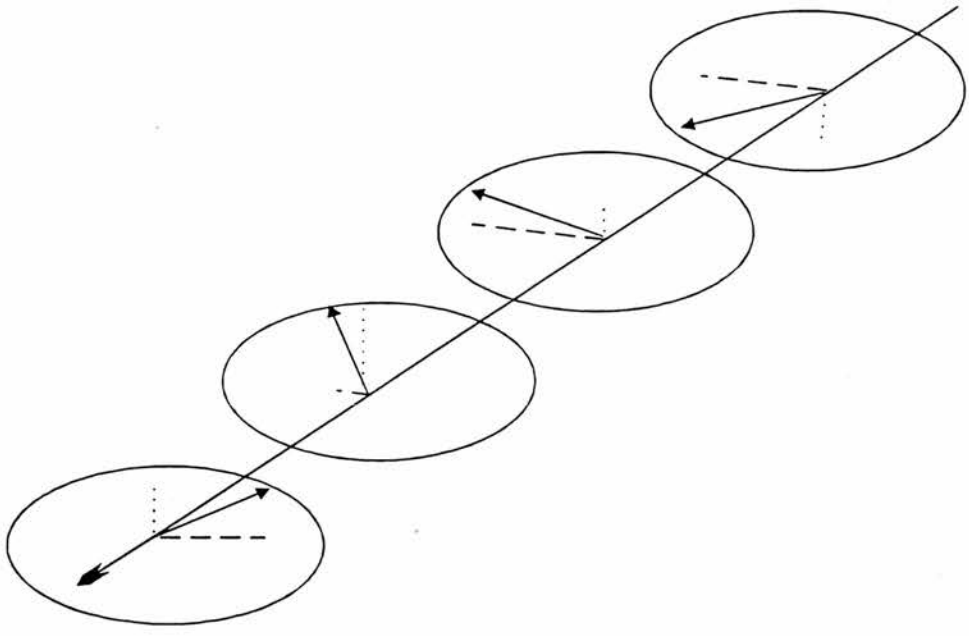

Elliptically Polarised Light (the combination of out of phase beams of plane polarised light)

Cholesteric liquid crystals also interact with light in unusual ways. When white light is incident on a cholesteric phase most of the light is transmitted (and circularly polarised). However, light of the wavelength equal to half the pitch of the cholesteric undergoes constructive interference and is reflected. This phenomenon is known as selective reflection. Because half the pitch of a cholesteric is often in the region of the wavelength of visible light this reflected light is brightly coloured. The pitch of the cholesteric is very sensitive to temperature therefore the wavelength (colour) of reflected light changes with temperature. The ability to react to minute variations in temperature by changing colour has many applications. In medicine for example it is used to determine temperature variations on the skin in the search for subcutaneous tumours.

Nematic liquid crystals are widely used as electronic displays. The prerequisite for materials to be used in this way is that they are in a LC state at room temperature.

One of the first stable room temperature liquid crystals was *p*-methoxybenzylidene-*p*-*n*-butylaniline MBBA.[2,8]

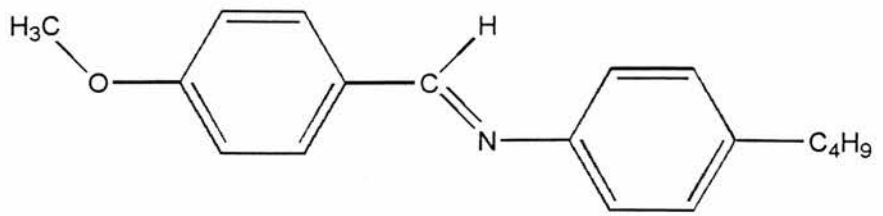

MBBA

The first liquid crystal display (LCD) was demonstrated at Radio Corporation of America in 1963 utilizing the light scattering properties of liquid crystals when large voltages are applied. This is known as the dynamic scattering mode and works because the large electric field causes charged impurities in the liquid crystal to flow, creating turbulence. This turbulence scatters light which previously passed through. The voltages applied are reversed about a thousand times a second to prevent build up of charge yet leave enough time for the charged impurities to move and create turbulence. The ability to modify ambient light rather than produce its own meant a low power consumption in comparison to other display technologies of the time. Dynamic scattering mode displays proved the feasibility and the enormous potential of LCDs.

In the early 1970s twisted nematic LCDs were developed by Wolfgang Helfrich at Hoffmann-La Roche, Inc.[9] (Figure 1.7). When a glass slide is rubbed, with a filter paper, in one direction it imposes certain constraints on nematic liquid crystals which come into contact with it. The director of these nematic liquid crystals align with the direction the glass was rubbed. This phenomenon was first discovered by Mauguin in 1911.[10] An electric field, when applied across certain nematic LC compounds, causes the director to align parallel to the field.

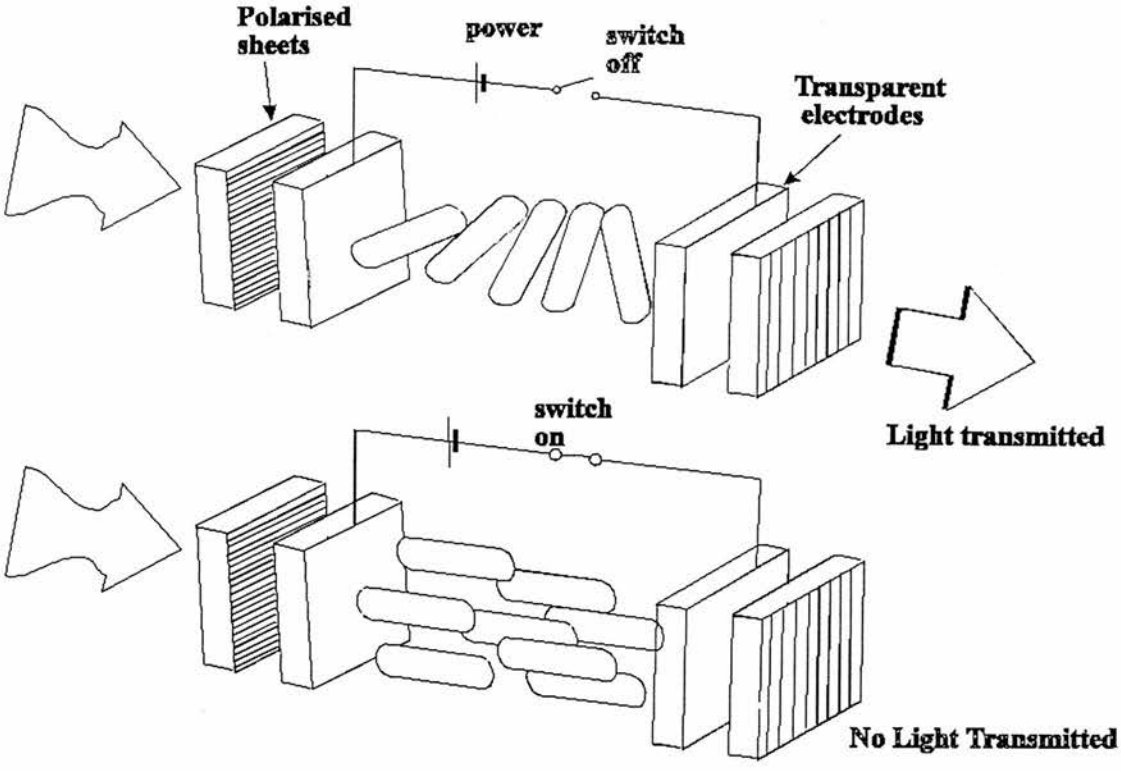

Figure 1.7 *Twisted nematic L.C. Display*

This is due to either a permanent electric dipole present in the molecule or an induced electric dipole interacting with the electric field and causing the molecule to rotate. Molecules must be chosen with the dipole in the correct position for the director to align parallel with the field for twisted nematic displays.

The transparent electrodes with coatings of indium tin oxide in figure 1.7 also have a thin polymer coating several hundred angstroms thick which is rubbed to impart a certain direction to the director of the liquid crystal at the surface.[11] The first electrode is rubbed at right angles to the second, so that, when no voltage is applied the director of the liquid crystal undergoes a 90° twist in the region between electrodes. Polarised sheets are positioned on both sides of the display in such a way that the direction of linear polarised light is parallel to the rub direction. The optical activity of the liquid crystal in this configuration is such that it rotates the direction of the plane

polarised light by 90°. Thus linear polarised light from the first polariser can propagate through the liquid-crystal layer and pass through the second polarised sheet. Application of a small voltage across the two electrodes orients the director, in the central portion of the liquid-crystal layer, parallel to the electric field and perpendicular to the electrodes. The voltage must be above the threshold value for this Freedericksz transition. This untwists the structure and destroys its optical activity. The polarised light passing through the cell is now absorbed by the second polarising sheet and the cell appears dark. Removal of the field allows the nematic liquid crystal to relax back into its preferred orientation, a 90° twist. The display can also utilise ambient light by placing a diffuse reflector behind the display; light passing through the display is reflected and simply retraces its path back through the cell.

The great advantage of this system is the fact that it only requires a few volts and a tiny current to operate. A small battery can therefore run this display for a very long time. The disadvantages include the switching time which is not very fast (0.02 to 0.05s) and the viewing angle and brightness which are restricted by the polarising filters. This type of display has been dominant for devices such as digital watches.

Another type of liquid crystal display utilises the smectic C* phase,[12] in which the director of this material rotates in a cone as you pass from one layer to the next. If the cell is made thin enough there is an interaction with the walls of the cell and no rotation occurs, instead it prefers to align with the glass. Normally the electric dipole of the molecules in the liquid crystal state would be averaged out because of the rotation. In this case because there is no rotation the sample possesses a macroscopic dipole. Samples which posses a permanent macroscopic dipole in the absence of an electric field are known as ferroelectric. This ferroelectric phase allows the molecules to align in

one direction with the electric field and the other when the electric field is reversed. Crossed polarisers at the correct angle will prevent light passing through with one orientation and induce a phase shift for the other orientation. If the thickness of the cell is adjusted so this phase shift is 180° the plane polarised light produced will be at 90° to the incoming plane polarised light and able to pass through the second polariser.

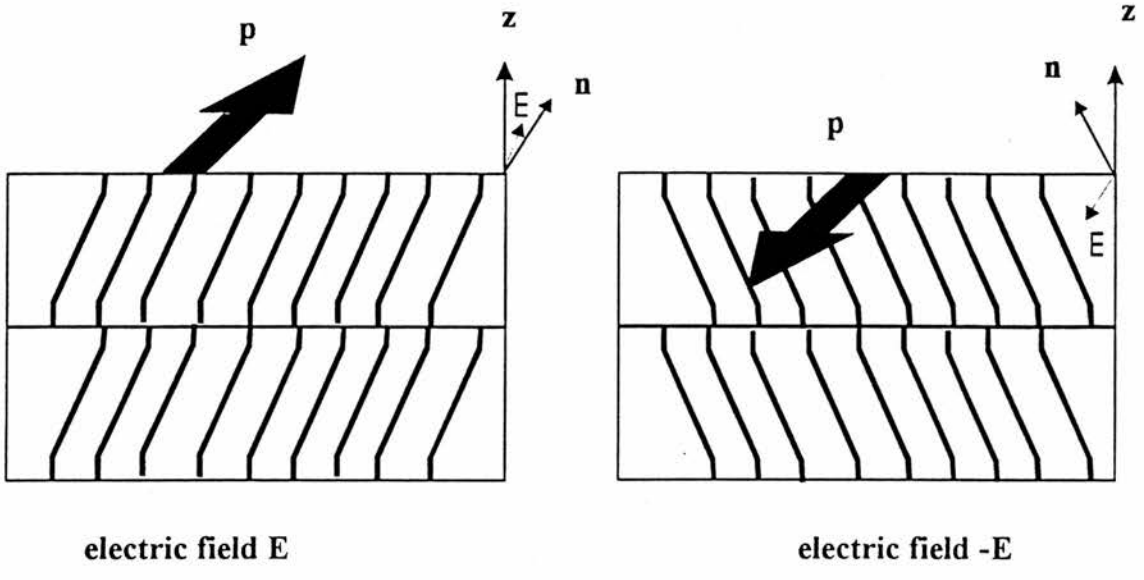

Figure 1.8 *Smectic C* with a macroscopic dipole p (ferroelectric polarisation) when exposed to two opposite electric fields*

The speed of switching in these displays is approx. 10-50 ns; this is order of magnitudes faster than the maximum theoretical value for twisted nematics. The molecules remain in a particular orientation, even in the absence of an electric field, until an opposite field is applied. The power consumption, as for a twisted nematic display, is very low and this may be the display technology of the future.

1.2 Metal containing liquid crystals (metallomesogens)

With the many diverse properties present in organic liquid crystals, the aim of incorporating metals might seem pointless; however, metals can and do impart many additional properties to these remarkable compounds.

The incorporation of transition metal ions in LC compounds provide the means to alter the shape beyond the constrictions of the coordination geometry around carbon, hydrogen, oxygen and nitrogen. They offer the possibility of square planar, square pyramidal, trigonal bipyramidal, octahedral and so forth. The shape of the molecule has great influence on the properties exhibited in LC phases.

Anisotropic materials commonly display birefringence, in which a beam of light enters the material at an angle and is then split into two beams. This is because light polarised in one direction travels through this medium at a different speed from light polarised at right angles. The difference in speed is caused by the shape and electrostatic properties of the material being different in different directions. Liquid crystals, which tend to be rod-like molecules, have different properties depending on which direction they are orientated (*i.e.* anisotropic), display this birefringence. The difference in the two refractive indices, parallel and perpendicular to the molecular axis is the birefringence, Δn. Very large birefingences can be obtained with the addition of metals into liquid crystals.[13]

In addition whilst organic materials tend in general to be colourless, organometallic complexes, are often highly coloured by virtue of the intense metal to ligand charge transfer absorptions.[14] Although filters are used to provide colour in liquid crystal displays, coloured liquid crystals and possibly electrochromic liquid crystals may be useful in this area.

Thirdly, the electrical and magnetic properties of metals can be incorporated into the liquid crystal. Conducting,[15,16] paramagnetic[17] and ferromagnetic[18] properties along with a whole host of other useful properties which are only present when metals

are involved, are also present when in the LC phase. The addition of order in the liquid phase opens up a myriad of possible applications unavailable to solids.

Finally, the polar electron density found in metals is very large and this is an important feature in all liquid crystal compounds. The additional polarity may induce properties not seen in purely organic liquid crystals *i.e.* an ability to deviate from the rod like structure and still retain LC properties. This increase in interactions can be seen with the coordination of iridium to a non mesogenic ligand forming a metallomesogen with nematic and smectic phases.[19]

Drawbacks of Metallomesogens

There are drawbacks to incorporating metals into LC compounds.

The metal to ligand bond is the weak link in the compound.[12] It leads to decomposition at lower temperatures. The presence of a metal atom in the structure tends to increase the temperature at which LC phases are found. This is possibly due to intermolecular metal to ligand interactions. It is desirable from the point of view of most technological applications that LC phases be present at room temperature. Thus higher temperatures of LC phases and lower temperatures of decomposition mean fewer compounds are stable in the LC phase and this phase is less likely to be at room temperature.

Types of Metallomesogens

The first thermotropic metal containing LC compounds were prepared by Vorlander in 1910.[20] The long chain sodium carboxylates were found to form lamellar phases. He progressed from alkali-metals and in 1923 reported mercury compounds **1** which displayed smectic phases.[21]

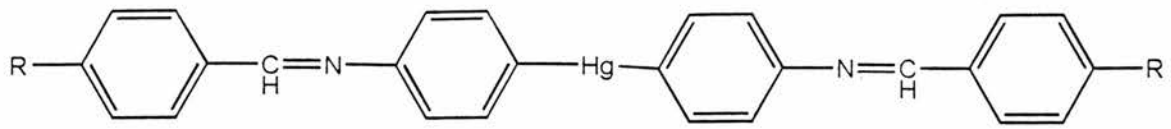

1

There are many types of metallomesogens; however, they can normally be categorised according to their shape. Linear, square planar and dinuclear are the main categories but there are also more exotic compounds like ionic melts, square pyramidal and octahedral complexes which also form liquid crystal phases

Linear

This configuration resembles the rod like molecules in organic liquid crystals and as such displays many of the same features. The sodium carboxylate compounds prepared by Vorlander come into this category, as do **2** and **3**:

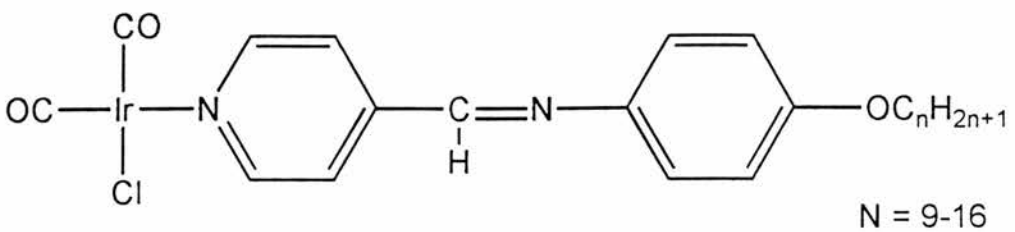

2

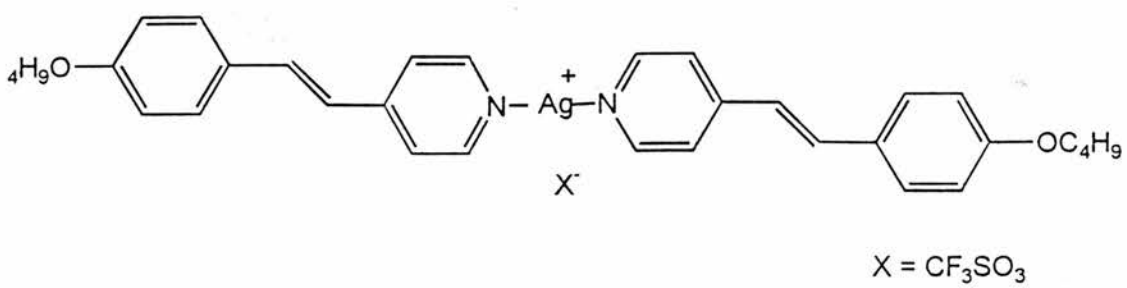

3

The short, strongly polar group on one end of **2** differs from the traditional organic liquid crystal which normally has long chains on both ends. It has been found that

organic compounds with short groups such as CN and NO_2 on one end of the rigid core often enhance the LC character. The highly polarisable group causes the molecules to pair up slightly, resulting in a dimer which is longer than the original molecule. Metals are very polarisable and hence the effect works well with molecules of this type. Compound **2**[22] gives a smectic A phase when the chain length is between 8 and 16. Rhodium complexes[23] of this material also show LC properties when the chain length is 8 or 9.

Linear organometallic silver salts[24] can show LC phases. Compound **3** has a nematic phase between 146°C and 153°C. These ionic melts have altered properties if a different anion used: with tetrafluoroborate, for example, the sample is hygroscopic, sensitive to light and has higher transition temperatures.

Only a few transition metal complexes show a nematic phase. The square planar complex **4** has a nematic phase between 126.8°C and 171.6°C. [25] An unusual feature of this compound is that the Cu^{II} complex is paramagnetic in the nematic phase and the Ni^{II} complex is diamagnetic in the nematic phase. Paramagnetic LC complexes were first described simultaneously in 1986 in β diketone Cu^{II} complexes[26] and in salicylaldimine Cu^{II} complexes.[27]

M= Ni II, Cu II

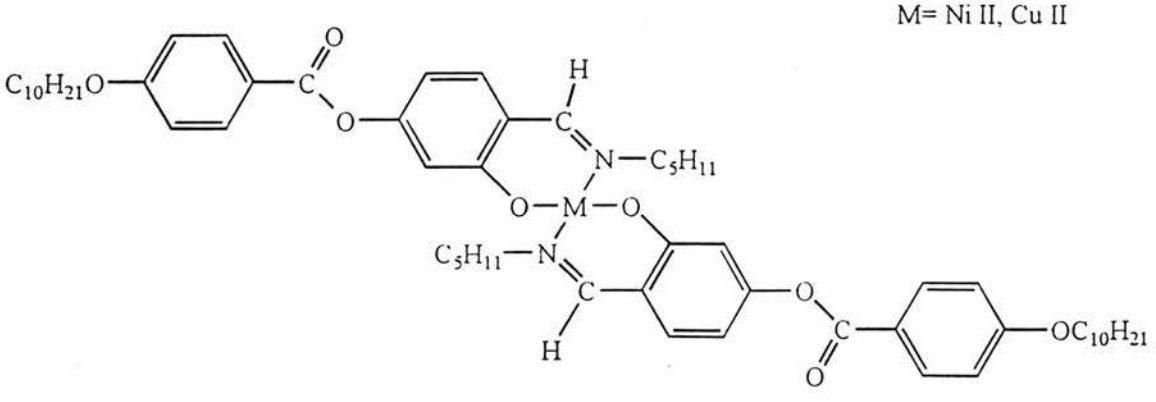

4

Smectic phases are more common with transition metal complexes, compound **5** has a smectic phase when the chain length is 10 however when the chain length is only 4 the compound displays nematic characteristics at the transition temperature. This compound is also an electron acceptor. Experiments were conducted with a mixture of the nematic nickel complex and an electron donor nematic molecule to determine whether the enhanced intermolecular interactions would lead to a smectic phase. [28]

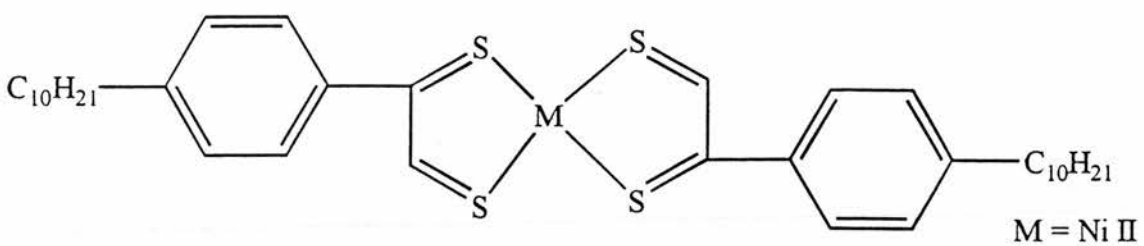

5

Square planar complexes can also form discotic mesophases. Compound **6** is similar to organic discotic liquid crystals in shape and mesophase form.[29] The compounds stack into columns in a hexagonal array at the transition temperature. These columns position the metal centres on top of each other. With Cu^{II} as the metal centre there is the possibility of a one-dimensional conductor along the spine of the mesophase. A molecular wire of this type has possible uses in molecular electronics. It also has a robust insulating apolar medium which can accept dopants without altering the conducting chains.

It is possible for a metallomesogen to contain two metals. The palladium dinuclear complex 7 displays smectic C* LC phases because of the chiral centres. Given the correct conditions it can be induced to display ferroelectric LC behaviour. This permanent macroscopic dipole is normally used in display technologies; however, the response time for this material is substantially slower than for organic molecules. The

slowness is thought to be a consequence of the shape of the molecule which is like a half opened book with the palladium atoms on opposite pages.[30]

Another dinuclear complex is dirhodium carboxylate **8** which forms a discotic mesophase.[31] It was investigated by Raman spectroscopy which was used both as the heat source and the detector of phase changes. The complexes have a certain degree of intermolecular interaction and stack into hexagonal columns (Figure 1.9). The metals in this case are not stacked directly on top of each other.

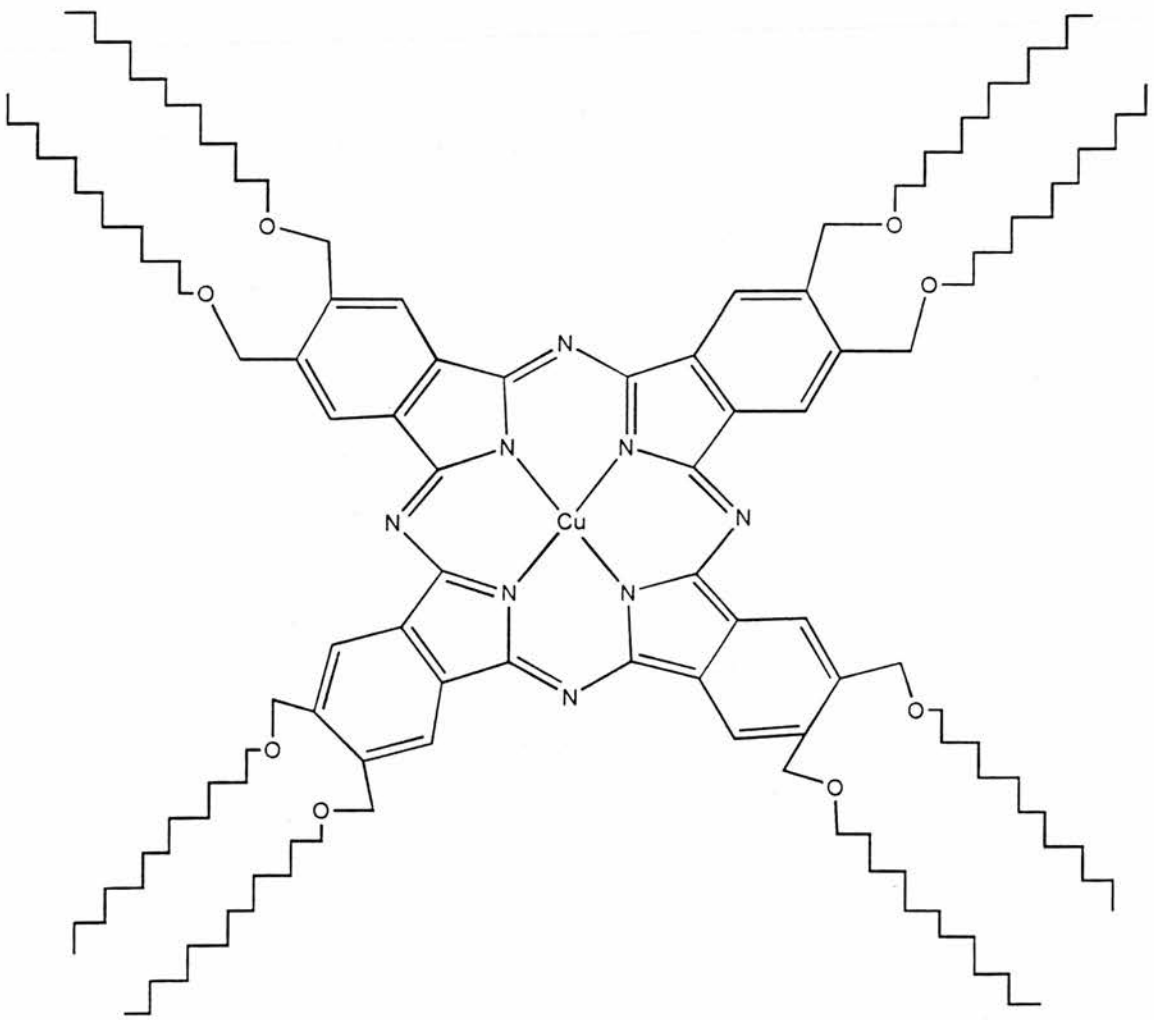

6

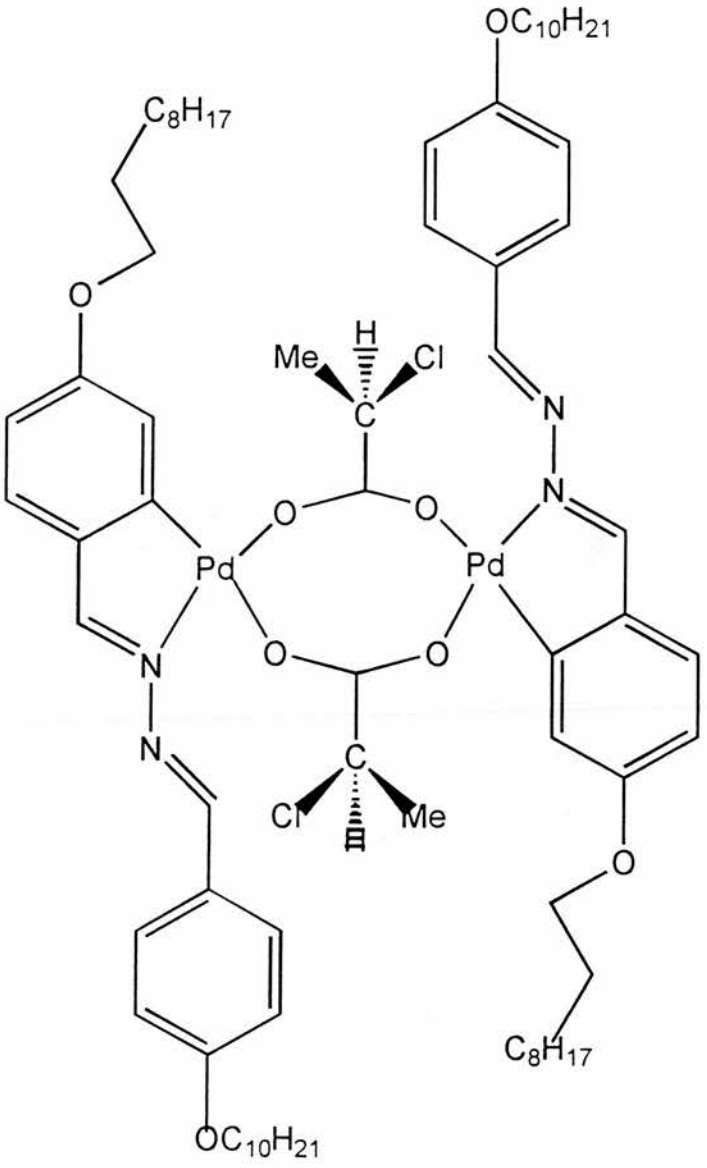
OC10H21
C8H17
O
Me
H
Cl
C
N
N
O
O
Pd
Pd
O
O
O
O
N
N
C
Cl
Me
O
C8H17
OC10H21

7

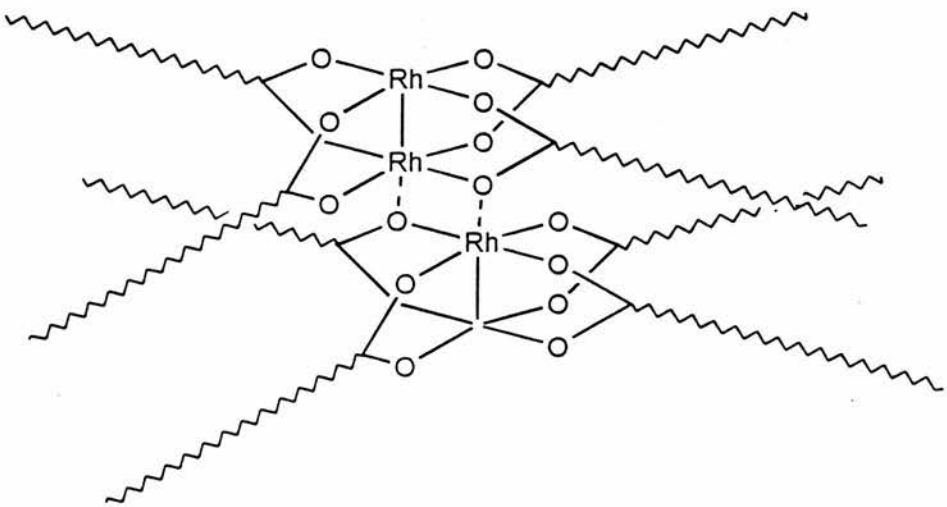
O
Rh
O
O
O
Rh
O
O
O
O
Rh
O
O
O
O
O
O
O
O

8

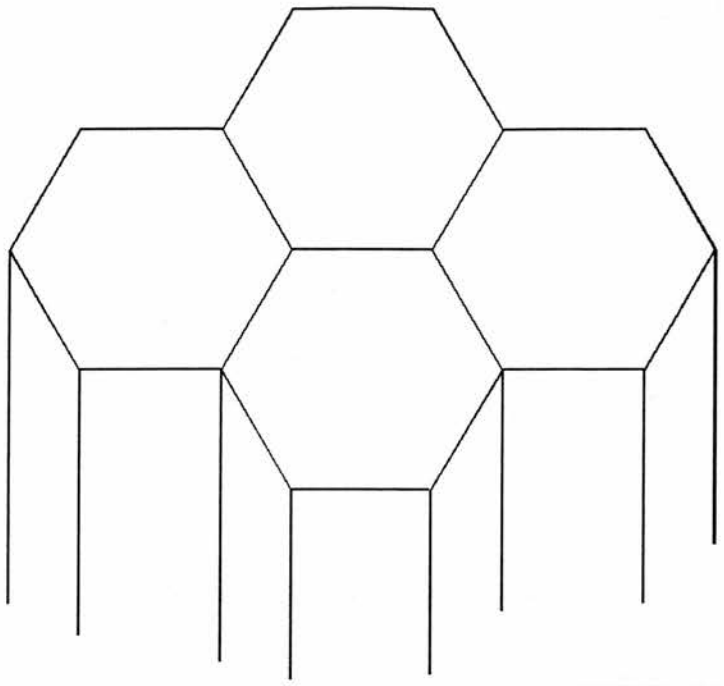

Figure 1.9 *Hexagonal columns*

Substituted ferrocene molecules can form mesogenic phases if the correct substrates are attached.[32] Complex **9** forms monotropic smectic C mesophases (present only on cooling).

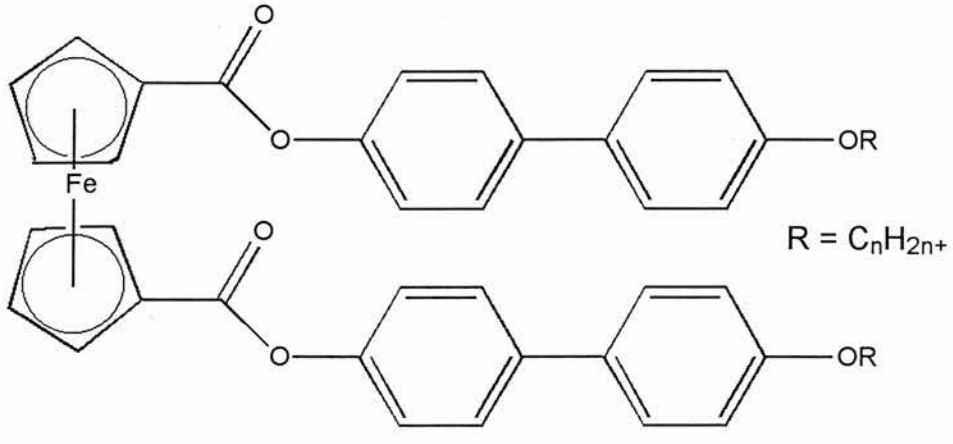

9

Octahedral Fe^{III} trisdiketonate[33] has endothermic transitions in the liquid phase and has a birefringent structure while in this state which strongly suggests that a LC phase has been formed. If this is correct then it would be the first octahedral metallomesogen.

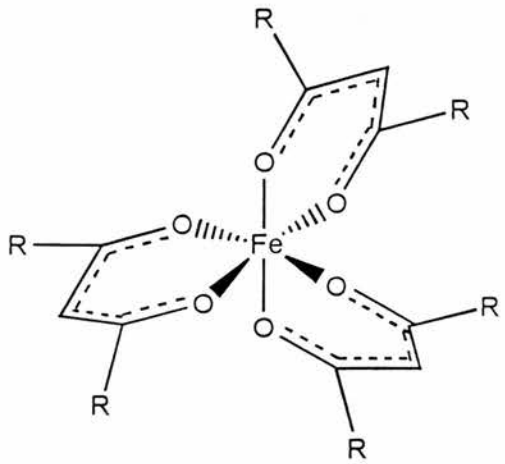

10

If a compound does not have the properties necessary to be used in display technology by itself it may have the desired properties when mixed with organic liquid crystals. Many compounds such as these are used in host guest displays. A complex which is highly dichroic *i.e.* the extinction coefficient is very much greater along the molecular axis than perpendicular to it, can be used to provide colour to an organic liquid crystal. The purple nickel complex[34] **11** aligns with the director of an organic liquid crystal when mixed and follows the director when an electric field is applied. The change from a highly coloured compound to a colourless one is something difficult to find in purely organic materials.

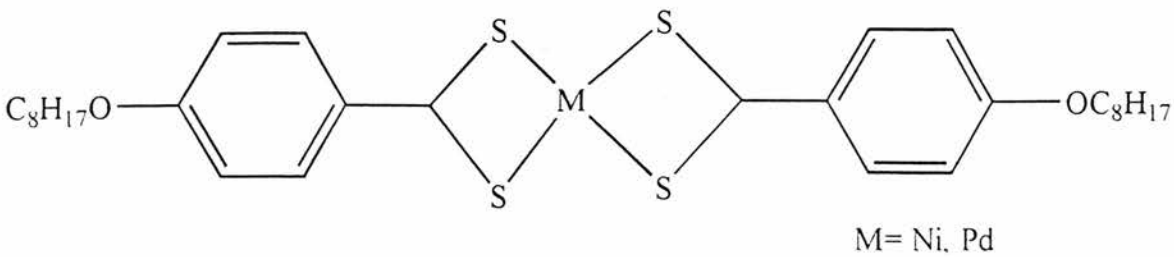

11

In general it can be said that the requirements for a metal complex to show mesophases is not dissimilar to organics. The length of the tail has to be longer than five

atoms.[3] The ligands used to complex the metal need not necessarily be liquid crystals in their own right.[18] The complexation of a metal to a liquid crystal only results in similar properties for the complex when the overall shape is not altered radically. Tetrahedral geometry at the metal centre is not conducive to mesophase generation. This is probably due to the fact that most of the metallomesogens have some degree of coordination with adjacent molecules through the metal centre which would be difficult with tetrahedral geometry. The strength of the intermolecular coordination at the metal is such that the transition temperatures are often higher than for purely organic liquid crystals. Deviations from strict rod like molecules does not necessarily destroy mesophase formation and brings the transition temperatures down.[35] Certain Cu-β diketonates[25] give discotic phases when the phenyl groups have alkoxy substituents but not with simple alkyl substituents showing that very small changes can result on the formation or destruction of mesogenic states.

As more is discovered about these complexes, more potential uses are proposed. Chemical sensors, and nonlinear optics[36] are just some of the areas in which metallomesogens might be useful.

1.3 Macrocycles

Macrocyclic ligands are polydentate ligands with their donor atoms, normally N, incorporated in a cyclic backbone. To be referred to as a macrocyclic ligand there should be at least nine atoms in the ring, at least three of which must be donor atoms.[37] Such atoms play major roles in many biological systems, e.g. photosynthesis, O_2 transportation and enzyme catalysis. The driving factor in the investigation of these complexes is the production of models and even replacements for bioorganic systems.

Living organisms maintain steady states far from thermodynamic equilibrium.[38] Their entropy decreases over time as they form ordered structures and grow. To maintain these states energy and materials must be harnessed at low temperatures. Bioinorganic macrocycles play important roles in many essential processes.

An efficient O_2 transportation system in animals is essential so energy-producing biochemical reactions can occur where they are needed. In mammals this job is done by haemoglobin, which transports and stores O_2 in the bloodstream, and myoglobin which transports O_2 in the muscle cells.[39] Both are large protein molecules and both contain a haem unit which is the active site for binding O_2. Haemoglobin, found in red blood cells, consists of four haem groups surrounded by a globin group. A globin group consists of two linked polypeptide chains. The protein molecule myoglobin has a molecular weight of 16700 about a quarter of haemoglobin and although the haem portion of the molecule stays the same the protein portion varies between species.

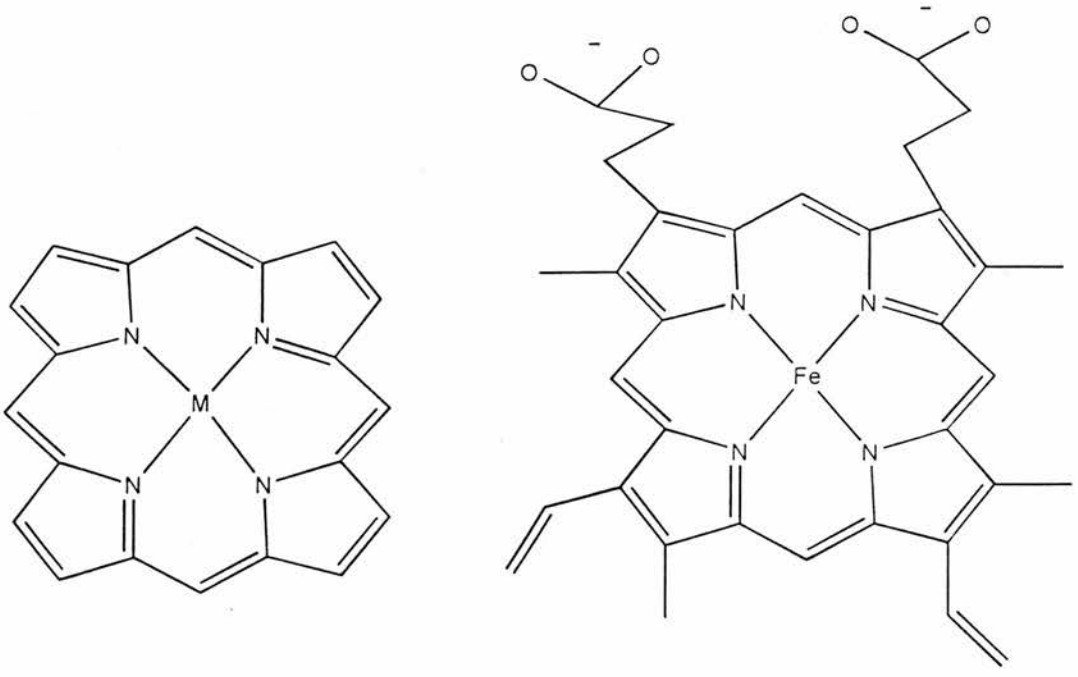

Figure 1.10 *Metalloporphyrin and haem unit*

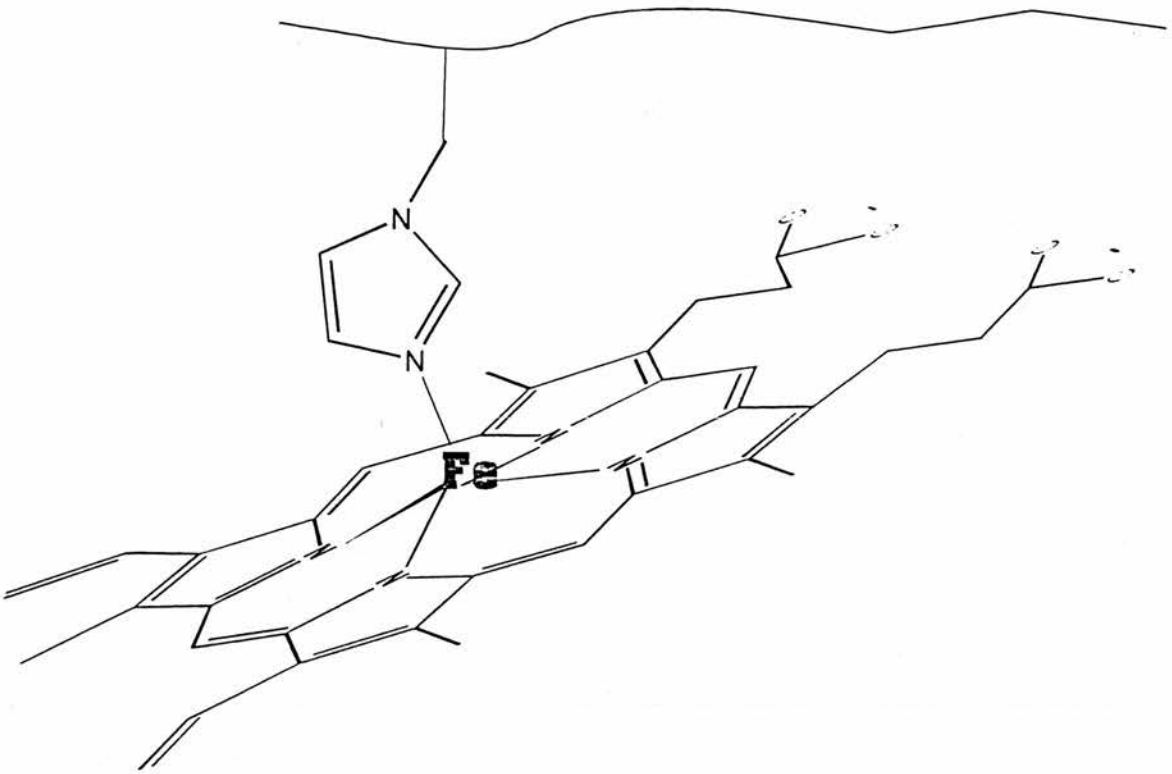

Figure 1.11 *The haem unit is axially coordinated to the protein*

O_2 is bound at the free axial position forming an octahedral complex

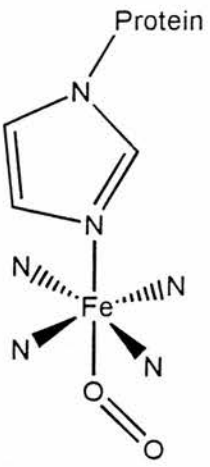

Figure 1.12 *Octahedral complex when bound to* O_2

These groups have a reversible bond with O_2 at the iron centre of the haem unit. The haem unit is based on a metalloporphyrin. (Figure 1.10). The binding site is not very selective and any π acid ligand of the correct size will bind.[35] NO, CO, CN^-, and O_2

will all bind but not necessarily reversibly, CO for example blocks this site and poisons the organism.

Naked haem units in the presence of O_2 are irreversibly oxidised from Fe^{II} to Fe^{III} giving a μ-oxo bridged dimer. It is the protein environment which prevents this happening in biological systems. The protein is shaped in such a way that it does not allow the approach of large molecules. Models of O_2 binding have had to prevent two porphyrin groups coming together. Three broad approaches have been taken to prevent Fe^{III} formation[37]: the use of low temperatures, the incorporation of steric barriers, and immobilisation on a solid surface. Two O_2 binding porphyrin models which elegantly solve this problem by steric hindrance are known as the picket fence model and the capped model. Collman *et al.*[40] prepared a compound based on Fe^{II} porphyrin with an axially coordinated N-methylimidazole base. The substituents on the porphyrin project out onto one side of the ring, effectively blocking approach by any large molecules (Figure 1.13). Baldwin *et al.*[41] went one stage further and added a protective cap to the molecule with dimensions large enough to allow O_2 inside but small enough to exclude solvent. Both these systems have demonstrated reversible O_2 uptake.

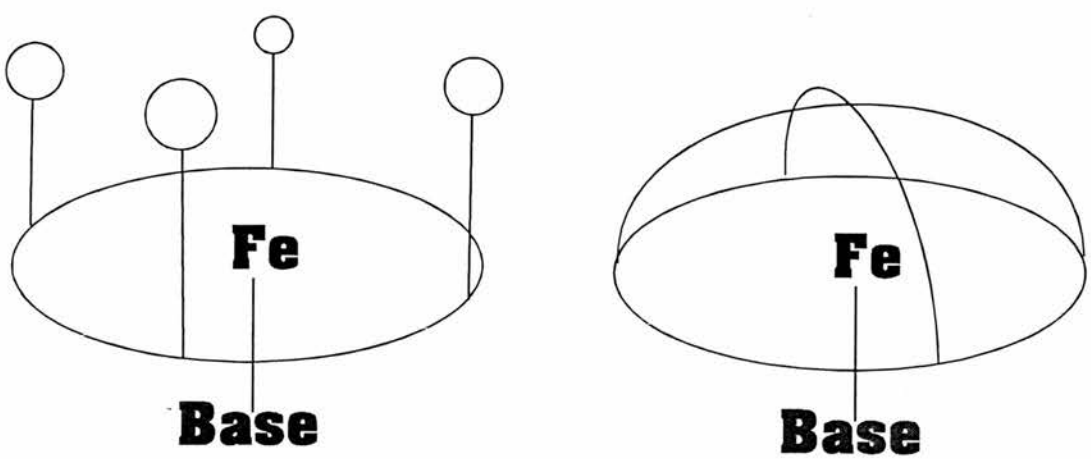

Figure 1.13 *Picket fence and capped models of haem group*

Magnesium macrocycles play an important role in photosynthesis. In the production of carbohydrates from O_2 and CO_2 the energy from the sun has to be harnessed. The role of chlorophyll in the photosynthetic reduction of CO_2 is the supply of electrons. This is achieved because of the unique redox properties of chlorophyll which can convert light to chemical energy. Chlorophyll was structurally defined by Willstätter, who won the Nobel Prize for this work in 1915.[42] Chlorophyll is a reduced porphyrin molecule with a magnesium metal centre (Figure 1.14).

The light which this complex does not adsorb is reflected and gives the characteristic green colour to plants. Harnessing energy from the sun in a quick efficient manner is a dream of many scientists. Macrocycles may be central to this process as it is developed into a direct source of power.

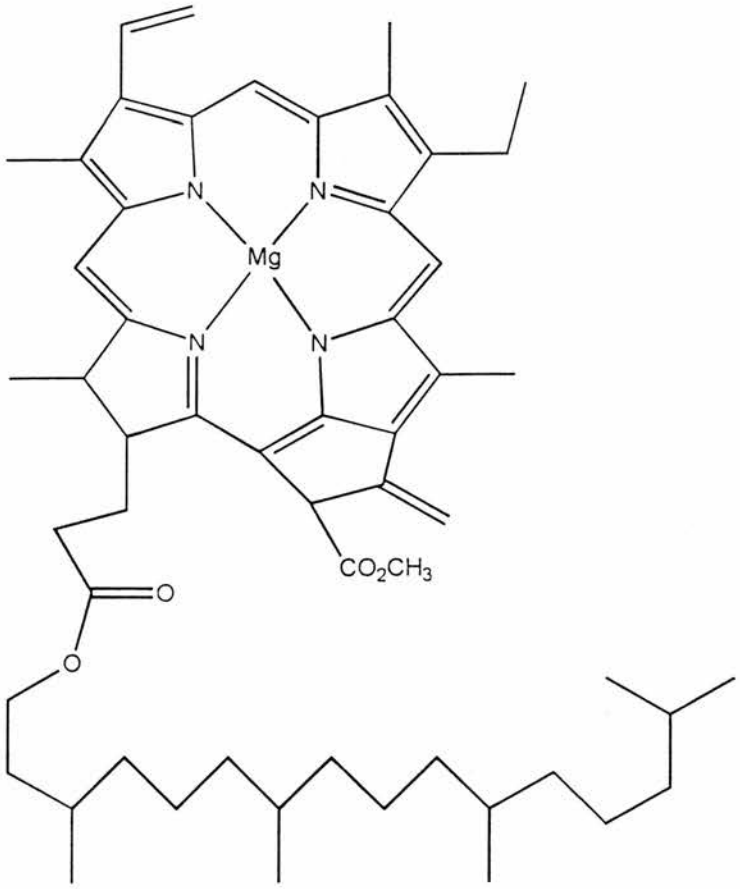

Figure 1.14 *Chlorophyll*

Other biologically active compounds such as vitamin B_{12} coenzyme and Cytochrome P-450 are macrocyclic complexes containing Co^{III} and Fe^{II} respectively. They have attracted much interest, the corrin-cobalt B_{12} coenzyme because it is involved in so many enzyme reactions and Fe-haem cytochrome P-450 because of its ability to catalyse aliphatic and aromatic hydroxylations and epoxidations. These investigations have revealed a lot about the individual compounds but also by modelling the complexes a lot has been learned about the synthesis and properties of macrocycles as a whole.

Macrocyclic compounds have certain characteristics:

1. A high thermodynamic stability. When compared to a complex formed with a comparable non cyclic ligand the macrocyclic complex is found to be more stable.[42]

2. A marked kinetic inertness both to the formation of the complexes from the ligand and the metal ion and to the reverse the removal of the metal ion from the complex. Once formed the metal is firmly held and not affected by competing demetallation reactions.

In most macrocycles the donor atoms are nitrogen but other atoms such as phosphorus, oxygen, and sulphur can also be used. Crown ethers, for example, are synthetic polyether ligands which form a macrocycle. Depending on the size of this macrocycle various metal ions can be complexed: Na^+ K^+ Mg^{2+} and Ca^{2+}. In natural systems, ionophores such as cyclodepsipeptides and macrotetrolides are the macrocycles involved in transport of ions through the cell walls (lipid bilayers). This is allowed because the ions are cloaked in an organic layer. This cloaking ability also allows metal ions to be soluble in organic solvents and take place in reactions not possible before.

The hole size or cavity is one of the most important features of a macrocyclic compound. In macrocycles containing four donor atoms the size of the ring is normally between 15 and 21 atoms. From this information the space available to the metal ion can be calculated, for fully saturated molecules,[43] (Figure 1.15):

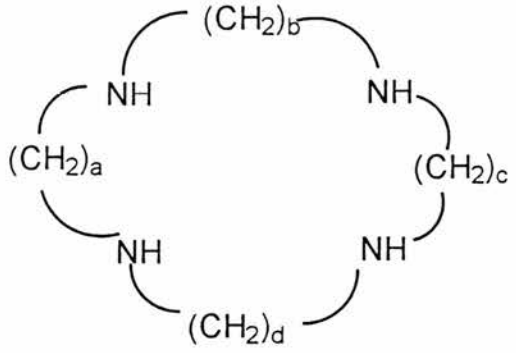

Figure 1.15 *The size of the cavity*

Molecular mechanics calculations showed that for each additional atom in the macrocycle there is a regular increment of 0.1-0.15 Å in the mean radius. The type of ions which will fit into this cavity can therefore be predicted. Metal ions which are too large for the hole may still be complexed: however, they will either sit outside the plane formed by the nitrogen atoms or they will distort the macrocycle, from planarity, into a folded position. The stability of the macrocycle can lead to unusual situations in which the donor metal bond length is either much shorter or much longer than normal, leading to exceptional properties, e.g. the stabilisation of high oxidation states.[44]

Unsaturated macrocycles are much less flexible and it is possible to form completely unsaturated macrocycles where a Hückel aromatic system can occur. Porphyrins form this state with $(4n + 2)$ π electrons. This increases the difference between a closed macrocycle and the corresponding non cyclic ligand.

Synthesis of macrocycles is normally either by direct organic synthesis or by template reactions. In a template reaction the metal ion can have two possible functions. It can sequester the cyclic product from an equilibrium solution forcing the reaction towards the product side. This role is called the thermodynamic template effect. It can otherwise be used to direct the atoms into the correct configuration for cyclisation. This is termed the kinetic template effect. In fact the metal often participates in both these effects.

The first recorded template synthesis was by accident in 1928 when phthalimide was prepared in an iron vessel. The dark blue compound formed was phthalocyanine. Later on the Curtis synthesis[45] became a landmark in template synthesis terms and involved the condensation of acetone molecules to form a stable compound (Figure 1.16).

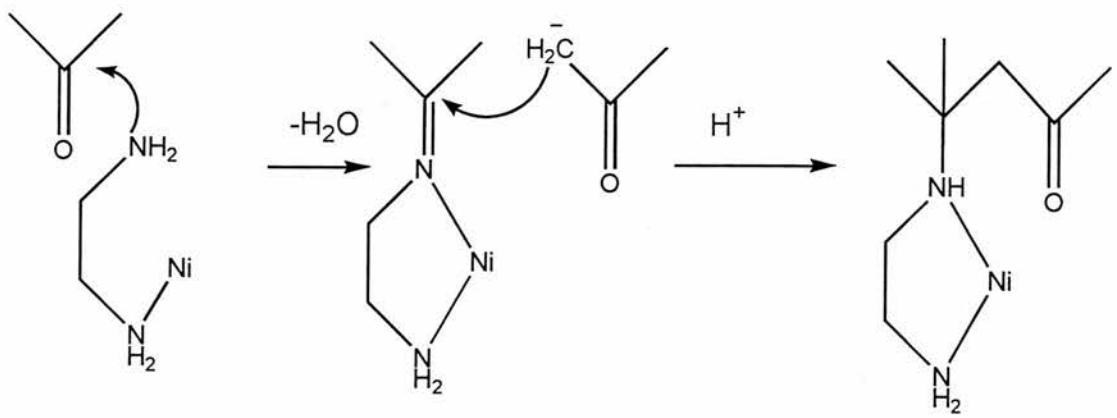

Figure 1.16 *Curtis condensation reaction (proposed mechanism)*

Direct macrocycle synthesis has the disadvantage that there is nothing to stop the reagents forming polymers rather than the complete macrocycle. There is also the possibility that the half formed macrocycle can condense with itself in a head to tail fashion rather than with another molecule. Production of the desired macrocycle is therefore very dependent on reaction conditions to eliminate the undesirable polymer

and half macrocycle products. The chief method of control is concentration. High dilution is favoured for a number of direct synthesis reactions because it virtually eliminates formation of polymers.

There are also reactions which are a mixture of template and direct synthesis, where it cannot be said for certain if a particular ion has any part in the reaction. Even though an ion can be used to bring a molecule into the correct conformation for cyclisation it does not necessarily complex to the resultant macrocycle.[46]

1.4 Tetraazaannulenes

Tetraazaannulene compounds (Figure 1.17) have all the characteristics necessary for the central portion of a metallomesogen. They are robust rigid molecules with aromatic groups and the ability to complex a variety of metal ions. They also have interesting chemical, electrochemical and catalytic properties which could be transferred to the LC phase.

In addition to the properties unique to tetraazaannulenes, they share certain characteristics with porphyrins.[47] In common with porphyrins the four nitrogen atoms are confined to a plane, metal complexations result in deprotonation to give a dianion and they both have a completely conjugated system of double bonds. There are also important differences between porphyrins and tetraazaannulenes. The ring size is smaller, containing only 14 atoms in comparison to porphyrins 16 atoms resulting in shorter metal to nitrogen distances. Despite being completely conjugated the tetraazaannulene system is anti-aromatic, according to Hückel's rules, whereas porphyrins are aromatic. The two negative charges are localised on the bridging top and

bottom portion of the molecule, rather than delocalised over the entire structure as in porphyrins.

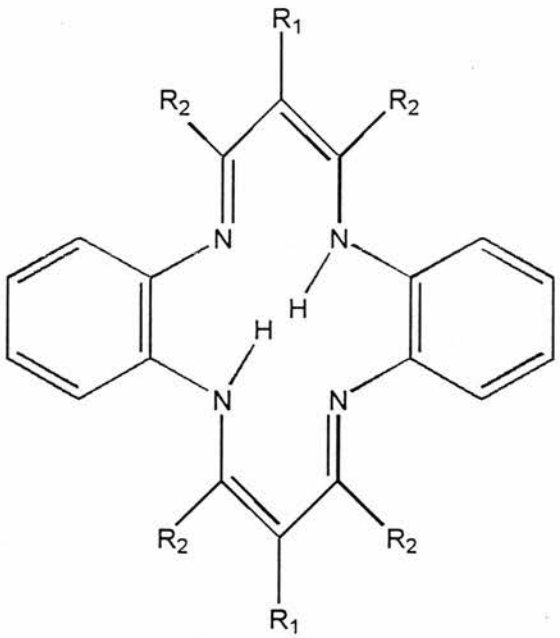

Figure 1.17 *Tetraazaannulenes;*

Tetraazaannulene TAA $R_1 = R_2 = H$,

Dimethyltetraazaannulene DMTAA $R_1 = CH_3$ $R_2 = H$,

Tetramethyltetraazaannulene TMTAA $R_2 = CH_3$ $R_1 = H$

Tetramethyltetraazaannulene was first prepared by Jäger in 1969 via a Ni template synthesis.[48] Its crystal structure revealed a saddle formation and a hole size of about 1.902 Å which is 0.1 Å smaller than porphyrin. The saddle shape is due to the steric interactions between the methyl groups and the phenyl groups. Because of this the coordinated metal is not in the plane of the N atoms which introduces an inequivalence in the two remaining coordination sites. TMTAA is much more soluble than the other tetraazaannulene molecules due to this buckled shape which prevents close π-π interactions in the solid state. Many metals have been complexed with this

ligand, Fe^{II}, Co^{II}, and Ni^{II} are known to form simple square planar complexes but can also utilise the uncoordinated sites to form more unusual structures. The first row of the transition metal series from Ti to Zn have been found to complex with this ligand and even ions in the second and third rows such as Zr^{IV}, Ru^{II} and W^{0} seem to be able to complex. The coordination geometries of these complexes vary considerably and each ion can have several different coordinations depending on the additional ligands. Because the ions are displaced from the plane of the macrocycle it is not unusual for additional ligands to be coordinated in a *cis* fashion. Goedken *et al.*[49] synthesised $Ti(TMTAA)Cl_2$ which was found to be in a *cis* arrangement (Figure 1.18) forming a trigonal prismatic structure (Figure 1.19).

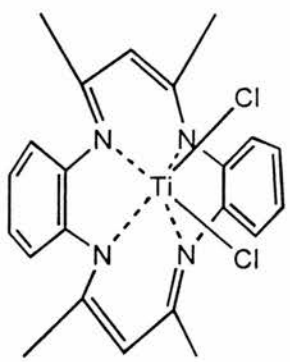

Figure 1.18 *Chlorine atoms in a cis configuration*

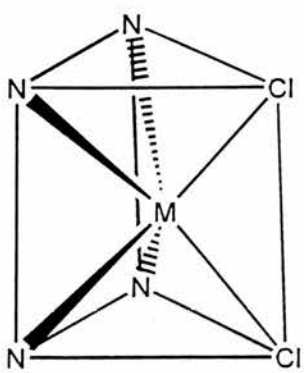

Figure 1.19 *Trigonal prism configuration.*

The chlorine atoms can be replaced by alkylation of the metal with a Grignard reagent leading to a product which is also in a *cis* configuration.

The atomic radii decrease along the transition metal series so as expected smaller ions which are not displaced as far from the N plane can often readily form octahedral complexes. In Fe(TMTAA)(CO)(NH_2NH_2),[50] for example, the Fe ion has an octahedral geometry as it does in many bioorganic complexes. Ions from the second and even third row are larger and hence displaced further from the plane of the N atoms and can display quite unusual coordination geometries. W(H_2TMTAA)(CO)$_4$ is only coordinated to two N atoms and is positioned well outside the ring.[51,52] The coordination in this case is achieved by reaction at high temperatures, and the ligand remains neutral upon complexation as one of the nitrogen protons migrates to the bridgehead carbon. Fe^{III} and Co^{III} and Cr^{III} can form square pyramidal structures bound to TMTAA and one chlorine atom. It is very unusual to find Cr^{III} in such a geometry.[53] Vanadium tetraazaannulene complexes form a very stable bond with oxygen at the fifth coordination site to form a square pyramidal structure V^{IV}(TMTAA)O and are otherwise quite inert[54,55]. A substituted TMTAA complex can even provide the fifth coordination site from an attached pendant arm should a suitable donor be in the correct position.[56]

Dinuclear complexes are possible; for example Ru^{II}, Rh^{III}, Cr^{II} and Mo^{II} complexes have been formed (Figure 1.20). Hanack and Koch[57] have developed the idea of ligand-bridged dinuclear tetraazaannulenes into a polymeric Fe^{II}(TMTAA) complex with a pyrazine molecule joining the metals (Figure 1.21).

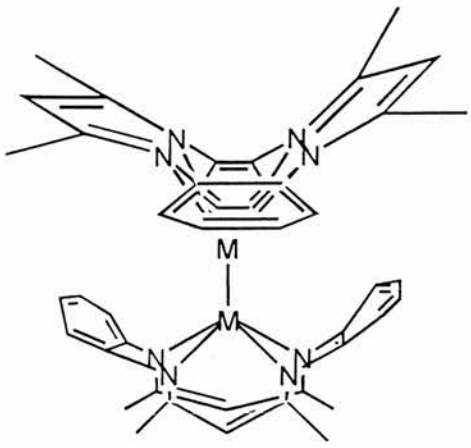

Figure 1.20 *Dinuclear TMTAA complex*

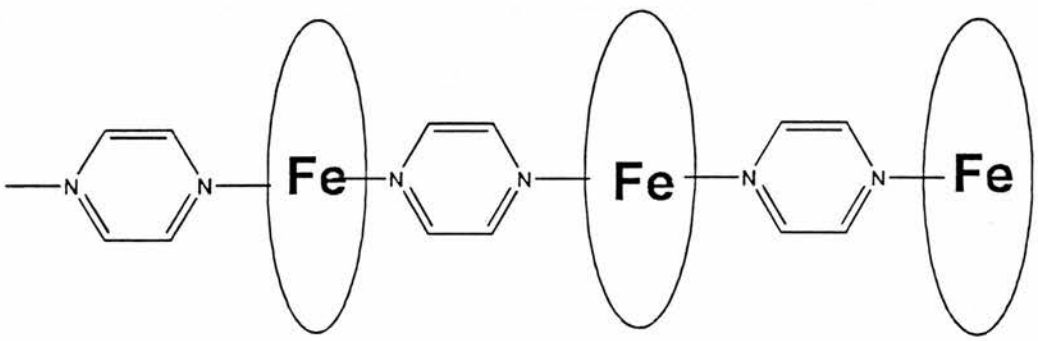

Figure 1.21 *Polymeric Fe^{II}(TMTAA) complex*

Ni^{II}(TMTAA),[58] Cu^{II}(TMTAA)[59] and VO(TMTAA)[54] can also form molecules containing two metal ions. When electrochemically oxidised they form a dication (Figure 1.22) which forms a neutral dimer in basic conditions.

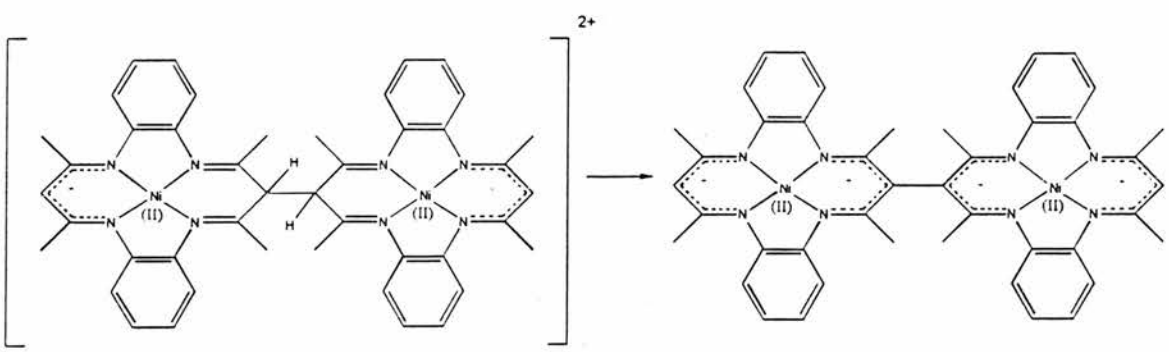

Figure 1.22 *Electrochemically induced dimers.*

Finally, a dimolybdenum complex uses a TMTAA molecule as a bridging ligand (both metals coordinated) producing unusually short Mo-Mo bond lengths.[60]

All these different metals and shapes have generated great interest and numerous uses for the interesting characteristics are being developed.

Bailey *et al.*[59] used Co^{II} and Cu^{II} tetraazaannulenes as models for the active site in metalloproteins: myoglobin, haemoglobin and copper-zinc superoxide dismutase. They succeeded in forming a reversible complex with O_2 during electrochemical experiments. Busch *et al.*[61] also had success with a substituted Co^{II}(TMTAA) compound. The demand for an efficient reversible O_2 binding complex comes from several quarters: portable devices to provide oxygen rich atmospheres in the treatment of certain medical conditions, underwater breathing apparatus and even as temporary whole blood substitutes.[62]

Workers have reported catalytic behaviour from some of these compounds. After examining the redox properties in solution,[63] and on surface modified electrodes[58] Bailey *et al.* reported evidence of catalytic CO_2 reduction to formate by Ni^{II}(TMTAA).[64] Such reductions would be easily accessible were it not for the large overvoltage required to drive this reaction electrochemically. Ni^{II} tetraazaannulene surface modified electrodes were found to catalyse the oxidation of water, methanol, ethanol, and propanol.[65] Ru^{II}(TMTAA) was found to catalyse the hydrogenation of unsubstituted alkenes[66] and Co^{II} tetraazaannulene has been used as a O_2 reduction catalyst at the cathode in fuel cells.[67] It is only a matter of time before the properties of the compounds are tailored to meet the needs of industry and electrochemists.

Adams *et al.*[68] are using tetraazaannulenes covalently bonded to electron acceptors as the basis for models of organic superconductors and light induced electron

transfer. Iodine-doped Ni and Cu tetraazaannulenes were found to be molecular conductors.[69-72] On partial oxidation the structures of highly conducting metal complexes are normally changed to a stacking pattern where the molecular planes are perpendicular to the stacking direction. This can result in short M-M bond lengths with the possibility of interaction.[73] However, with ditolyl substituents these compounds were found to be the first transition metals to be highly conducting when in a slipped stack configuration, where the molecular plane is not perpendicular to the stacking direction. This is because oxidation takes place on the ligand rather than the metal and conduction occurs because of the overlap of ligand π orbitals and is independent of stacking angle. Hunziker has developed this into lithium iodide batteries based on a metal dibenzotetraazaannulene iodine charge transfer complex.[74] The electronic properties of tetraazaannulenes and their metal complexes compounds have been investigated[75-77] and it was found that the π system was localised in the phenyl and diimine regions of the molecule. The in plane π-π^* transitions dominate the electronic spectra.

Tetraazaannulene is the core molecule in several investigations of electroactive Langmuir Blodgett (LB) films.[78,79] Substituted Ni^{II} and Cu^{II} complexes have been prepared which form stable semiconducting LB films. These are being tested for use as sensors for environmental gases. Sensors have already been prepared, by vacuum sublimation of tetraazaannulene ligands and complexes, which are sensitive to hydrochloric acid, nitrogen dioxide and nitrogen tetroxide.[80] These compounds have even been used as copolymers in non linear optical materials.[81]

1.5 Solid state NMR

The compounds which will be described in the subsequent chapters display crystalline transitions as well as LC transitions. The tetraazaannulene macrocyclic ligands on which they are based also have internal molecular motion as the protons migrate around the four N atoms. Solid state NMR is a powerful tool for investigating chemical structure and dynamics in the solid state. When molecules do not form crystals large enough for X-ray crystallography and are unsuitable for X-ray powder diffraction, solid state NMR can reveal much about the structure in the solid state. It can also be used in conjunction with the above methods give great insight into the underlying chemistry.

Nuclear magnetic resonance was once the province of physicists and the Nobel Prize for Physics was awarded jointly to Felix Bloch and Edward M. Purcell in 1952 for their pioneering work in this field.[82] It is chemists however, who have benefited most from its discovery and development. Today it is the most valuable spectroscopic technique for elucidating chemical structure in solution. It is only in the last twenty years that this technique has been expanded to include solids.

On the atomic level angular momentum is quantized, and so has discrete values. These values are vector quantities possessing a magnitude and direction. In NMR the angular momentum of certain atomic nuclei are examined in a magnetic field. Motion of a charged body has an associated magnetic field, the angular momentum of the nuclei produce a magnetic moment and as the angular momentum is quantized, so is the magnetic moment. Spin angular momentum for different constituents of the nucleus combine to give a spin quantum number. For ^{1}H and ^{13}C the spin quantum number **I** is ½ but for other atoms can take values of integral, a half, or zero. In a magnetic field the

magnetic moment generated by the angular momentum can take up 2**I**+1 orientations. Spin ½ therefore have two possible orientations in a magnetic field, a high and low energy configuration. Essentially NMR is the transition between these energy levels induced by electromagnetic radiation. Because each nucleus in a molecule is also affected to a different extent by the electron density from nearby atoms the resonance frequency is dependent on molecular environment. The relative number of nuclei in the high and low energy state at any give time can be calculated by the Boltzman distribution:

$$N_\beta/N_\alpha = \exp(-\Delta E/kT)$$

As the two populations are not equal there is a small overall magnetic moment in one direction. In the two energy states the magnetic moment precesses in a cone shape around the direction of the magnetic field. If subjected to a strong pulse of electromagnetic radiation for a certain amount of time, to generate an oscillating magnetic field perpendicular to the static magnetic field (B_o), the magnetic moments of the nuclei are tipped through an angle. By carefully selecting the time duration of the electromagnetic radiation, the magnetic moments of the nuclei can be made to precess at 90° to the static magnetic field (Figure 1.).

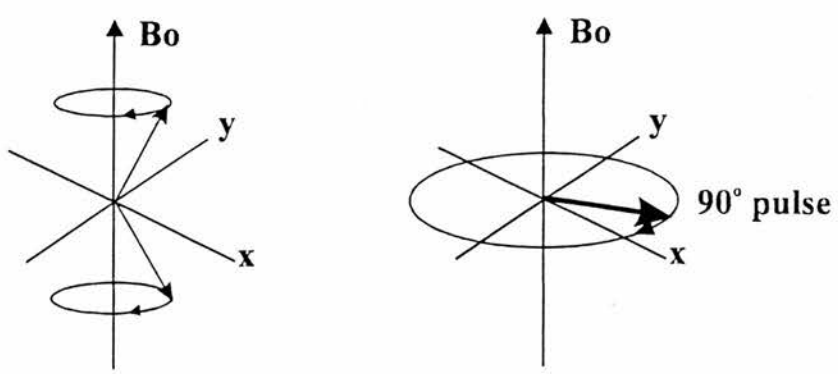

Figure 1.23 *90° pulse changes the precession of magnetic moment*

As they relax back to equilibrium, with the energy dissipated to the lattice, the oscillation is detected by a receiver coil. This free induction decay lasts a few seconds and consists of all the nuclei in different chemical environments. The complicated wave pattern produced can be converted into a spectrum by Fourier analysis.[83,84]

The most obvious difference between NMR of solutions and solids is the line-widths of the resonances. Solution resonances have linewidths of < 1 Hz whereas those in the solid have line widths of tens of kHz.[85] This is due to direct dipolar interactions, nuclear spins acting as magnets, and the dependence of shielding constants on orientation. Experimental techniques have been developed to simulate the averaging motion of liquids and overcome other inherent problems.

Magic-angle spinning and cross polarisation are two of the most important of these techniques.[86] The powder of amorphous solids contain molecular groups which are orientated in every direction, giving rise to a large number of chemical shifts and a broad resonance. The motion in a solution reduces the shielding to the isotropic value in addition to removing dipolar interactions. All the relevant anisotropic magnetic interactions have the term,

$$(3\cos^2\theta-1)$$

where θ is the angle between the symmetry axis and the static magnetic field. When this function is made equal to zero the anisotropic effects disappear. This is achieved by rotating the sample at an angle of 54°44' to the static magnetic field. This is known as the magic angle.[87]

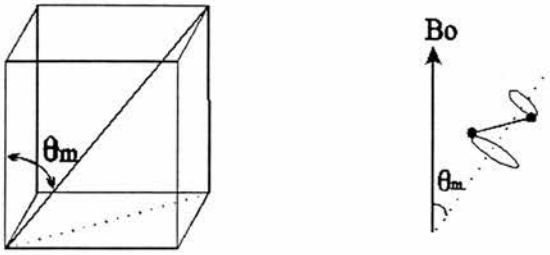

Figure 1. 24 Interacting spins rotating around the magic angle

The magic angle is the angle between opposing vertices of a cube. Three orthogonal directions in space are averaged in this way. When the sample is spun around this angle to the static magnetic field, each pair of interacting spins are also spun around the magic angle θ_m. The average direction experienced by all the spin pairs is thus θ_m 54°44'. The term $(3\cos^2\theta-1)$ is now zero and all interactions containing this term become zero.

Provided the rotation rate is greater than the linewidths, dipolar couplings are also averaged out by magic angle spinning. However dipolar couplings are often 50 kHz or more and rotation cannot remove them completely. These interactions can be removed by decoupling. If a nucleus has a neighbour which is changing its spin state rapidly the nucleus is only experiencing an average of all the states of its neighbour. In ^{13}C the neighbouring nuclei are normally ^{1}H which can be irradiated with a frequency which will cause all ^{1}H to exchange between spin states. This leaves a simple decoupled signal for the ^{13}C. The powers necessary to enable this state in solids are orders of magnitude greater than solution.

For dilute spins such as ^{13}C spectral broadening due to dipolar interactions are not the only problem in achieving solid state spectra. Spin-lattice relaxation times can also be very long, making multipulse experiments inefficient. The technique of cross polarisation has been developed to enable experiments to be conducted in a reasonable

time period.[88] Under the appropriate conditions magnetisation flows from protons to ^{13}C during the contact time. Protons are much more abundant and possess a stronger spin polarisation than ^{13}C. The protons are spin locked into the xy, plane then the ^{13}C spin is irradiated and the amplitude of the magnetic field B_1 at right angles to the static magnetic field B_o is adjusted so that the Hartmann-Hahn matching condition is fulfilled.

$$\gamma_c B_{1c} = \gamma_H B_{1c}$$

where γ_c and γ_H are the magnetogyric ratios (the ratio of the magnetic moment to the angular momentum) and B_1 is the appropriate field strength. Both nuclei now have the same resonance frequency and exchange of magnetisation is allowed. The shorter relaxation times of the protons will now determine the recycle rate of the experiment.

When combined these methods produce spectra for solid state samples which while not quite as good as solution is a vast improvement on early attempts. Because the physical and chemical properties of solids differ from those in solution specialised techniques have had to be developed to investigate this state. Solid state NMR is amongst the most useful of these techniques. When combined with non quaternary suppression and variable spinning rate (to identify spinning side-bands) the spectra can be assigned with confidence and the solid state chemistry probed.

The following chapters will describe how various tetraazaannulenes were synthesised and modified into LC shaped compounds by the addition of flexible aliphatic chains. The synthetic strategies are detailed and the respective chemical properties investigated, for a range of chain lengths in each case. The tautomeric processes involved in the tetraazaannulene ligands are also investigated, in the final chapter, by variable temperature solid state NMR.

References

1 F. Reintzer, *Monatsh. Chem.*, 1888, **9**, 421.

2 P. J. Collins, *Liquid Crystals - Natures Delicate Phase of Matter*, Adam Hilger, Bristol, 1990.

3 A. M. Giroud-Godquin and P. M. Maitlis, *Angew. Chem. Int. Ed. Engl.*, 1991, **30**, 375.

4 A. M. Guinier, *The Structure of Matter*, Edward Arnold, London 1984.

5 P. Espinet, M. A. Esteruelas, E. Sola, L. A. Oro, and J. L. Serrano, *Coord. Chem. Rev.*, 1992, **117**, 215.

6 A. Walton, *Three States of Matter*, OUP, 1983.

7 S. Chandrasekhar, B. K. Sadashiva and K. A. Suresh, *Pramana*, 1977, **9**, 471.

8 H. Kelker and B. Scheurle, *Angew. Chem. Int. Ed. Engl.*, 1969, **8**, 884.

9 M. Schadt and W. Helfrich, *J. App. Phys. Lett.*, 1971, **18**, 127.

10 C. Mauguin, *Bull. Soc. Fr. Miner.*, 1911, **34**, 71.

11 M. F. Toney, T. P. Russell, J. A. Logan, H. Kikuchi, J. M. Sands and S. K. Kumar, *Nature*, 1995, **374**, 709.

12 T. Ikeda, T. Sasaki and K. Ichimura, *Nature*, 1993, **361**, 428.

13 D. W. Bruce, D. A. Dunmur, P. M. Maitlis, M. M. Manterfield and R.Orr, *J. Mater Chem.*, 1991, **1**, 255.

14 D. W. Bruce, D. A. Dunmur, P. M. Maitlis, S. E. Hunt and R.Orr, *J. Mater Chem.*, 1991, **1**, 857.

15 H. Tokuhisa, K. Kimura S. Shinkai and M. Yokoyama, *J. Chem. Soc. Faraday Trans.*, 1995, **91**, 1237.

16 Z. Belarbi, C. Sirlin, J. Simon and J. J. Andre, *J. Phys. Chem.*, 1989, **93,** 8105.

17 J. L. Serrano, M. Marcos, P. Romero and P. J. Alonso, *J. Chem. Soc. Chem. Commun.*, 1990, 859.

18 D. Lelievre, L. Bosio, J. Simon, J. J. Andre and F. Bensebaa, *J. Am. Chem. Soc.*, 1992, **114**, 4475.

19 M. A. Esteruelas, E. Sola, L. A. Oro, M. Ros and J. L. Serrano, *J. Chem. Soc. Chem. Commun.*, 1989, 55.

20 F. Reintzer, *Monatsh. Chem.*, 1888, **9**, 421.

21 D. Vorlander, *Ber. Dtsch. Chem. Ges.*, 1910, **43**, 3120.

22 M. A. Esteruelas, E. Sola, L. A. Oro, M. B. Ros and J. L. Serrano, *J. Chem. Soc. Chem. Commun.*, 1955, 55.

23 M. A. Esteruelas, E. Sola, L. A. Oro, M. Marcos, M. Ros and J. L. Serrano, *J. Organomet. Chem.*, 1990, **387**, 103.

24 D. W. Bruce, D. A. Dunmur, P. M. Maitlis, P. Styring, M. A. Esteruelas, E. Sola, L. A. Oro, M. Ros and J. L. Serrano, *Chem. Mater.*, 1989, **1**, 479.

25 M. Marcos, P. Romero and J. L. Serrano, *J. Chem. Soc. Chem. Commun.*, 1989, 1641.

26 S. Chandrasekhar, B. K. Sadashiva, S. Ramesha and B. S. Srikanta, *Pramana.*, 1986, **27**, L713.

27 Y. G. Galyametdinov, D. Z. Zakieva and I. V. Ovchinnikov, *Izv. Akad. Nauk. SSSR Ser. Khim.*, 1986, **2**, 491.

28 U. T. Muller-Westerhoff, A. Nazzal, R. J. Cox and A. M. Giroud, *J. Chem. Soc. Chem. Commun.*, 1980, 497.

29 C. Piechocki, J. Simon, A. Skoulios, D. Guillon and P. Webber, *J. Am. Chem. Soc.*, 1982, **104**, 5245.

30 P. Espinet, J. Etxebarria, M. Marcos, J. Perez, A. Remon and J. L. Serrano, *Angew. Chem. Int. Ed. Engl.*, 1989, **28** 1065.

31 O. Poizat, D. P. Strommen, P. Maldivi, A. M. Giroud-Godquin and J. C Marchon, *Inorg. Chem.*, 1990, **29**, 4851.

32 J. Bhatt, B. M. Fung, K. M. Nicholas and C. D. Poon, *J. Chem. Soc. Chem. Commun.*, 1988, 1439.

33 A.-M. Giroud-Godquin and A. Rassat, *C. R. Seances Acad. Sci. Ser.*, 1982, **294**, 241.

34 H. Adams, N. A. Bailey, D. W. Bruce, R. Dhillon, D. A. Dunmur, S. E. Hunt, E. Lalinde, A. A. Mags, R. Orr, P. Styring, M. S. Wragg and P. M. Maitlis, *Polyhedron*, 1988, 1861.

35 A. B. Blake , J. R. Chipperfield, S. Clark and P. G. Nelson, *J. Chem. Soc. Dalton Trans.*, 1991, 1159.

36 D. W. Bruce, A. Thornton, B. Chaudret S. Saboetienne, T. L. Axon and G. M. Cross, *Polyhedron*, 1995, **14**, 1765.

37 L. F. Lindoy, *The Chemistry of Macrocyclic Ligand Complexes*, Cambridge, 1989.

38 D. Shriver, P. W. Atkins and C. Langford, *Inorganic Chemistry*, OUP, 1990.

39 R. W. Hay, *Bio-Inorganic Chemistry*, Horwood, Wiley, Chichester, 1984.

40 J. P. Collman, R. R. Gagne, H. B. Gray and J. W. Hare, *J. Am. Chem. Soc.*, 1974, **96**, 6522.

41 J. Almog, J. E. Baldwin, R. L. Dyer and M. Peters, *J. Am. Chem. Soc.*, 1975, **97**, 226.

42 M. J. Kendrich, M. May, M. Plishka and K. Robinson, *Metals in Biological Systems*, Ellis Horwood, 1992.

43 D. H. Busch, *Acc. Chem. Res.*, 1978, **11**, 392.

44 M. Micheloni and P. Paoletti, *Inorg. Chim. Acta*, 1980, **43**, 109.

45 N. F. Curtis, Y. M. Curtis and H. K. J. Powell, *J. Chem. Soc. A.*, 1966, 1015.

46 M. G. Reen, J. Smith and P. Tasker, *Inorg. Chim. Acta*, 1971, **5**, 17.

47 F. A. Cotton and J. Czuchajowska, *Polyhedron*, 1990, **9**, 2553.

48 E. G. Jäger, *Z. Anorg. Chem.*, 1969, **364**, 177.

49 V. L. Goedken and J. A. Ladd, *J. A. Chem. Soc. Chem. Commun.*, 1982, 142.

50 V. L. Goedken, S. M. Peng, J. Molin-Norris and Y Park, *J. Am. Chem. Soc.*, 1976, **98**, 8391.

51 L. G. Bell and J. C. Dabrawiak, *J. Chem. Soc. Chem. Commun.*, 1975, 512.

52 F. A. Cotton and J. Czuchajowska, *Polyhedron*, 1990, **9**, 1217.

53 F. A. Cotton, J. Czuchajowska, L. R. Falvello and X. J. Feng, *Inorg. Chim. Acta*, 1990, **172**, 135.

54 V. L. Goedken and J. A. Ladd, *J. Chem. Soc. Chem. Commun.*, 1981, 910.

55 D. L. Davies and A. J. Grist, *Inorg. Chim. Acta*, 1994, **216**, 217.

56 M. C. Weiss, G. C. Gordon and V. L. Goedken, *J. Am. Chem. Soc.*, 1979, **101**, 857.

57 J. Koch and M. Hanack, *Chem. Ber.*, 1983, **116**, 2109.

58 C. L. Bailey, R. D. Bereman and D. P. Rillema, *Inorg. Chem.*, 1986, **25**, 933.

59 C. L. Bailey, R. D. Bereman and D. P. Rillema, *Inorg. Chem.*, 1986, **25**, 3149.

60 J. M. Kerbaol, E. Furet, J. E. Guerchais, Y. Lemest, J. Y. Saillard, J. Salapala and L. Toupet, *Inorg. Chem.*, 1993, **32**, 713.

61 D. H. Busch and S. J. Dzugan, *Inorg. Chem.*, 1990, **29**, 2528.

62 D. H. Busch, *Oxygen complexes and Oxygen Activation by Transition Metals*, Plenim Press, 1988.

63 C. L. Bailey, R. Bereman, R. Nowak and D. P. Rillema, *Inorg. Chem.*, 1984, **23**, 3956.

64 C. L. Bailey and R. D. Bereman, *Inorg. Chim. Acta*, 1986, **116**, L45.

65 D. I. Issahary, G. Ginzburg, M. Polak and D. Meyerstein, *J. Chem. Soc. Chem. Commun.*, 1982, 441.

66 L. B. Luo, E. D. Stevens and S. P. Nolan, *Inorg. Chem.*, 1996, **35**, 252.

67 B. Clauberg and G. Sandstede, *J. Electroanal. Chem.*, 1976, **74**, 393.

68 F. Adams, R. Gompper and E. Kujath, *Angew. Chem. Int. Ed. Engl.*, 1989, **28**, 1060.

69 M. Hunziker, B. Hilti and G. Rihs, *Helv. Chemica. Acta*, 1981, **64**, 82.

70 L. S. Lin, T. J. Marks, C. R. Kannewurf, J. W. Lyding, M. S. McClure, M. T. Ratajack and T. C. Wang, *J. Chem. Soc. Chem. Commun.*, 1980, 954.

71 Y. M. Wuu, S. M. Peng and H. Chang, *J. Inorg. Nucl. Chem.*, 1980, **42**, 839.

72 F. Lelj, G. Morelli, G. Ricciardi, M. Romanelli, A. Rosa and M. Ottaviani, *Polyhedron*, 1991, **10**, 1911.

73 M. Hunziker, H. Loeliger, B. Hilti and G. Rihs, *Helv. Chemica. Acta*, 1981, **64**, 2544.

74 M. Hunziker and I. Exnar, *J. Power Sources*, 1988, **22**, 69.

75 M. Casarin, E. Ciliberto, S. Di Bella, A. Gulino, I. Fragala and T. J. Marks, *Inorg. Chem.*, 1992, **31**, 2835.

76 A. Rosa, G. Ricciardi, F. Lelj and Y. Chizhov, *J. Chem. Phys.*, 1992, **161**, 127.

77 S. Bell, J. A. Crayston, T. J. Dynes, S. Ellahi and C. Smith, *J. Phys. Chem.*, 1996, **100**, 5252.

78 F. Bonosi, F. Lely, G. Ricciardi, M. Romanelli and G. Martini, *Langmuir*, 1993, **9**, 268.

79 A. Wegmann, M. Hunziker and B. Tieke, *J. Chem. Soc. Chem. Commun.*, 1989, 1179.

80 C. L. Honeybourne, R. J. Ewan and C. A. S. Hill, *J. Chem. Soc. Faraday Trans. 1*, 1984, **80**, 851.

81 L. Yu, D. W. Polis, F. Xiao, L. S. Saochak, M. R. McLean, L. R. Dalton, C. W. Spangler, T. J. Hall and K D. Havelka, *Polymer*, 1992, **33**, 3239.

82 R. K. Harris, *International Laboratory*, Dec. 1996, 32.

83 D. H. Williams and I. Fleming, *Spectroscopic Methods in Organic Chemistry 4th ed.*, McGraw-Hill, London, 1987.

84 R. K. Harris, *Nuclear Magnetic Resonance Spectroscopy*, Longman, Harlow, England, 1986.

85 M. E. A. Cudby, *European Spectroscopy News*, 1988, **78**, 18.

86 R. K. Harris, *Chemistry in Britain*, 1993, **29**, 601.

87 J. D. Wright, *Molecular Crystals*, Cambridge University Press, 1987.

88 E. A. V. Ebsworth, D. W. H. Rankin and S. Cradock, *Structural Methods in Inorganic Chemistry*, 2nd Ed, Blackwell, Oxford, 1991.

CHAPTER 2

Tetraazaannulene Precursors

2.0 Introduction

There are two types of compound which form liquid crystals: rod-like molecules which form nematic and smectic mesophases; and disc-like molecules which form discotic mesophases. Being rod or disc shaped in itself is not enough for a compound to exhibit liquid crystalline (LC) behaviour; rod-like molecules require strongly polarising groups *e.g.* aromatic rings or metals. They also require a long rigid group and several long flexible, *n*-alkyl or *n*-alkoxy tails. Disc-like molecules tend to have a flat aromatic core surrounded by several long *n*-alkyl or *n*-alkoxy chains. These characteristics must be incorporated into our molecules if LC phases are to be observed.

Having worked with tetraazaannulenes (**1** to **5**) previously, we were aware that they offered a suitable core for the LC materials, with both a rigid centre and strong polarising groups in the form of metals and aromatic rings. The advantage of these compounds is that they can easily be made to exchange the metal centre which in turn would impart widely different electronic properties to the macrocycle.[1,2] The precursors are diverse and offer a wide scope for substitution and modification of the periphery to tailor the LC complex to the optimum properties.[3-8] We also have the possibility of producing discotic and nematic LC complexes from the same family of compounds, depending on how many long chains are attached to the parent macrocycle.

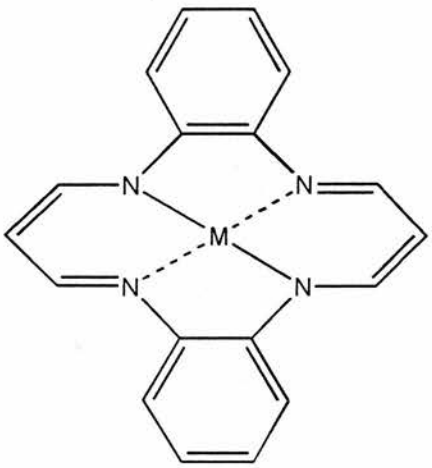

1

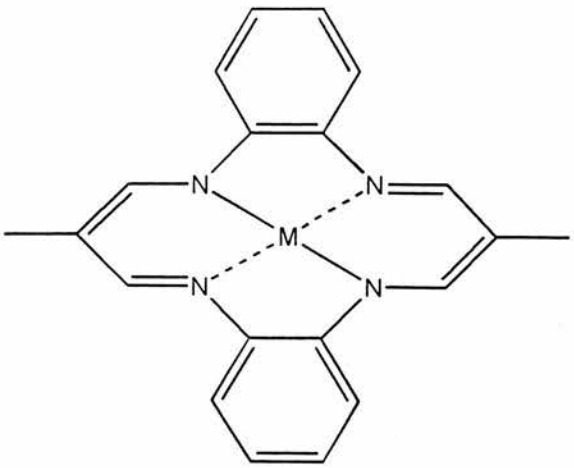

2

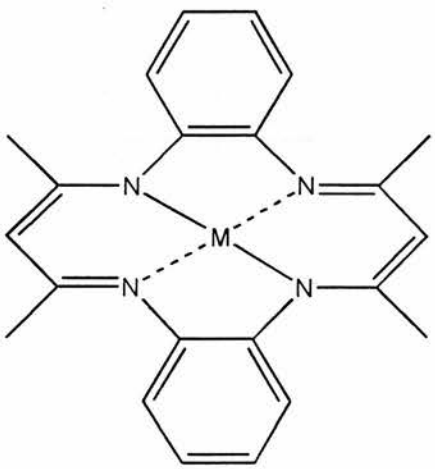

3

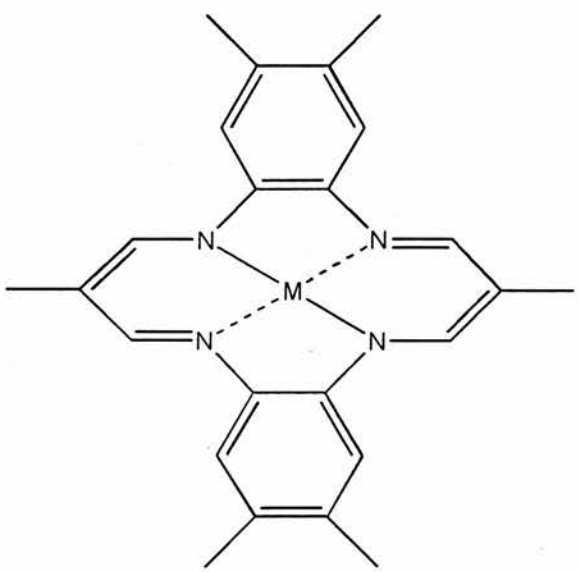

4

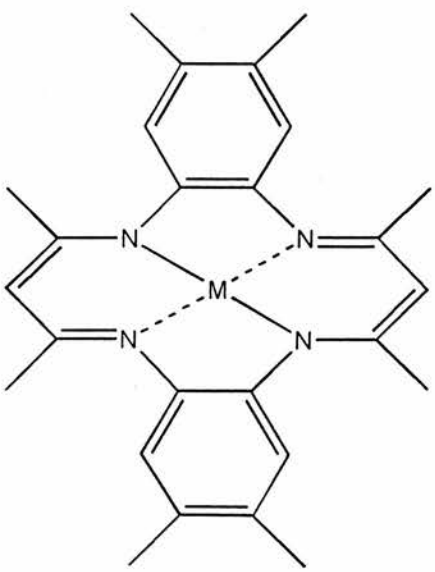

5

The primary objective was to establish a reliable method of attaching long alkyl chains of the type found in other metallomesogens to our coordinated macrocycles. Before the methods described in chapters three and four were developed several other routes were pursued. Outlined in this chapter are some of the less successful routes investigated.

2.1 Bromination

The macrocycles taken by themselves are relatively inert molecules and it was thought that to obtain interesting molecules they would have to be altered in some way to induce greater reactivity. By replacing protons with bromine atoms on the methyl groups of the macrocycle a large number of reactive sites would be created, depending on the macrocycle. These sites would then be rendered susceptible to alkylation by the Wurtz-Fittig reaction with long chain alkyl halides.[9] The best method to obtain this bromination was thought to be by using *n*-bromosuccinimide[10,11](NBS) in CCl_4 (Scheme 2.1).

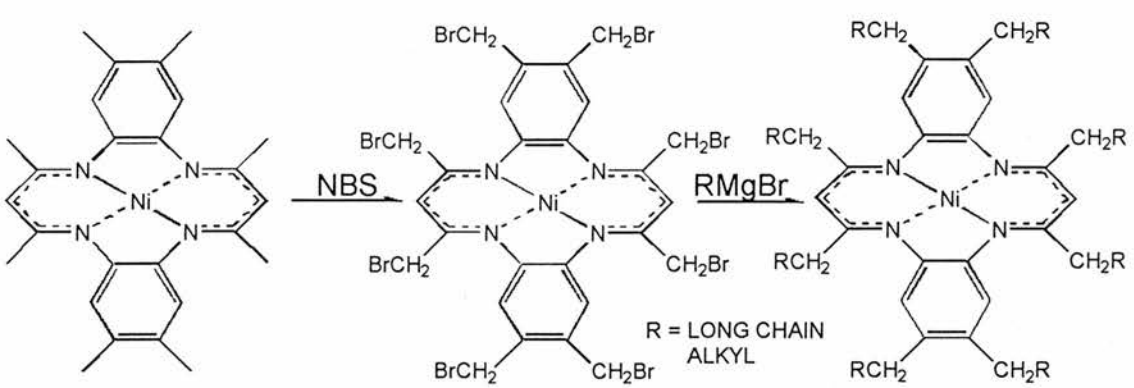

Scheme 2.1

This method consistently failed to produce the octobromosubstituted macrocycle. The bridgehead position in **5** is known to be reactive and as the compound is thermally and chemically stable it was thought that a polymer may have been formed. The starting material was changed from **5** to **4** which does not have a reactive site thus preventing bridgehead coupling. However, the black polymeric solid formed was still not the desired product and gave peaks on the FAB (Fast Atom Bombardment) mass spectrum of 1200 and above.

Stoichiometric amounts (two equivalents) of *n*-bromosuccinimide were used to attempt dibromination of **4** on the two bridgehead methyl groups most susceptible to attack (. This too failed to give a single, clean product. Thin layer chromatography revealed several different products and the FAB. mass spectra displayed high mass peaks which could not be assigned to possible product fragments. The product had no UV-vis peak at ca. 520 nm characteristic of the ligand to metal charge transfer (LMCT) Ni chromophore.

Thus this method was abandoned on the grounds that it was not producing the desired product and as the desired product was only the starting material for future reactions it was considered prudent at the time to turn our attention to different avenues.

2.2 Quaternisation of nitrogen

As previously mentioned one of the great advantages of this class of compound seemed to be the potential to replace substituents with more reactive groups. One such attempt was the replacement of the phenyl rings with pyridine rings. The pyridine rings incorporated on macrocycles can be quaternised by long chain alkyl

halides.[2] Literature preparations required amounts of alkyl halide up to 14 times molar excess which only succeeded in alkylating one of four equivalent nitrogens.

By substituting diaminopyridine for o-phenylenediamine in the macrocycle synthesis a molecule **6** was prepared which in theory could be alkylated in a manner similar to the Co porphyrin described in the literature preparation of Majda and Galen[12] (Figure 2.1).

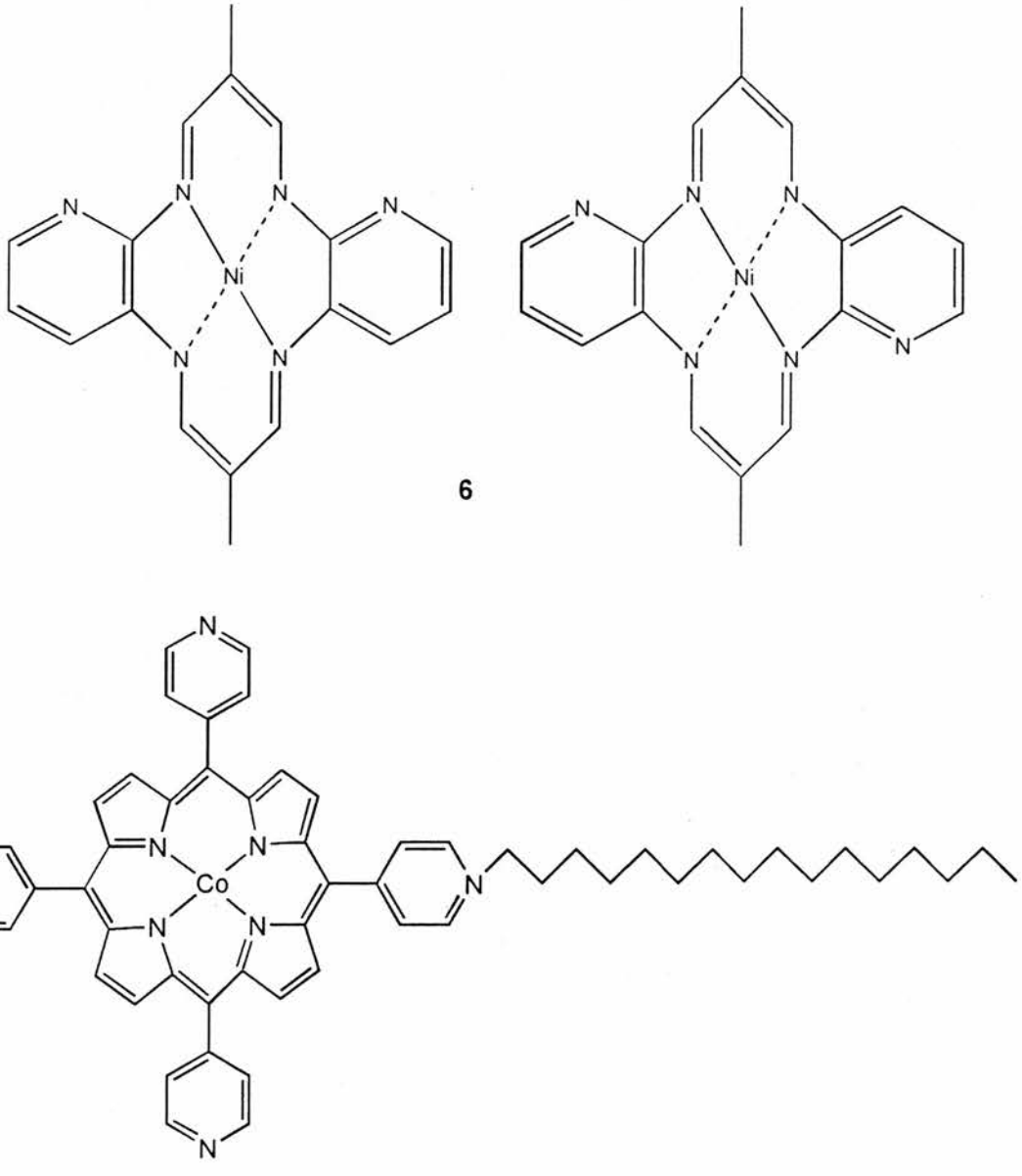

Figure 2.1

It was expected that the dication would be balanced by the association of two Br^- counter ions (Scheme 2.2).

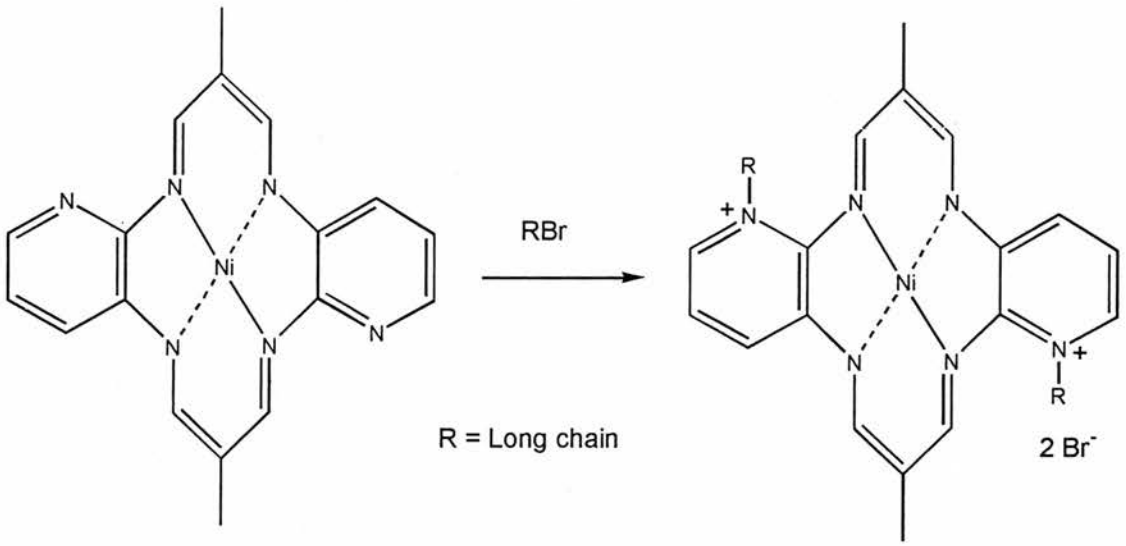

Scheme 2.2

The compound proved difficult to obtain in any degree of crystallinity or purity. FAB gave high mass peaks (592,-1179) which could not be assigned readily to possible products. The product was too insoluble for NMR (DMSO solvent), whilst UV-vis spectroscopy gives no characteristic peaks at 520 nm for the LMCT chromophore.

2.3 Phenyl and pyridyl acroleins

Attempts to modify the precursors of the macrocycles, to incorporate a long chain alkyl group, proved most successful with the acrolein family of compounds. Previously acetyl acetone **8** was used to make **3,** 3-ethoxymethacrolein **9** was used for **2,** and propargyl alcohol **10** was used to make **1.** By arranging for a long chain to be

present in the precursors at a position which did not interfere with the template reaction a liquid crystalline rod shaped molecule could be formed.

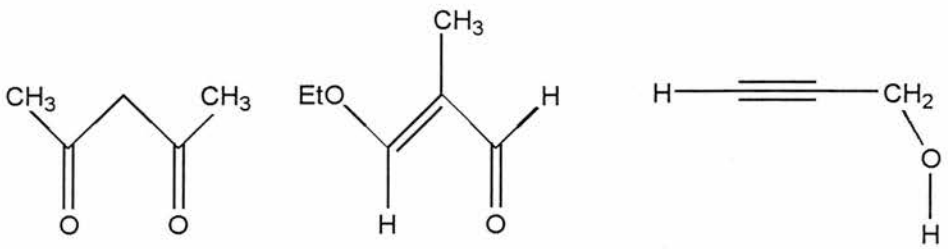

8 **9** **10**

Figure 2.2

Literature searches revealed a paper which claimed to produce 2-phenyl-3-dimethylaminoacrolein **11** and other associated compounds.[13] These compounds can be converted to the alcohol derivative **12,** but such a step would be superfluous as **11** should be able to take the place of 3-ethoxymethacrolein directly in the template. The synthesis involved utilising the Vilsmeier-Haack active electrophile[14-16] (Scheme 2.3).

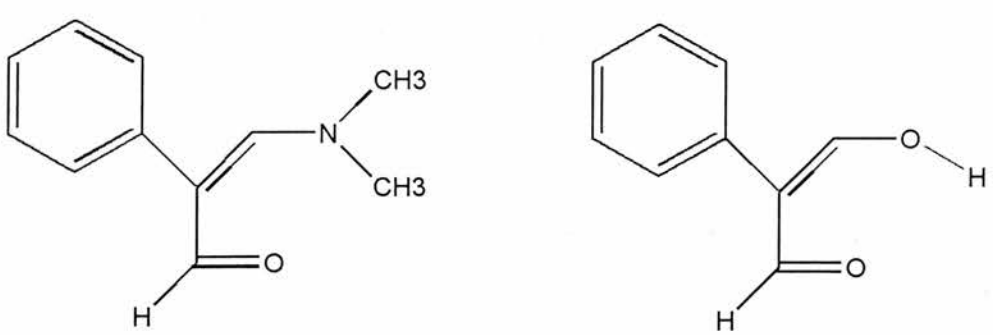

11 **12**

Unfortunately, the dimethylaminoacrolein compound **11** was reported to be a crystalline product, and considerable time and effort was expended in trying to obtain crystals. The oil which was produced turned out to be the product in quite high purity.

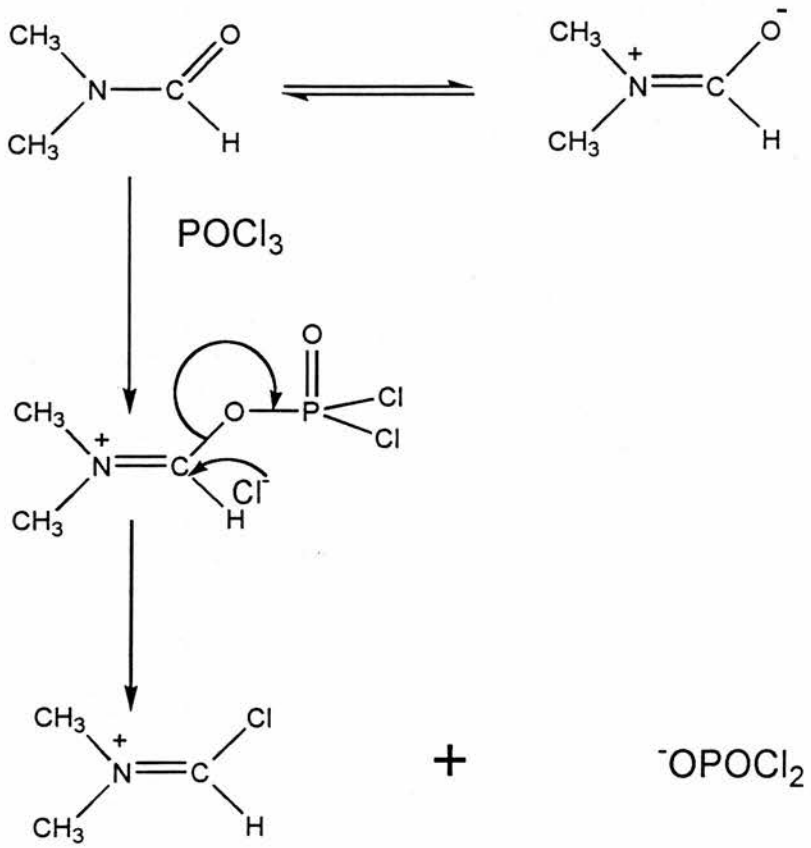

Vilsmeier active electrophile

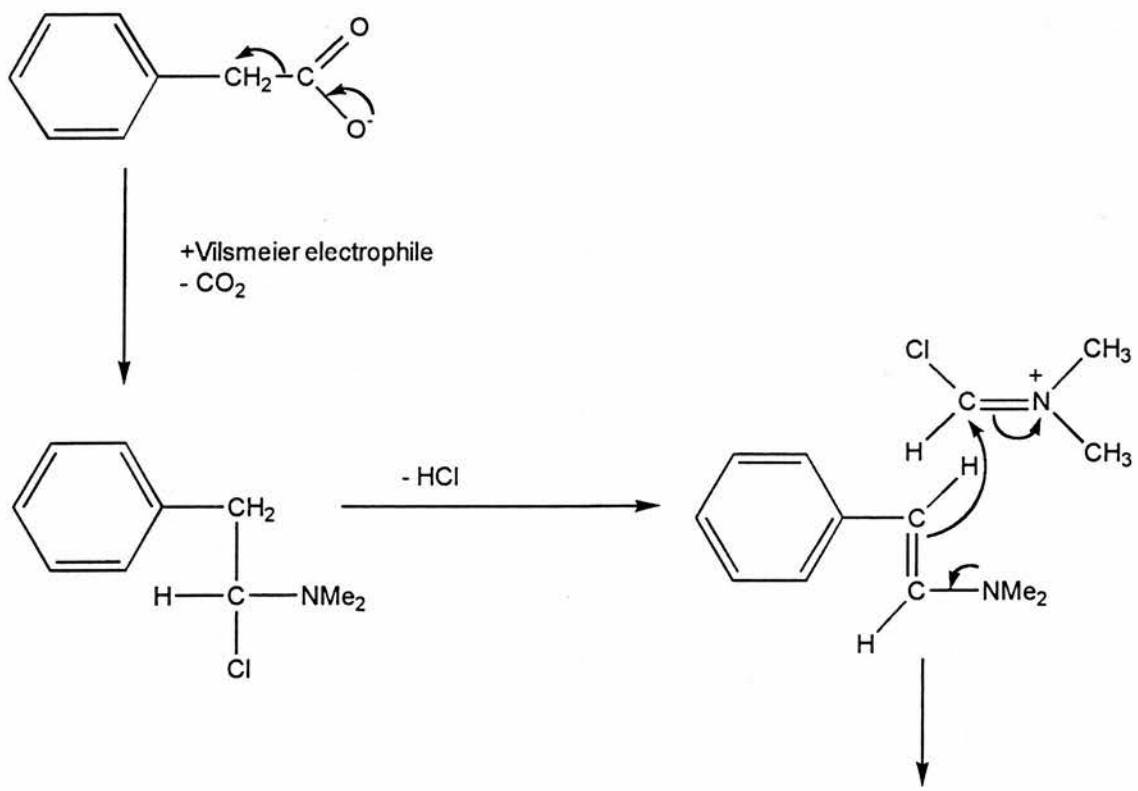

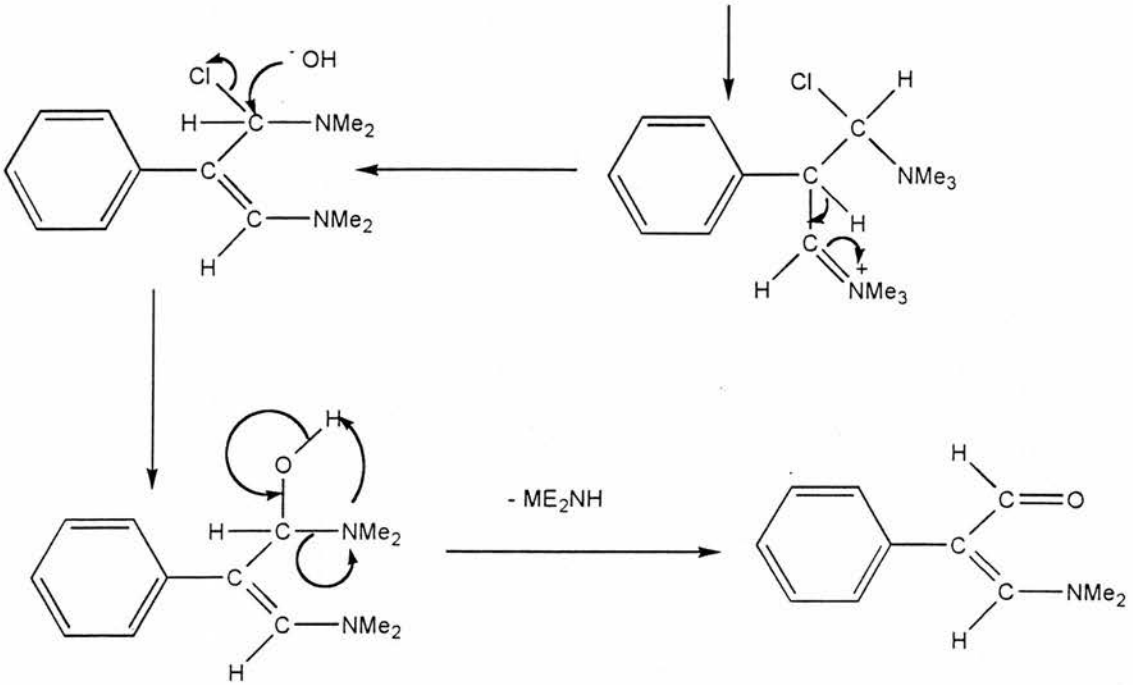

Scheme 2.3

Mass spectra and NMR confirmed that **11** had been made. The pyridine analogue of this compound 2-pyridyl-3-dimethylaminoacrolein **14** was also prepared and also would not form crystals, but gave the correct NMR and mass spectra. It was also found that simple long chain carboxylic acids and other useful compounds could be transformed in this manner[17-21] (Scheme 2.4)

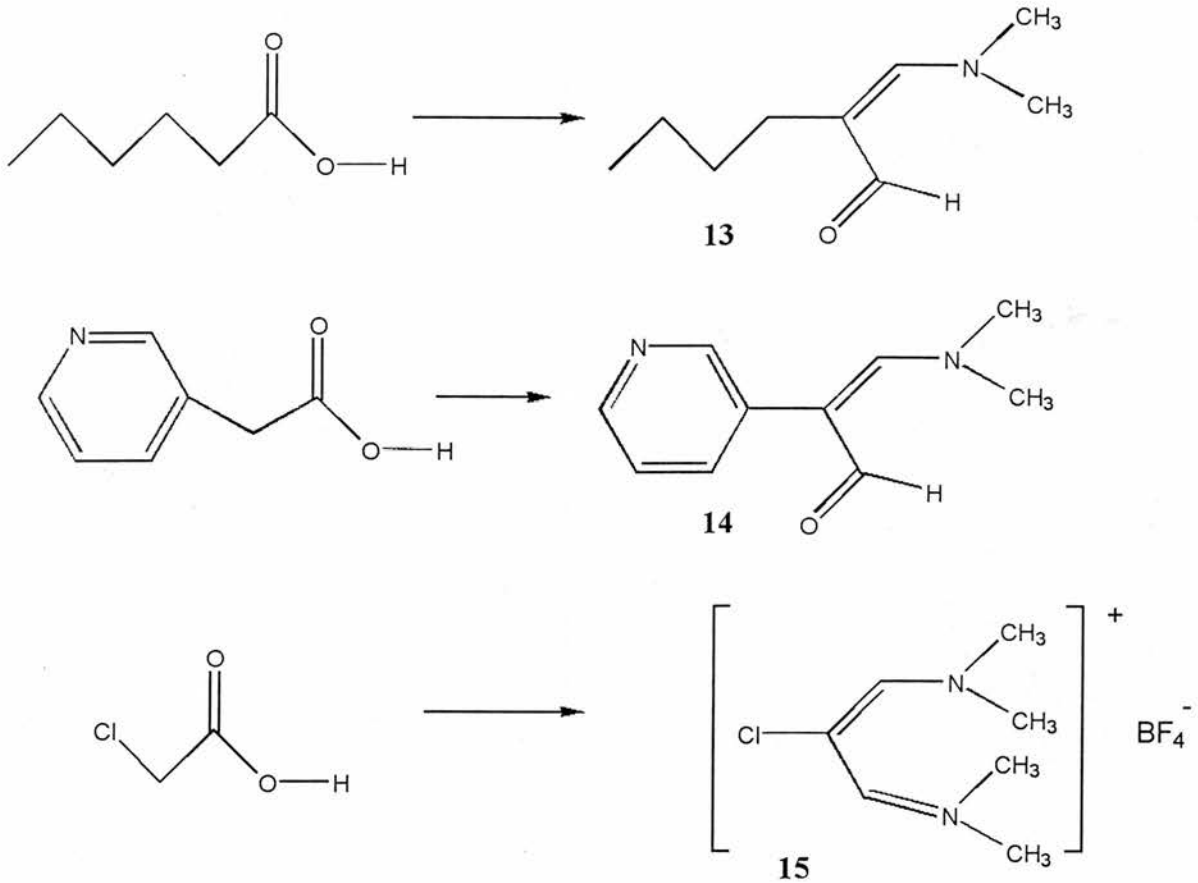

Scheme 2.4

These three precursors were being purified and made into macrocycles by reacting with nickel acetate and *o*-phenylenediamine when a European patent by Max Hunziker *et al.*[22,23] from CIBA GEIGY was discovered. They utilised a number of long chain acroleins from carboxylic acids to prepare macrocycles (Figure 2.3).

The compounds described exhibited discotic behaviour at temperatures above 130 °C. They had proposed to use these compounds as colouring agents in organic liquid crystals which would also reduce the transition temperatures. The pursuit of this line of research, therefore, came to an abrupt halt. Later work in this thesis will show that these materials, in the absence of substituents on the benzene rings, are unlikely to show nematic or smectic liquid crystalline behaviour.

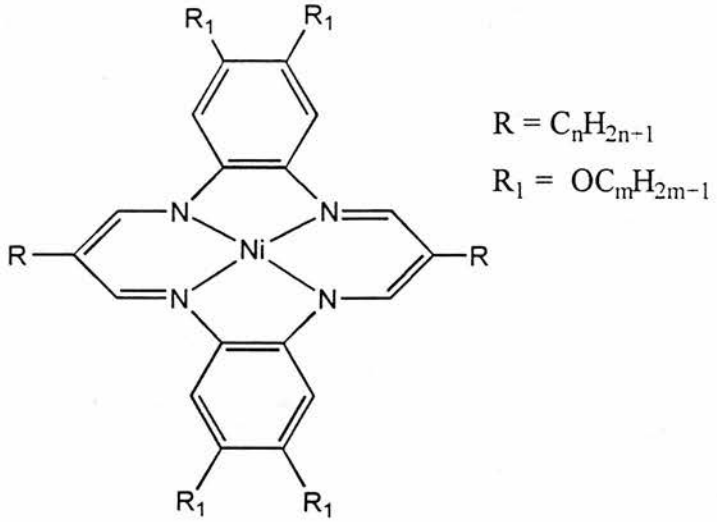

Figure 2.3

2.4 Precursor rearrangement

Other methods were used to prepare macrocycles with reactive sites, however they did not prove very successful. Despite being similar in nature to the precursors in the simple macrocycle the ring closure step has proved to be notoriously difficult for these altered compounds. Examples include[24-30](fig 2.5):

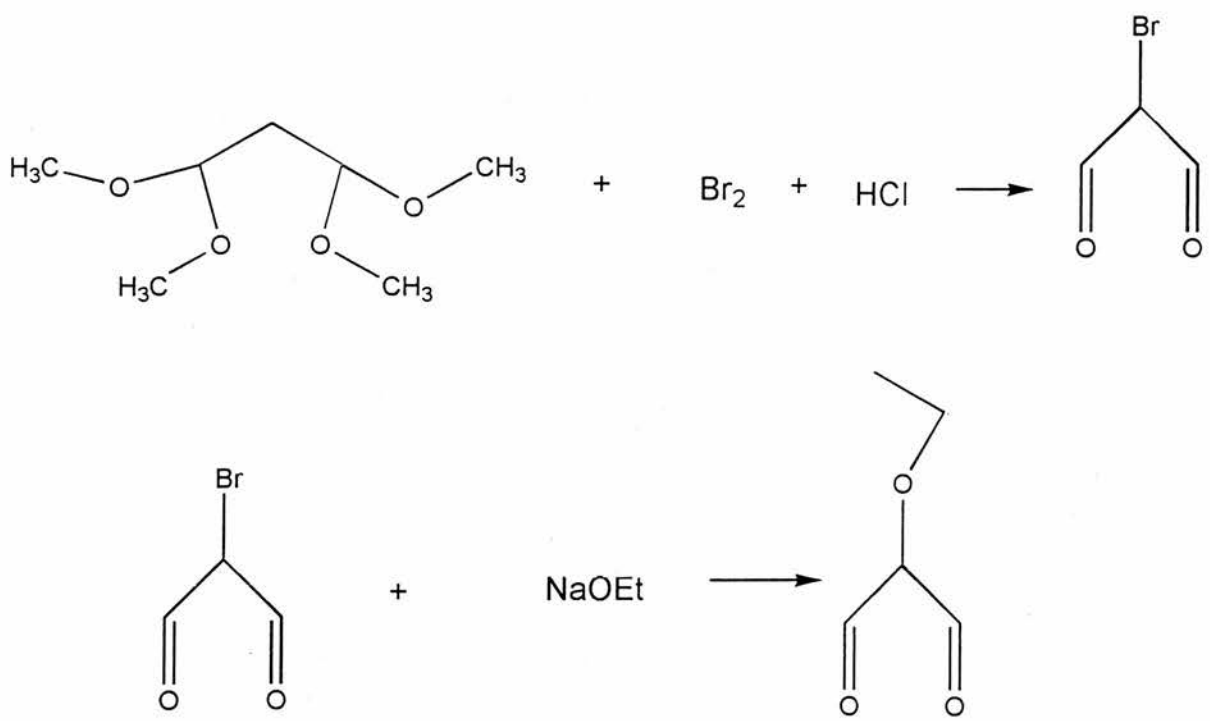

Fig 2.5

It was decided that the precursor route to the production of macrocyclic liquid crystals was not as practical as the other methods outlined in the next two chapters. Despite producing pure analogues of the reagents used in the production of the simple macrocycle, production of macrocycle derivatives was not successful. The one case we found where it was possible to use this route had already been investigated and patented by other workers.

2.4 Experimental

Solution NMR spectra were recorded using a Varian Gemini-200 spectrometer (200 MHz, ^{1}H and 50 MHz, ^{13}C). FTIR spectra were obtained with a Perkin-Elmer 1710 spectrometer and were run as KBr discs. Cyclic voltammetric data were recorded using a Pine Instruments RDE4.

Reagents containing an amine group were purified by distillation or recrystallisation prior to use. All other reagents were used without purification unless specifically stated. Solvents were dried prior to use, HPLC grade DMF was used.

[5, 7, 12, 14-Me_4-2, 3: 9, 10-Xyl_2[14] hexaenato(2-)N_4] Ni(II)- Ni **5**

Acetylacetone (Lancaster) (4.6 ml) was added dropwise into a refluxing solution of nickel acetate tetrahydrate (Aldrich) (5.5 g) and 4,5-dimethyl-*o*-phenylenediamine (Aldrich) (6 g) in DMF. This was refluxed for 6 h. The product was cooled, filtered and recrystallised from toluene. Dark blue/purple crystals (green in solution) were obtained. Yield 53 %.

$\delta_H(CDCl_3)$ 1.25 (12 H, s, CH_3), 2.05 (12 H, s, $arCH_3$), 4.8 (2 H, s, Bridgehead), 6.5 (4H, s, ar).

[6,13-Me_2-2, 3: 9, 10-Xyl_2[14] hexaenato(2-)N_4] Ni(II)- Ni **4**

3-Ethoxy-2-methylacrolein (Aldrich) (4.2 g) was added dropwise to a refluxing solution of nickel acetate tetrahydrate (Aldrich) (4.57 g) and 4, 5 dimethyl-*o*-phenylenediamine (Aldrich) (5 g) in DMF (150 ml). This was refluxed for 5 h cooled filtered and washed with acetone. Yield 44 %.

$\delta_H(CDCl_3)$ 2.2 (12 H, d, $arCH_3$), 7.0 (4 H, s, ar), 7.05 (4 H, s, iminato H).

M/z 429 (M^+).

Bromination *N*-Bromosuccinimide (1.56 g) was added to **5** (0.5 g) in refluxing carbon tetrachloride (50 ml). This was refluxed for 3 h. Black polymeric material was formed and FAB mass spectroscopy gave peaks which could not be related to the starting materials or desired product.

An intractable product was also obtained using **4.**

[6,13-Me_2-2, 3: 9, 10-dipyridyl[14] hexaenato(2-)N_4] Ni(II)- Ni **6**

2-methyl-3-ethoxyacrolein (Aldrich) (1.04 g) was added dropwise to a refluxing solution of 2,3-diaminopyridine (Aldrich) (0.3 g) and nickel acetate tetrahydrate (Aldrich) (0.34 g) in methyl benzoate 80 ml under N_2 for 9 h. The mixture was cooled and filtered and dried under vacuum. Very insoluble dark microcrystals formed. Yield 70 %. *M/z* 375 (M^+).

Alkylation of **6**

A seven-fold excess of bromotetradecane was refluxed with **6** in DMF under N_2 for 4 h. This was evaporated, washed with ether to remove bromotetradecane, dissolved in MeOH, filtered, evaporated and recrystallised from EtOH. Brown crystals were produced which were not product. FAB indicated a peak at 439 which is probably unreacted **6** solvated with two MeOH molecules. Peaks in the region of the product are very small and do not correlate to any expected values.

2-Pyridyl-3-dimethylaminoacrolein **14**

DMF (1.97 ml) was added dropwise to phosphorous oxychloride (Aldrich) (3.35 g) with the temperature held at 30 °C. Pyridylacetic acid (1 g) in DMF (8 ml) was added dropwise. The resulting solution was stirred at 70 °C for 10 h. The solution was poured onto 30 g ice and neutralised with K_2CO_3. NaOH (10 ml 50 %) was added and the temperature maintained at 50 °C until evolution of DMF had ceased. The mixture was cooled and filtered, and the filtrate was extracted with CH_2Cl_2. The brown oil did not form crystals even after CH_2Cl_2 had been removed.

The brown oil gave a *m/z* of 176 (M^+).

2-Phenyl-3-dimethylaminoacrolein **11**

This was prepared in a similar manner to **14** using phenylacetic acid (Aldrich) as the starting material. The oil formed also would not crystallise but gave an *m/z* 175 (M^+).

$\delta_H(CDCl_3)$ 2.8 (6 H, m, NCH_3) , 6.8 (1 H, s, CHN), 7.1-7.4 (5 H, m, ar), 9.0 (1 H, s, COH).

2-Butyl-3-dimethylaminoacrolein **13**

This was prepared in the same manner as **14** using hexanal (Aldrich) as the starting material. This product was purified by vacuum distillation. Yield 20 %.

$\delta_H(CDCl_3)$ 0.9 (3 H, m, CH_3), 1.3 (2 H, m, CH_2), 2.35 (2 H, m, CH_2), 3.1 (6 H, s, NCH_3), 6.5 (1 H, s, CHN), 8.8 (1 H, s, COH).

2-Chlorovinamidinium tetrafluoroborate **15**

$POCl_3$ (46 g) was added to DMF (87.7 g) stirred and cooled in an ice bath. chloroacetic acid (Fisons) (14.2 g) was added and the mixture heated at 60-100 °C for 8 h. DMF was removed, using a rotary evaporator, and $NaBF_4$ (16 g) in H_2O (60 ml) was added. After cooling the yellow solid was filtered off, washed with EtOH and recrystallised from MeOH. Yield 22 %. $\delta_H(CDCl_3)$ 2.6 (12 H, s, NCH_3), 8.6 (1 H, s, CH). M.p. 300 °C.

Macrocycles utilising **11,13,14** and **15** were being prepared and purified when this course of action was abandoned.

2-Bromomalonaldehyde

Bromine (Aldrich) (54.6 g) was added dropwise to a mixture of HCl (20 ml) H_2O (100 ml) and malonaldehyde bisdimethylacetal (Fluka) (44.8 g). This was left overnight then taken to a slush on a rotary evaporator. This was filtered to yield yellow crystals. Yield 70.9 %. *M/z* 152 (M^+).

2-Ethoxymalonaldehyde

2-Bromomalonaldehyde (1 g) was added to sodium (Fisons) (0.7 g) dissolved in dry EtOH and refluxed for 1 h. The EtOH was evaporated off, H_2O was added and the product was extracted with CH_2Cl_2 . M.p. 135 °C.

References for Chapter 2

1 V. L. Goedken and M. C. Weiss, *Inorg. Synth.*, 1980, **20,** 115.

2 F. A. Cotton and J. Czuchajowska, *Polyhedron*, 1990, **9**, 2553.

3 A. R. Cutler, C. S. Alleyne and D. Dolphin, *Inorg. Chem.*, 1985, **24**, 2276.

4 A. R. Cutler, C. S. Alleyne and D. Dolphin, *Inorg. Chem.*, 1985, **24**, 2281.

5 C. L. Honeybourne, *Inorg. Nucl. Chem. Lett.*, 1975, **11**, 191.

6 Y. Nishida, A. Sumita, K Hayashida, H. Ohshima, S. Kida and Y. Maeda, *J. Coord. Chem.*, 1979, **9**, 161.

7 D. A. Place, G. P. Ferrara, J. J. Harland and J. C. Dabrowiak, *J. Heterocycl. Chem.*, 1980, **17**, 439.

8 M. C. Weiss and V. L. Goedken,. *J. Am. Chem. Soc.*, 1976, **98**, 3389.

9 J. March, *Advanced Organic Chemistry*, McGraw Hill, London, 1968.

10 M. Hanack, A. Beck and H. Lehmann, *Synthesis*, 1987, 703.

11 M. Hanack and G. Pawlowski, *Synthesis*, 1980, 287.

12 D. A. Van Galen and M. Majda, *Anal. Chem.*, 1988, **60**, 1549.

13 G. M. Coppola, G. E. Hardtmann and B. S. Huegi, *J. Heterocycl. Chem.*, 1974, **11**, 51.

14 A. Vilsmeier and A. Haack, *Chem. Ber.*, 1927, **60**, 119.

15 E. Breitmaier and S. Gassenman, *Chem. Ber.*, 1971, **104**, 665.

16 M. R. Maheas, *Bull. Soc. Chim. Fr.*, 1962, 1989.

17 Z. Arnold, *Collect. Czech. Chem. Commun.*, 1961, **26**, 3051.

18 Z. Arnold and F. Sorm, *Collect. Czech. Chem. Commun.*, 1958, **23**, 452.

19 Z. Arnold, *Collect. Czech. Chem. Commun.*, 1965, **30**, 2125.

20 M. Keshavarz, S. D. Cox, R. O. Angus and F. Wudl, *Synthesis*, 1988, 641.

21 H. Bredereck, H. Herlinger and J. Renner, *Chem. Ber.*, 1960, **93**, 230.

22 M. Hunziker, A. Wegmann, and B. Tieke, (CIBA-GEIGY), EP0341201 A2.

23 M. Hunziker, (CIBA-GEIGY), EP0162804 A1.

24 C. L. Honeybourne, *Chem. and Ind.*, 1975, 350.

25 C. L. Honeybourne, M. Gery and B. B. Wayland, *Inorg. Synth.*, 1978, **18**, 49.

26 C. E. Dalgliesh, A. G. Long and G. J. Tyler, *Chemistry of Carbon Compounds*, E. H. Rodd, **1b**, 1012.

27 A. Brandstrom and U. Junggren, *Acta Chem. Scand.*, 1969 **23**, 3585.

28 J. H. Clark and J. M. Millar, *J. Chem. Soc. Perkin Trans. 1*, 1977, 1743.

29 E. G. Jäger, *Z. Anorg. Allg. Chem.*, 1965, **337**, 80.

30 C. L. Mao, F. C. Frostick, E. H. Man, R. M. Manyik, R. L. Wells and C. R. Hauser, *J. Org. Chem.*, 1969, **34**, 1425.

CHAPTER 3

Diazotisation of Tetraazaannulenes

3.0 Introduction

Macrocyclic complexes have been studied in a wide range of molecular electronics applications, including liquid crystals,[1-6] novel electronic conductors[7-10] and monolayer films.[11-15] There has also been interest in the modification of electrode surfaces by macrocycle complexes in order to exploit their useful redox properties.[16-18] In this section the synthesis of a number of tetraazaannulene compounds is described prior to their conversion into liquid crystalline type molecules.

Diazo compounds have long been known for their liquid crystalline behaviour. For example, diazophenyl compounds such as **1** have nematic and smectic phase transitions. As the length of the organic chains are increased the corresponding transition temperatures decrease. The example shown is a member of the *p*-azoxyanisole (PAA) series of compounds. PAAs were one of the earliest liquid crystals series discovered and made a significant contribution to the development of this field.[19]

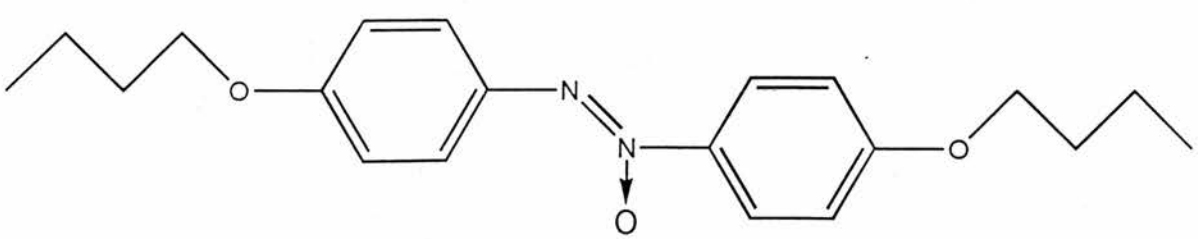

1

Other compounds of almost identical structure but with a straightforward diazo linkage also exhibit liquid crystal transitions.[20] This class of compounds is easy to prepare, relying on the fact that an amine group attached to an aromatic ring can be converted to a diazonium salt. This salt acts as a weak electrophile and can be used as a coupling reagent to compounds with nucleophilic sites (*e.g.* phenoxide anions) to produce brightly coloured azo-dyes[21] (Scheme 3.1).

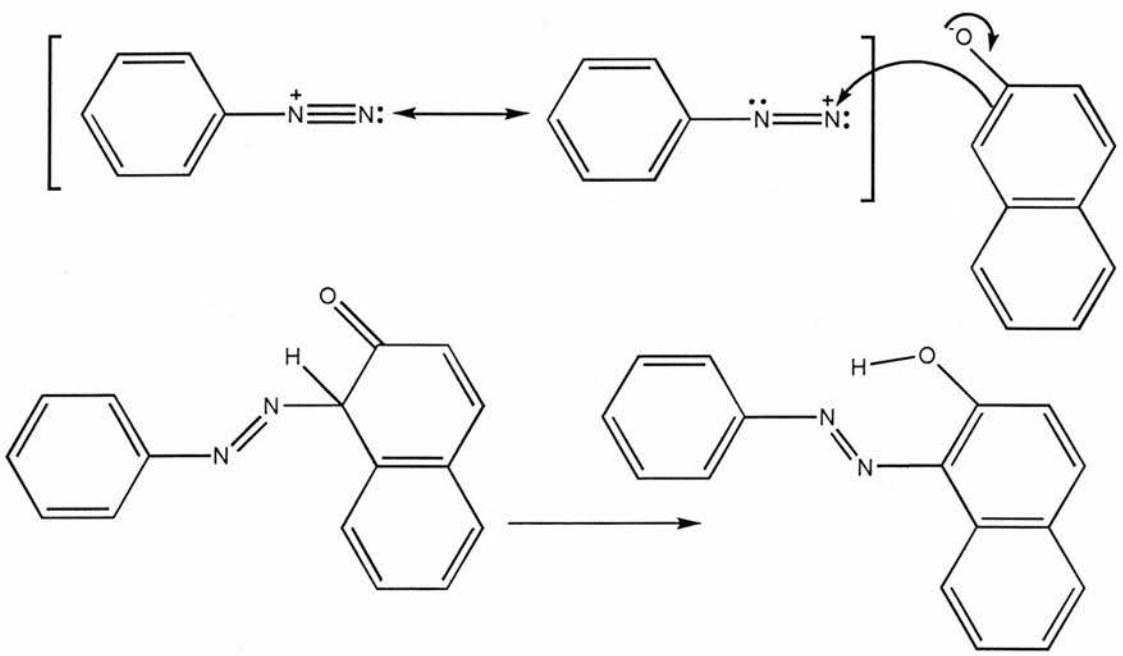

Figure 3.1 *Synthesis of Benzeneazo-2-naphthol a bright red azo dye by electrophilic aromatic substitution.*

The intense colours displayed by these compounds are due to the azo linkage which brings the two aromatic rings into conjugation. This extended system of delocalised π electrons allows absorption of light in the visible region of the electromagnetic spectrum. The coupling reaction is a simple electrophilic aromatic substitution; however, it must be carried out at low temperatures to prevent the decomposition of the diazonium salt. The explanation of the high instability of the

diazonium salt lies in the great stability of N_2 which is formed by the breakdown. The diazonium salt is generally formed *in situ*, as attempted isolation of the solid form carries the risk of detonation. The amine is converted to a diazonium salt at 0°C in acidic conditions by the addition of sodium nitrite[22] according to Scheme 3.2.

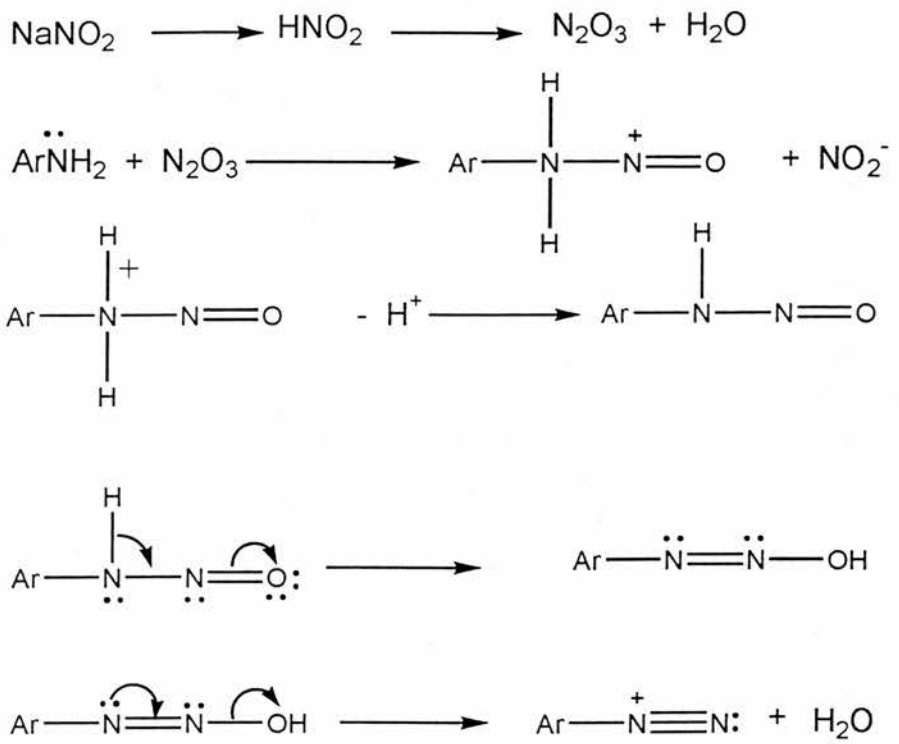

Scheme 3.2

Diazo compounds also have interesting photochemical properties, isomerising from the stable *trans* isomer at room temperature to the less stable *cis* form under irradiation. The dibenzotetramethyltetraazaannulene (TMTAA) **2** has previously been diazotised.[23] Dabrowiak *et al.*[24-28] in an effort to introduce substituents into unsaturated macrocyclic Schiff bases such as TMTAA, noted that they were susceptible to attack by various electrophilic reagents at the bridgehead position. They had problems with purification and could only isolate the bis(*p*-chlorophenyldiazo)TMTAA and the Ni complex thereof. The solubility of the Ni complex was so low that an NMR spectrum could not be obtained

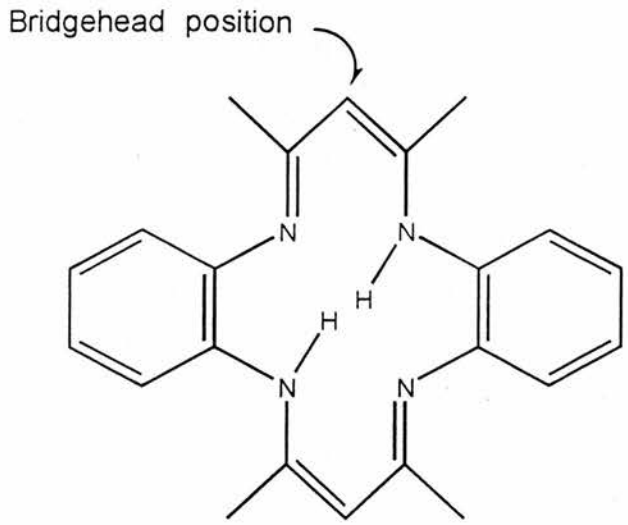

2

An interesting feature of their research was the observation that the ligand existed as a tautomer with a hydrozone linkage (Figure 3.2) and as such gave two peaks for CH_3 groups in the solution ^1H NMR spectrum.

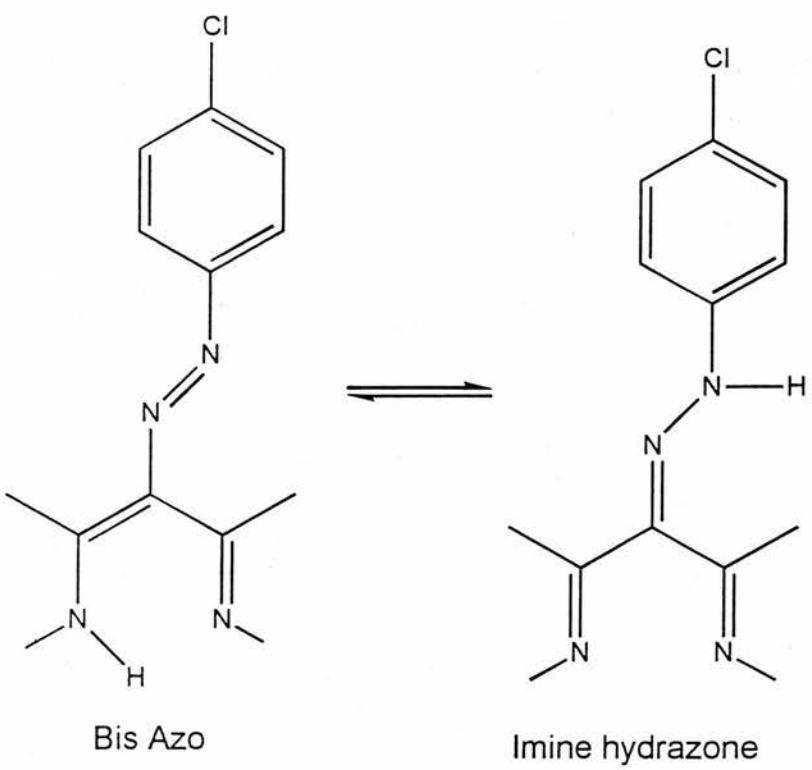

Figure 3.2

They reported that other reagents such as phenyldiazo and *p*-nitrophenyldiazo salts may have formed complexes but could not be purified. In this chapter we describe

the first attempts at using the diazo coupling to prepare potentially liquid crystalline metal tetraazaannulene complexes **3**.

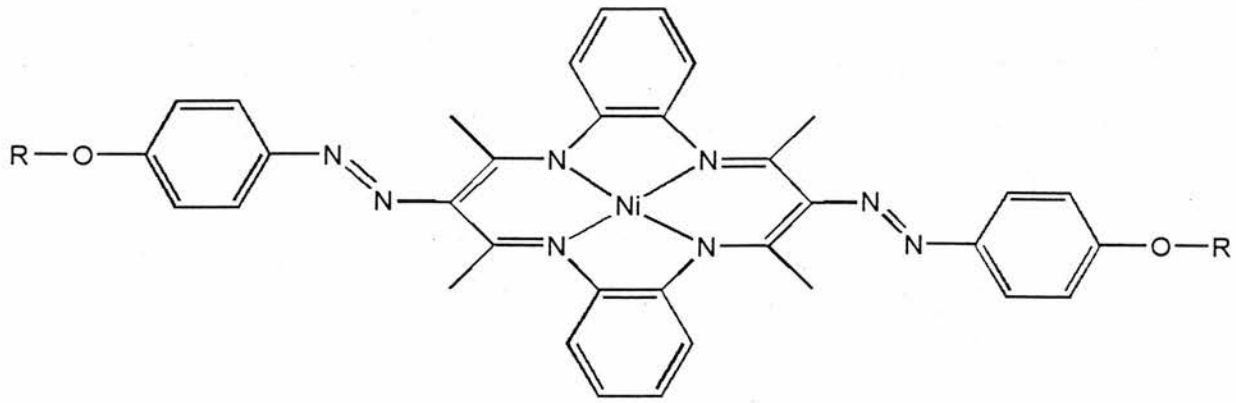

3

It will be demonstrated that the synthesis of such materials is relatively straightforward for the dibenzo compounds. However, these compounds were not liquid crystalline, instead they appeared to undergo unusual glass to crystalline transitions. This behaviour may be associated with the bulkiness of the molecules[29] (*i.e.* the benzene side groups interfere with molecular packing). We then proceeded to prepare for the first time diazo derivatives of other tetraaza macrocycles **8**.

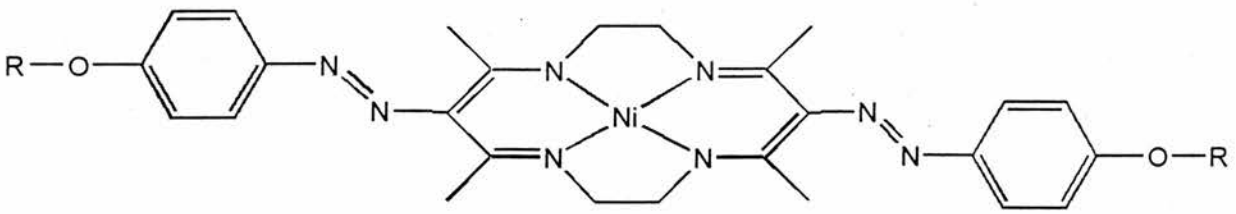

8

The thermal behaviour of these materials will be compared to the dibenzo derivatives. Finally, in order to optimise the liquid crystalline properties we sought to dispense entirely with the methyl groups on the macrocycle to give the ultimate rod-like macrocycle **5**.

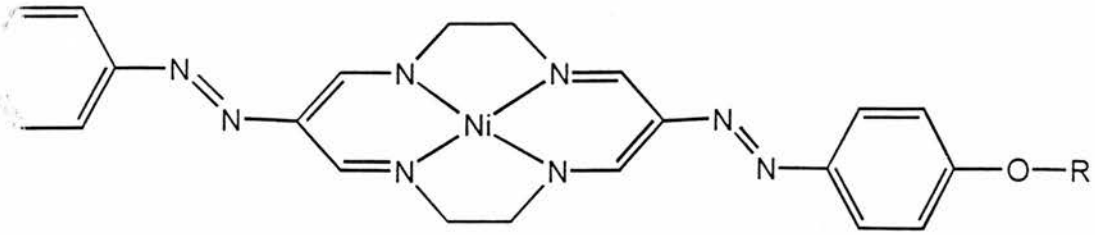

5

the unsubstituted members of the family have been shown to be planar,[30] ...yltetraazaannulene complex, which proved to be one of the most useful, ...shaped structure due to steric interactions between the methyl groups on ...he benzene protons.[31] This confers a high solubility and low melting points ...lexes and ligands. In this section I will describe the lateral substitution of ...esogenic phenylazo groups (complexes 6a-d, M = Ni, H_2 and Co) and the ...viour observed will be described.

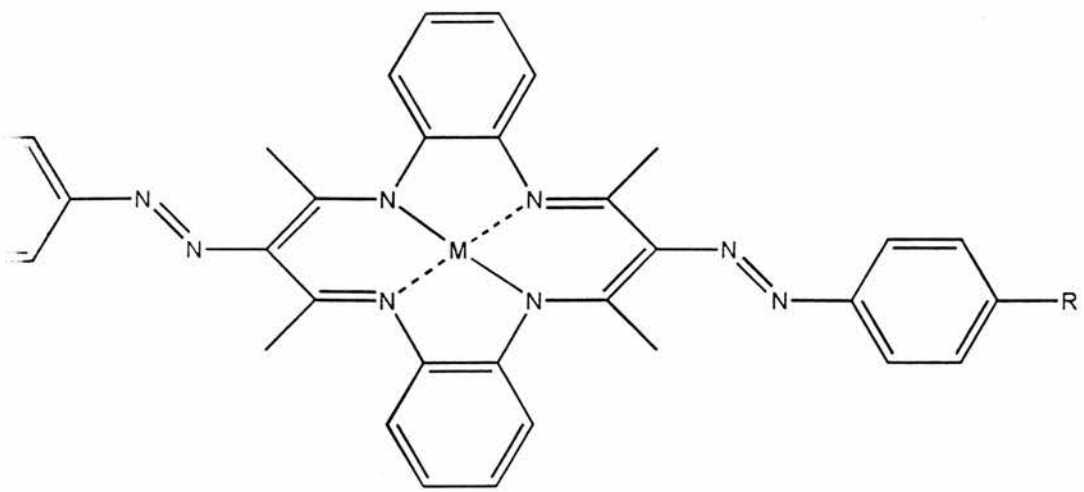

6

... R = H **6b** M = Ni, R = C_4H_9 **6c** M = H_2, Ni and Co, R = O-C_8H_{17}

6d M = Ni, R = O-$C_{14}H_{29}$

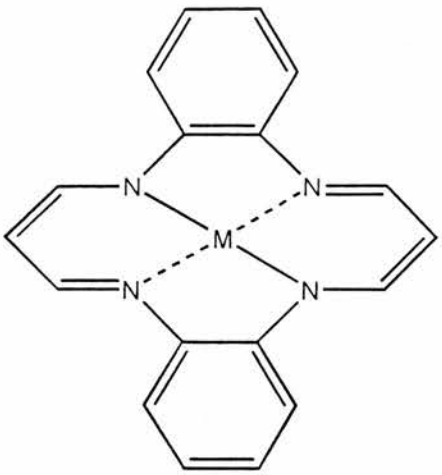
N
N
M
N
N

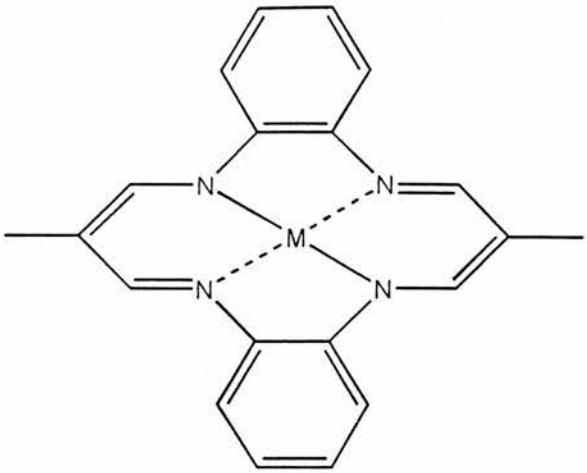
N
N
M
N
N

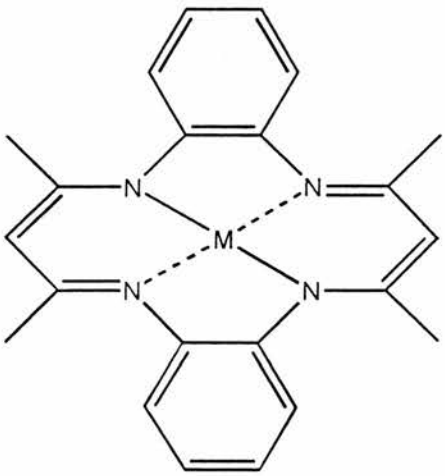
N
N
M
N
N

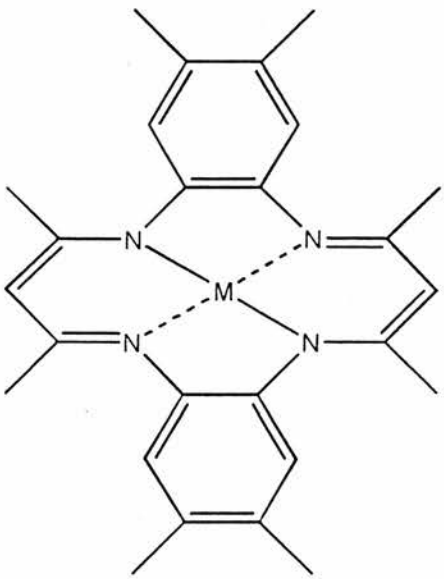
N
N
M
N
N

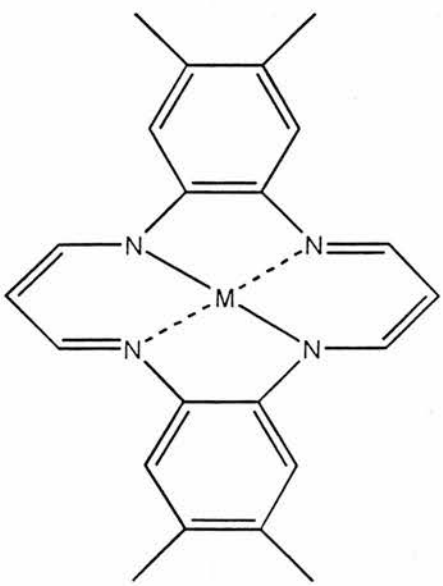
N
N
M
N
N

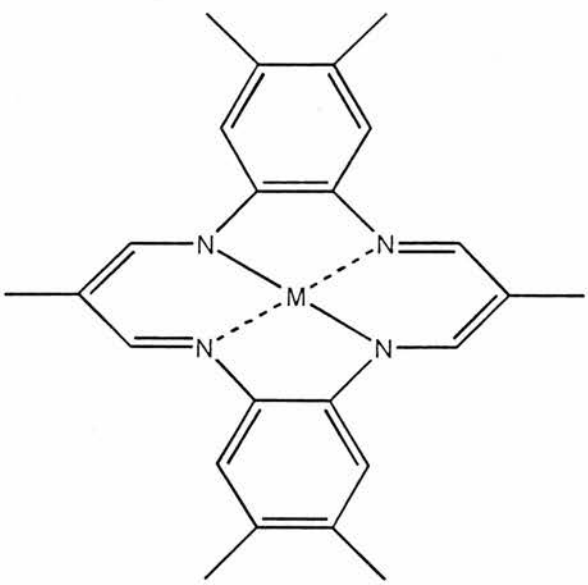
N
N
M
N
N

3.1 Results: Diazotisation of Dibenzotetramethyltetraazaannulene

The starting material Ni(TMTAA) **4** (7,16-dihydro-6,8,15,17-tetramethyldibenzo[b,i]-[1,4,8,11]tetraazacyclotetradecinato(2-)Ni(II)) is readily prepared by the template reaction between nickel acetate, pentan-2,4-dione and 1,2-diaminobenzene.[32]

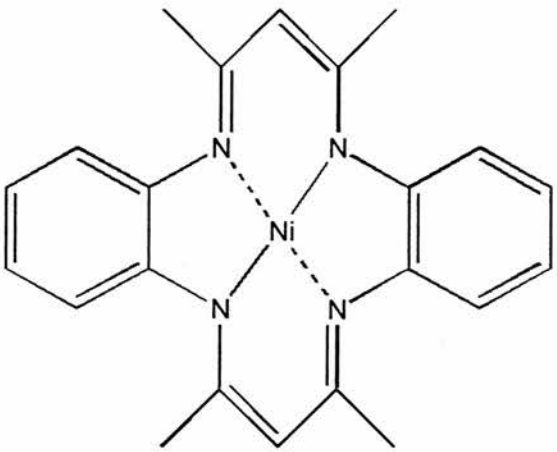

4

The pendant chains, however, posed a greater problem. They had to be stable enough to withstand the reaction conditions during the coupling reaction, posses an amine group adjacent to a benzene ring and ideally exhibit liquid crystalline properties which would be transferred to the completed complex. It was decided that a series of compounds based on *p*-alkoxyaniline would be suitable (Scheme 3.3). The starting material *p*-aminophenol is protected by acetic anhydride and the resulting *p*-hydoxyacetanilide (acetamidophenol) is converted to the potassium salt before reaction with a long chain alkyl bromide.[20] The product is deprotected by hydrolysis in an alkaline environment at elevated temperatures. As the chain length increases physical properties of the *p*-alkoxyanilines change and purification methods had to be altered for each new compound, a feature prominent throughout this work. The results of CHN microanalysis, an indicator of the purity of compounds, are, in some cases, quite far

away from the results expected from the molecular formula. This could be due to the fact that with some organometallics / inorganic compounds the involatile metal residue coats and protects the material underneath from burning.[33] Or the discrepancy could be due to a solvent of crystallisation coordinating with a metal centre.

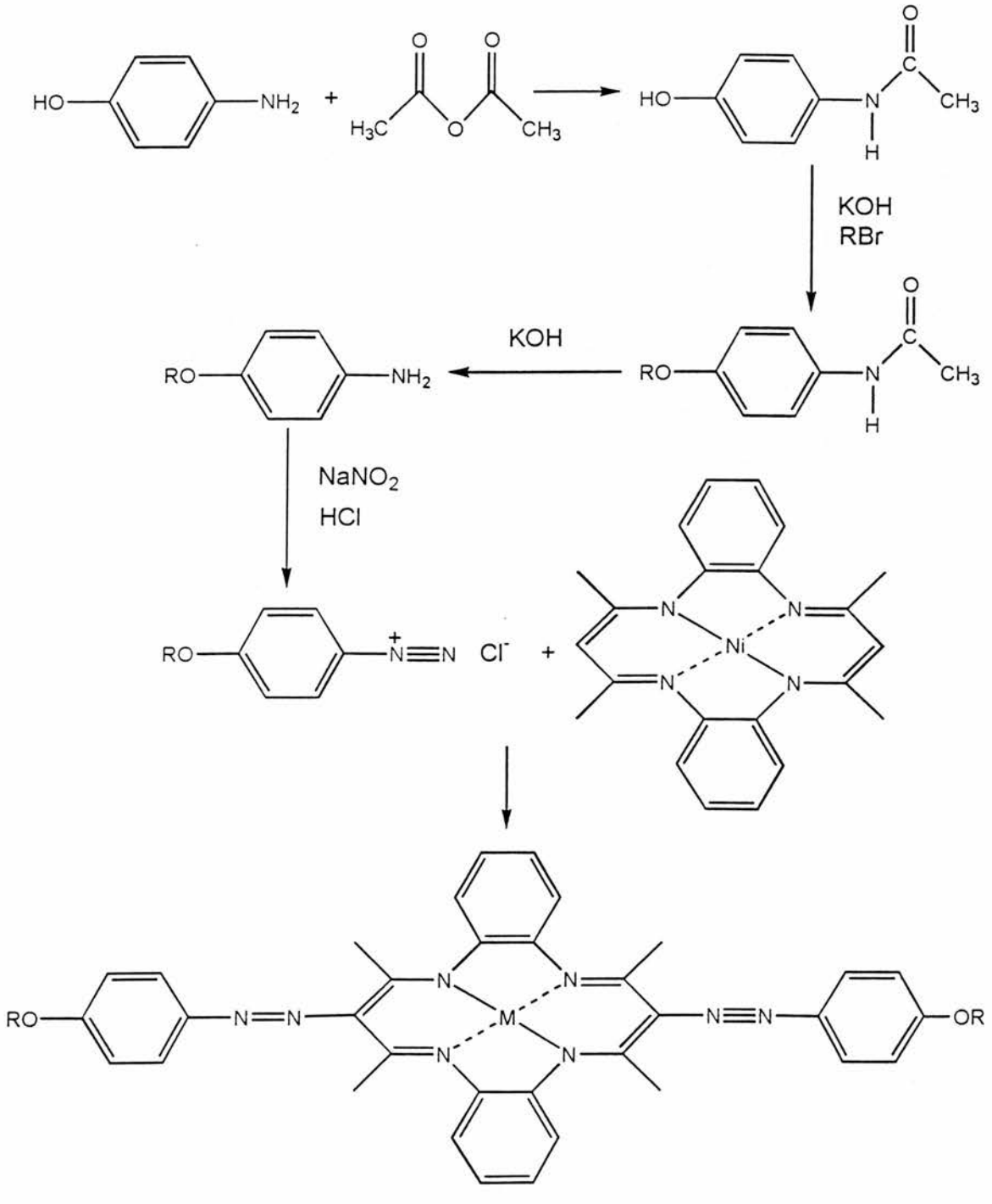

Scheme 3.3 *Synthesis of Ni (diazoTMTAA) complexes.*

There are commercially available *p*-alkylanilines and one was used to prove that it was possible to couple in this manner. Further investigation with this class of compounds was not pursued because the final product of these complexes proved to be more unstable, rupturing sealed aluminium pans during DSC.

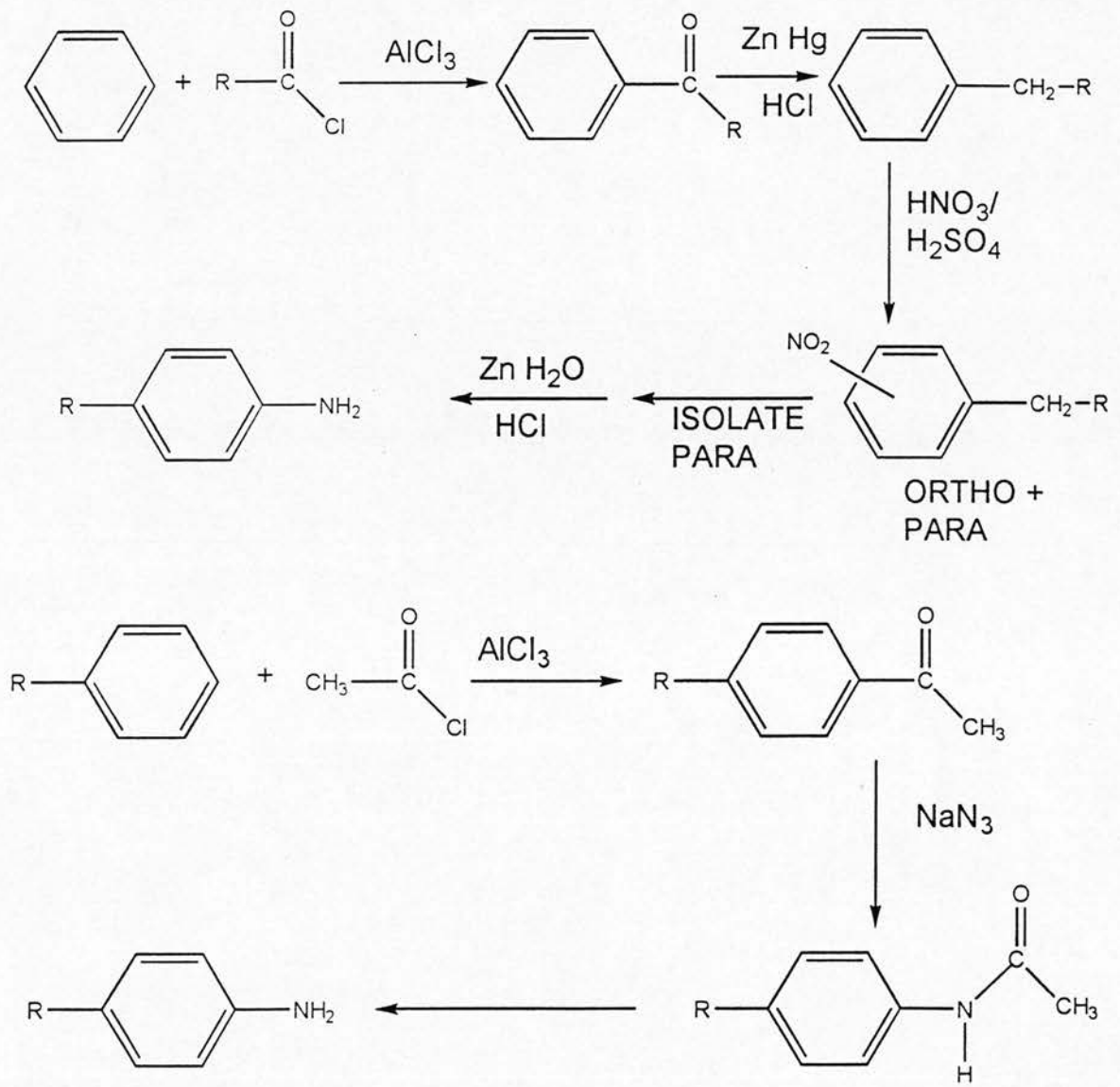

Scheme 3.4.

A recent paper[34] claimed to make alkylanilines by reacting aniline with the corresponding alcohol in zinc chloride at 255-258 °C without solvent, using a Dean and Stark condenser. This was attempted but did not produce the desired product. The more conventional methods to the same compounds are more time consuming,

requiring a number of steps (Scheme 3.4). This was not continued further because the complex made from butylaniline was found to decompose before any liquid crystal mesophases were detected by differential scanning calorimetry (DSC). One other type of ligand chain was proposed but proved difficult to produce in the required yield and purity. Thus the product of the Friedel Crafts acylation of aniline (Scheme 3.5), showed that acylation of the amine dominated.

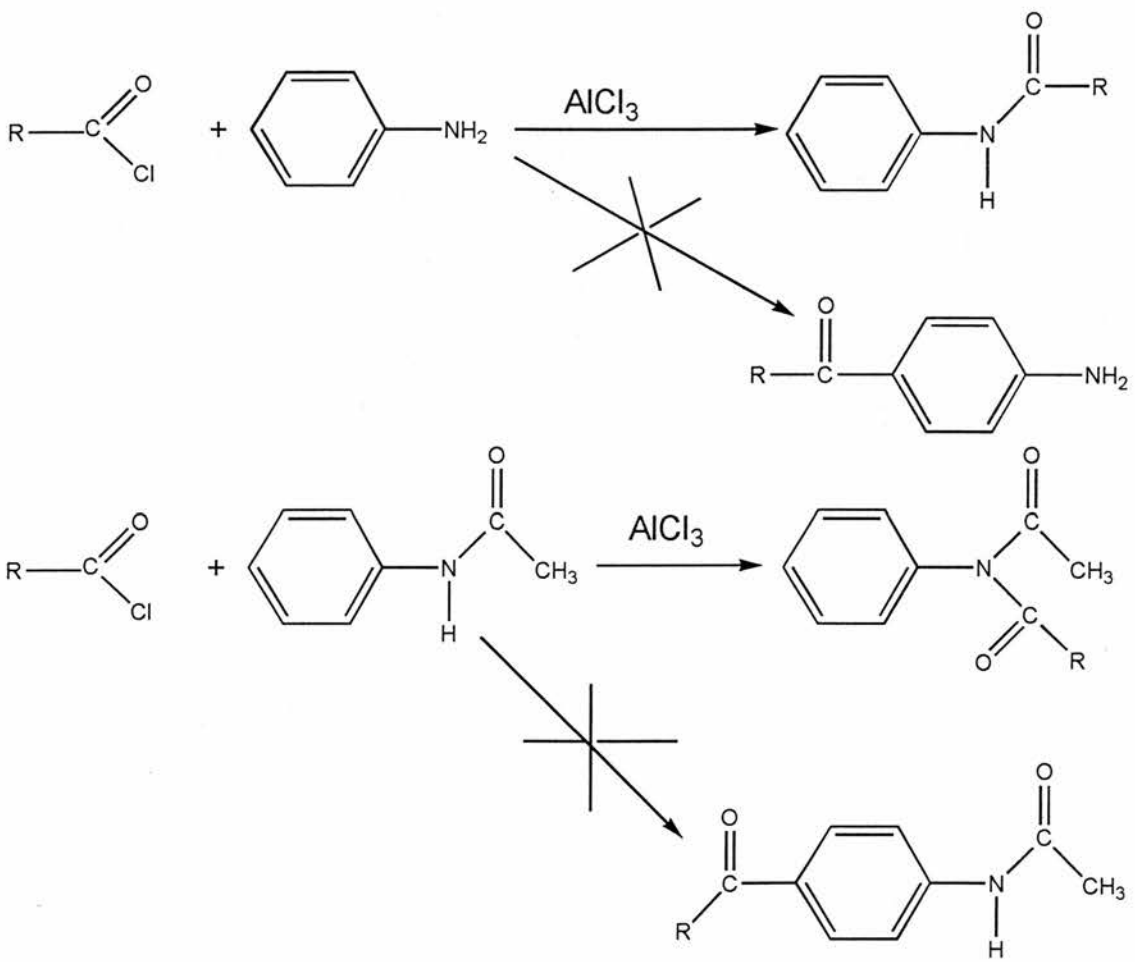

Scheme 3.5

Even after the amine was protected via acetanilide (which in theory should also be activating towards *o* and *p* attack by electrophiles) the desired product was not obtained. This could be due to insufficient activation of the ring by the amide group to electrophilic attack.

3.2 Solid state nuclear magnetic resonance

The solid state ^{13}C CP-MAS NMR spectrum of TMTAA displays two resonances in the methyl region (20.51 and 22.09 ppm) *cf.* the solution spectrum ($CDCl_3$) 22.6 ppm. Its crystal structure has one molecule in the asymmetric unit and no centre of symmetry, so we would expect four methyl resonances. Presumably further splitting of the two signals observed is too small to be observed. The solution NMR of the free ligand **6c**(M = H_2) showed evidence of tautomerism[35-38]with two peaks for the macrocycle core methyl groups. The non equivalence of the methyl groups in solution must be due to imine hydrazone formation which restricts rotation about the N=C bond and thus induces inequality in the methyl group chemical shifts (Figure 3.2).

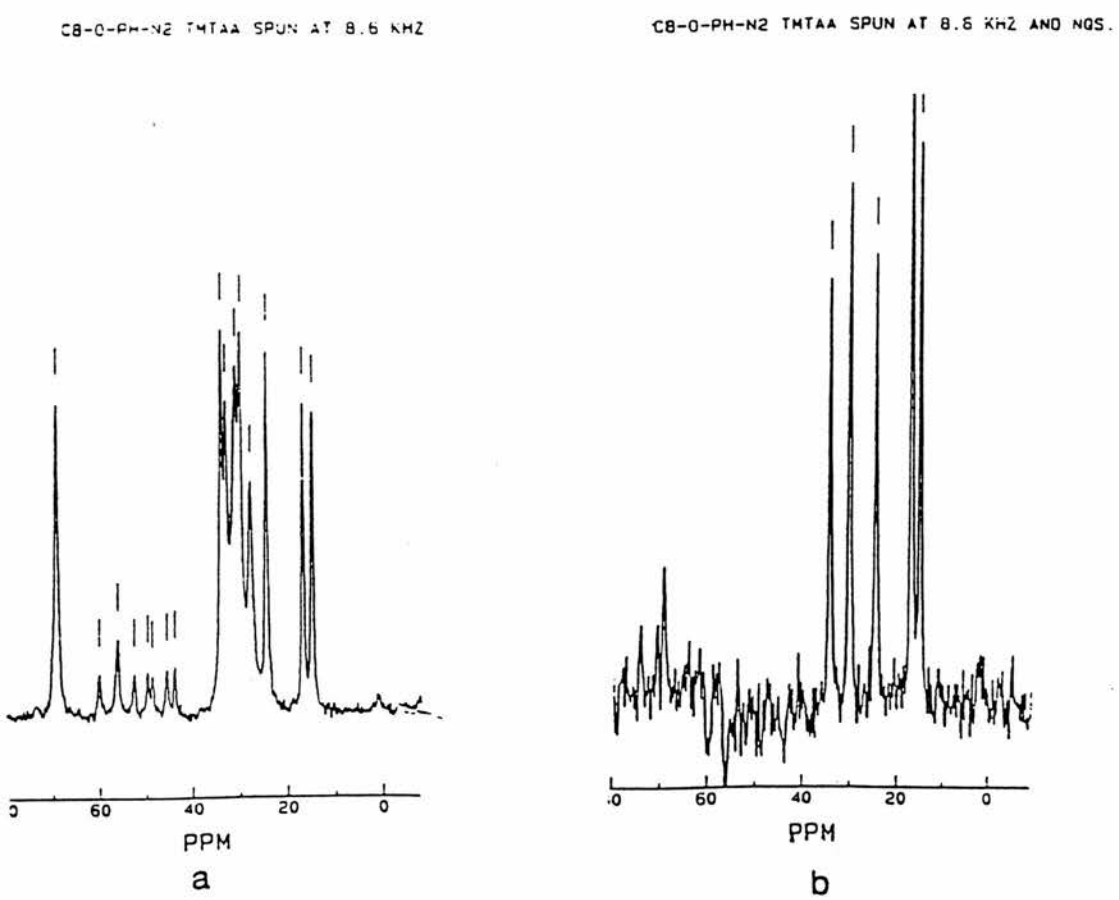

Figure 3.3 *(a) Solid-state NMR spectrum (^{13}C CPMAS) of* **6c** *(M = H_2); (b) NQS spectrum with 50ms delay time. Spectra obtained on a Bruker MSL 500 at 125.8 Mhz.*

The solid-state ^{13}C CP-MAS NMR of **6c**(M = H_2) (Figure 3.3a) shows five different methyl group environments which are clearly distinguishable from the CH_2 carbons in the non-quaternary suppression (NQS) spectrum, (Figure 3.3b). The resonances at 16 and 14 ppm. are clearly due to terminal methyl groups of the alkyl chains. The presence of two signals suggests either that the molecule is not symmetric or that there are two different molecules in the asymmetric unit. There are three resonances in the region expected for the methyl groups associated with the inner core of the macrocycle one more resonance than for TMTAA. This could indicate that we have two different molecules in the unit cell or alternatively that the two possible *cis* and *trans* isomers are present:

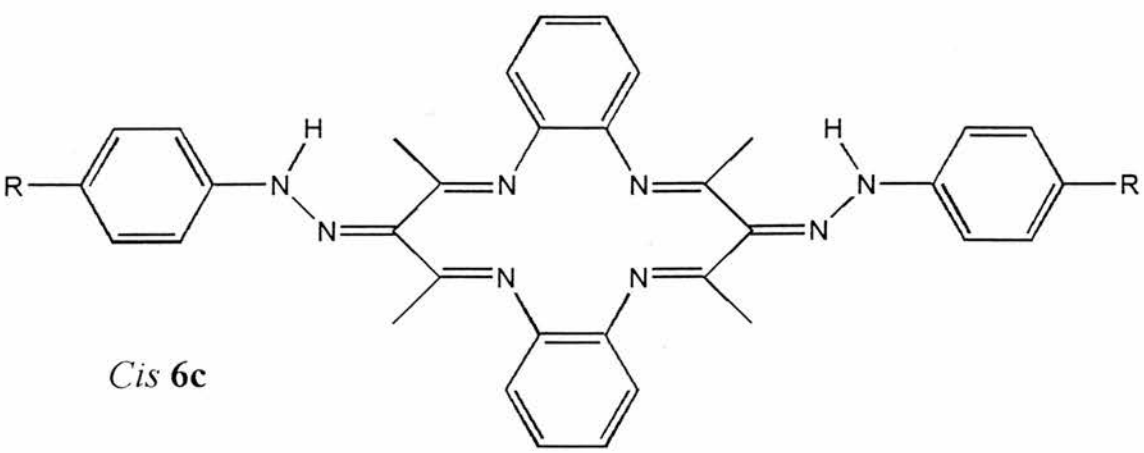

Cis **6c**

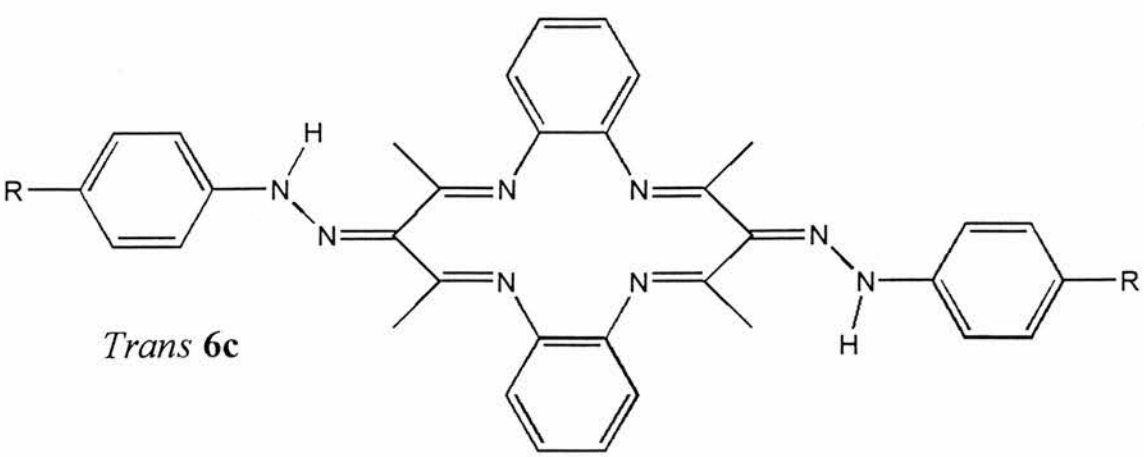

Trans **6c**

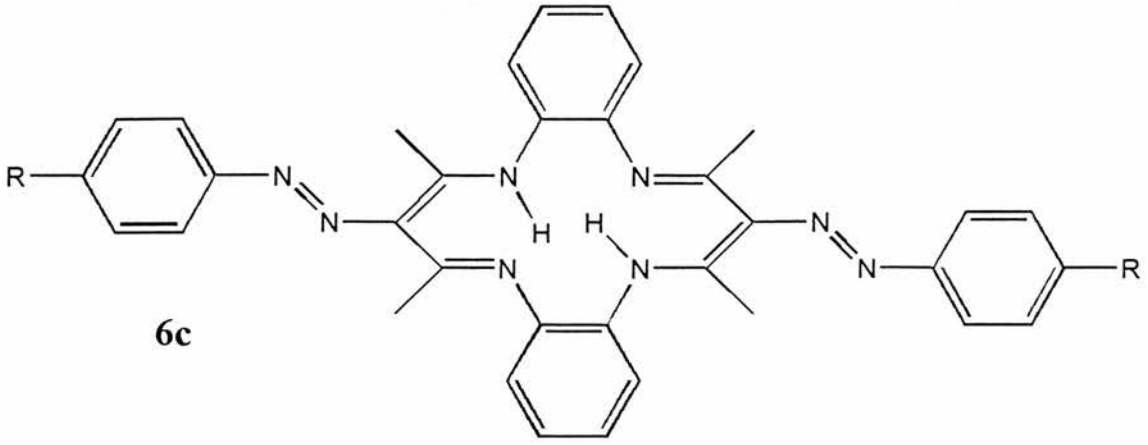

6c

A full elucidation of the assignments must await a detailed crystal structure for this sample.

3.3 Thermal behaviour

Differential scanning calorimetry (DSC)[39] was used to screen the complexes for mesophase transitions (Table 3.1). A phase transition of the type we were searching for solid to liquid crystalline or the change from one type of liquid crystalline structure to another would be accompanied by an absorption of energy. Absorption of heat is observed when non LC compounds change state from solid to liquid. The most interesting behaviour was noted for **6d** (Figure 3.4).

On the first heating cycle (Figure 3.4a), a transition from the crystalline phase is observed at 125.5 °C, with no corresponding exothermic phase transition observed on the cooling cycle, apart from a small exotherm (X) at 54.6 °C which is due to the isotropic to highly viscous nematic phase (N) transition. It is only during the second heating cycle that an exothermic peak is observed at 92.3 °C due to the crystallisation process (Figure 3.4b). This behaviour was also observed after 8 heating and cooling cycles for compound **6c** (M = Ni). Amorphous and glassy states often have enhanced

electron and ion transport properties compared to the crystalline state.. The glassy state was confirmed by microscopic observation of the phase transitions; the green crystals change colour to orange-red when the glassy state is formed. Deformation of the glass by shearing the lower slip failed to produce birefringent textures seen in vitreous organic compounds.[40] This state is characteristic of mesogens containing bulky central core groups.[29]

Table 3.1 *DSC Data for Macrocycle and Complexes*

Sample	Transition	T/°C	ΔH kJ mol^{-1}
6a	C → I decomp	>240	-
6b	K → I decomp	>250	-
6c (M = Ni)	K → K2	144.5	91.7
	K2 → I	183.9	15.4
on 9th heating	G → K2	123.5	-44.2
	K2 → I	188.8	42.9
6c(M = H2)	K → I	151.0	35.5
6d	K → K2	125.5	86.6
	K2 → I	131.0	0.7
on 2nd heating	Tg	69.8	5.2
	G → K2	92.3	-43.22
	K2 → I	130.6	38.4

Temperatures, and absorption (+) or emission (-) of energy of the peaks found in DSC heating curves of 6

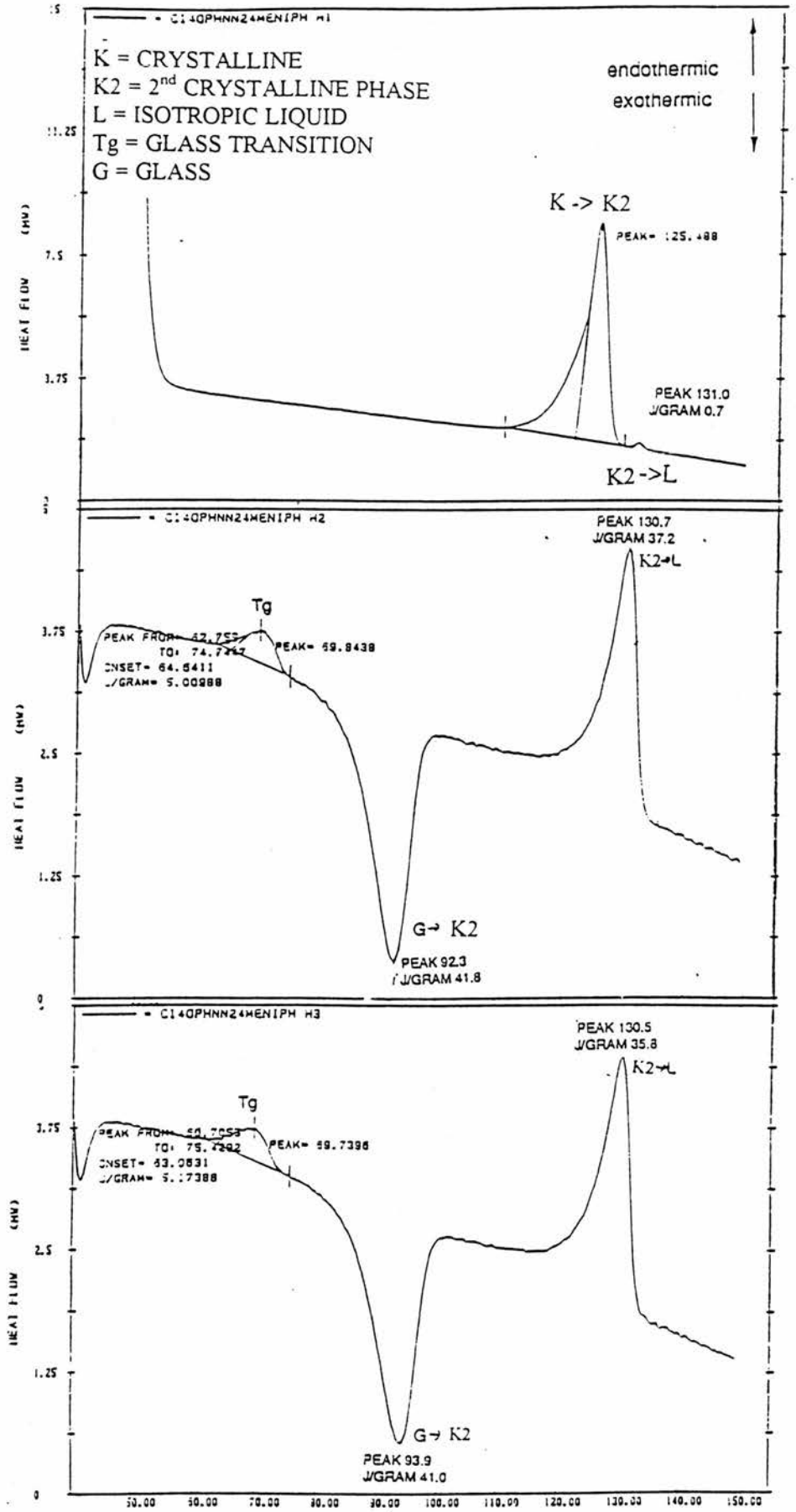

Figure 3.4 *DSC traces for compound* ***6d****, a) first heating curve, b) second heating curve, c) third heating curve. Scan rate 10 °C min^{-1}*

3.4 Solvatochromism

The compound **6c** (C_8O, M = Ni) when dissolved in $CHCl_3$ forms a green solution which rapidly turns red, accompanied by broadening of the ^1H NMR peaks suggesting that a square planar (diamagnetic) to octahedral (paramagnetic) equilibrium is set up through a dimerization or oligomerization process (Scheme 3.6).

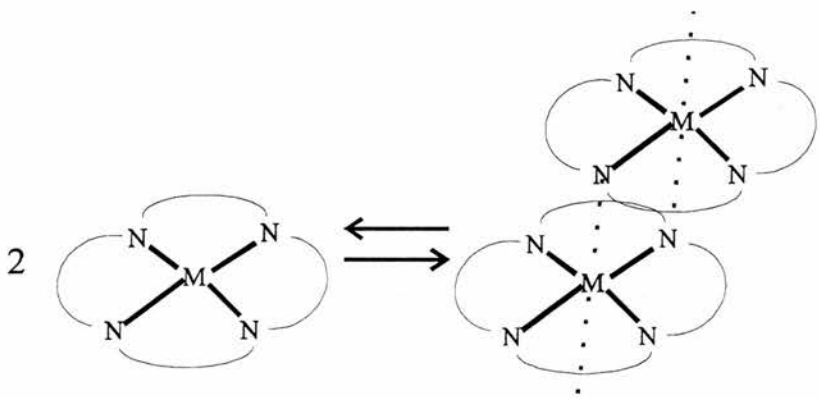

Scheme 3.6

Compound **6d** ($C_{14}O$ M = Ni) also turns red but takes longer and a considerable decrease in the resolution of the NMR signal can be observed. The slower colour change corresponding to the longer chain lengths suggests that the setting up of the octahedral complex is hindered by the length of the side chains.

3.5 Electrochemistry

The surface activity of the new compounds were studied by cyclic voltammetry. In order to detect monolayer coverage we used the Co complex since Co tetraazaannulenes are active towards O_2 reduction in alkaline solution giving

measurable catalytic currents.[16] Figure 3.5 (a) shows the response at a freshly polished gold electrode, with a broad O_2 reduction wave commencing at –0.3V vs SCE.

After coating with Co (**6c**) we observe (Figure 3.5b) a large decrease in capacitive current and the absence of any O_2 reduction current, in contrast to the complex without azo groups (Figure 3.5c) which shows a catalytic reduction wave commencing at –0.2V. The blocking behaviour of Co (**6c**) is characteristic of surface–active thiols such as $C_{18}H_{37}SH$ (Figure 3.5d).[41-43]

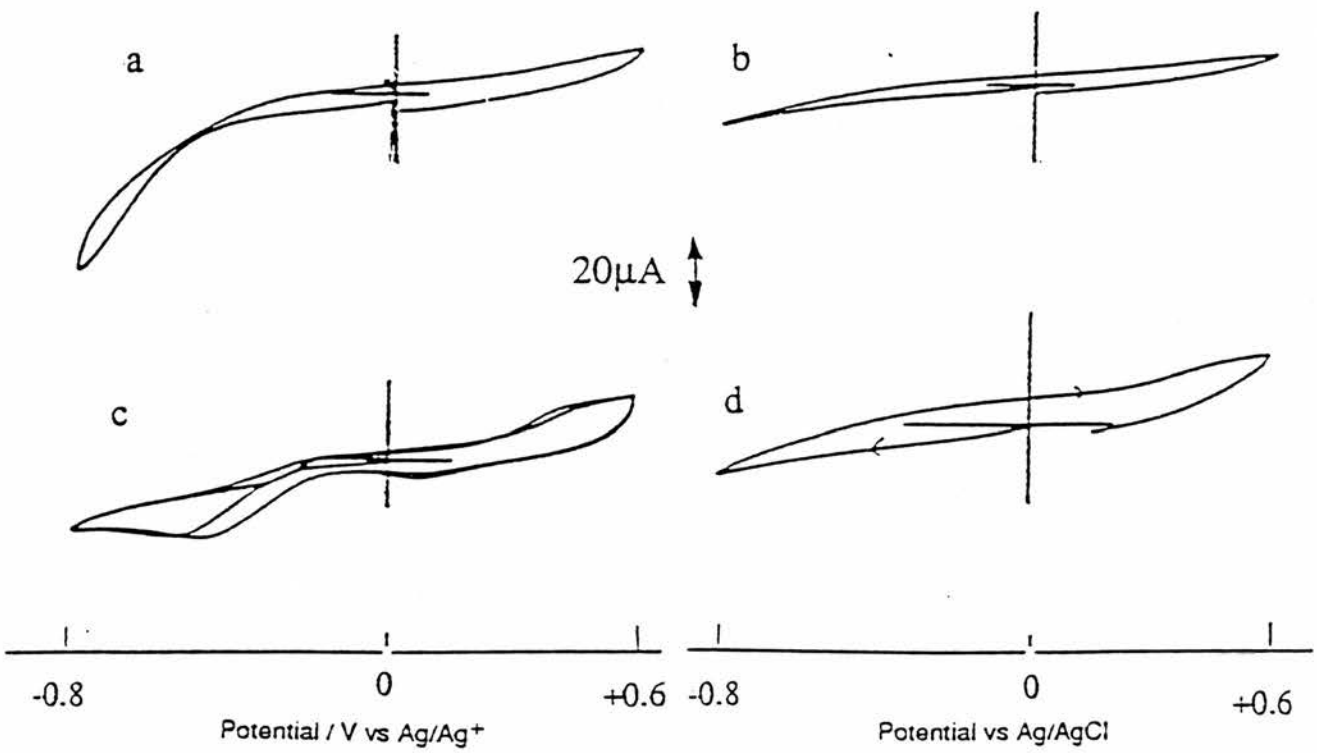

Figure 3.5 *Cyclic voltammograms (50 mVs^{-1}) for O_2 reduction in O_2–saturated (1.2mM)/0.1M NaOH at 291K for: (a) a bare gold disk electrode (area = 0.07 cm^2); (b) electrode dipped in 10^{-4} M Co (**6c**) in CH_2Cl_2 for 10 mins; (c) electrode dipped in 10^{-4} M 6,13,-Me_2-2,3:9,10-Xyl_2[14]hexaenato(2-)N_4 Co; (d) electrode coated with $C_{18}H_{37}SH$.*

The mode of adsorption of Co (**6c**) is therefore similar to the thiols in that the long alkyl chains are directed away from the surface preventing the access of O_2 and ions to the Co centre. It is interesting to compare this behaviour with that of a C_{16}–alkylated cationic Co porphyrin which remains active for O_2 reduction after adsorption on gold.[44] We attribute this difference to the greater hydration of the cationic head group of the porphyrin.

3.6 Attempted Synthesis Of A Flatter Macrocycle:

Non-Methylated Dibenzo TAA

As the original macrocycle did not display liquid crystalline behaviour alterations could be made to it to determine exactly what property was preventing the organisation of the molecules in the liquid state. The saddle shape of the molecule was one such possibility. To prevent this buckling the interaction between the benzene side groups and the methyl groups had to be prevented. A new approach to the formation of the complex was taken to remove the four methyl groups and return the structure to planarity (Scheme 3.7). Instead of using the long chain diazo salts to couple to the completed macrocycle they were attached to intermediates in the formation of the macrocycle.[35] This new strategy avoided isolation of the reactive and insoluble parent macrocycle.

Unfortunately reaction of this modified aldehyde derivative with o-phenylenediamine and nickel acetate did not produce the desired macrocycle. The "three quarter" formed macrocycle was all that could be isolated despite preformation

of nickel *o*-phenylenediamine complex and the use of various solvents and reaction conditions.

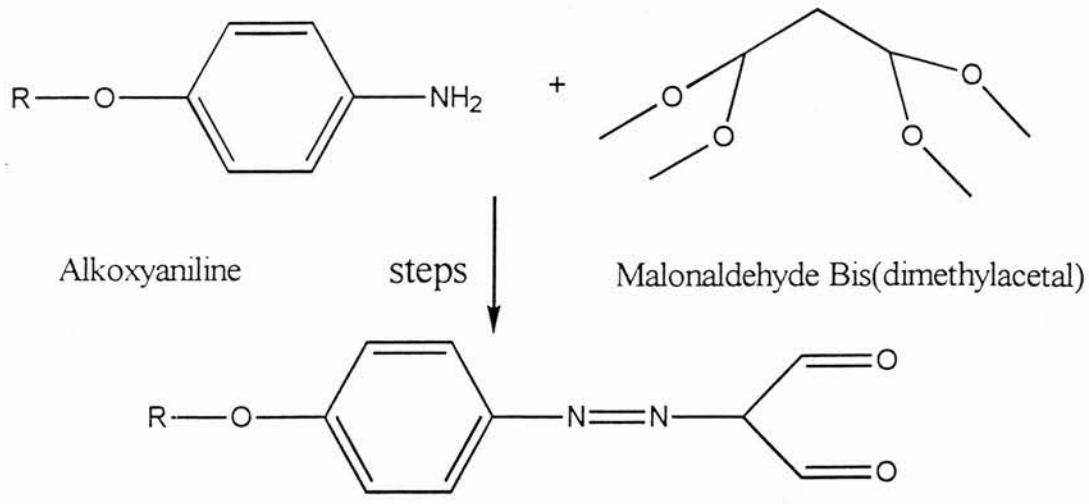

12 Alkoxyphenyldiazomalonaldehyde (i)HCl; (ii)$NaNO_2$; (iii) Et_3N

Scheme 3.7

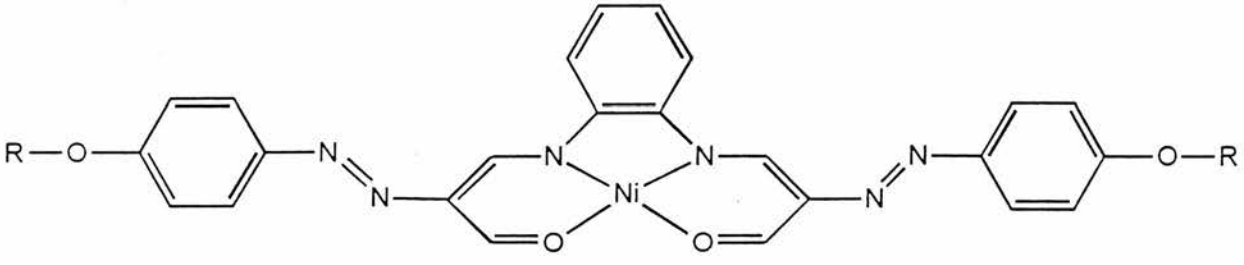

7 ("3/4")

3.7 A Slimmer Macrocycle: Diazotisation of 1,6,8,13-Me_4tetraazaannulene

Communications with Professor John Goodby of Hull University resulted in the conclusion that the glassy type behaviour could be a direct result of the bulky benzene side group and to achieve true liquid crystalline mesophases an attempt should be made to make the macrocycle core thinner. The obvious replacement of *o*-phenylenediamine

with ethylenediamine in the synthesis of the simple macrocycle again resulted in only a 3/4 formed macrocycle. Prolonged refluxing of this ¾ formed macrocycle in pure ethylenediamine did not result in the formation of the closed macrocycle (Scheme 3.8). After various attempts to produce a suitable macrocycle we became aware of a paper by Costes et al[45,46]which prepared a desirable macrocycle from a preformed intermediate complex 7-amino-4-methyl-5-aza-3-hepten-2-one (AEH) (Scheme 3.8). The literature yield was 30 %, however, our yields varied between zero and a maximum of 5 %. As this compound is a starting material for the preparation of the LC complexes a large quantity of material was required. Suggested improvements by Professor J. P. Costes were very informative, but neither they or the many variations of the reaction conditions to improve yield were fruitful. Refluxing for 18 h rather than the 20 mins suggested in the literature proved most successful. However, batches of this compound were prepared almost on a continual basis.

The macrocycle formed from AEH can be used in the same manner as the original TMTAA in the formation of diazo linked rod-like molecules. A series of these compounds were prepared each having its own distinct solubility properties which made purification difficult. It is essential that all impurities are removed before testing with DSC as any foreign matter can give rise to peaks which are irreproducible. Some of the compounds did not give good CHN microanalysis results and as discussed in section 3.1 this could be due of an involatile metal residue which coats and protects the material underneath from burning.[33]

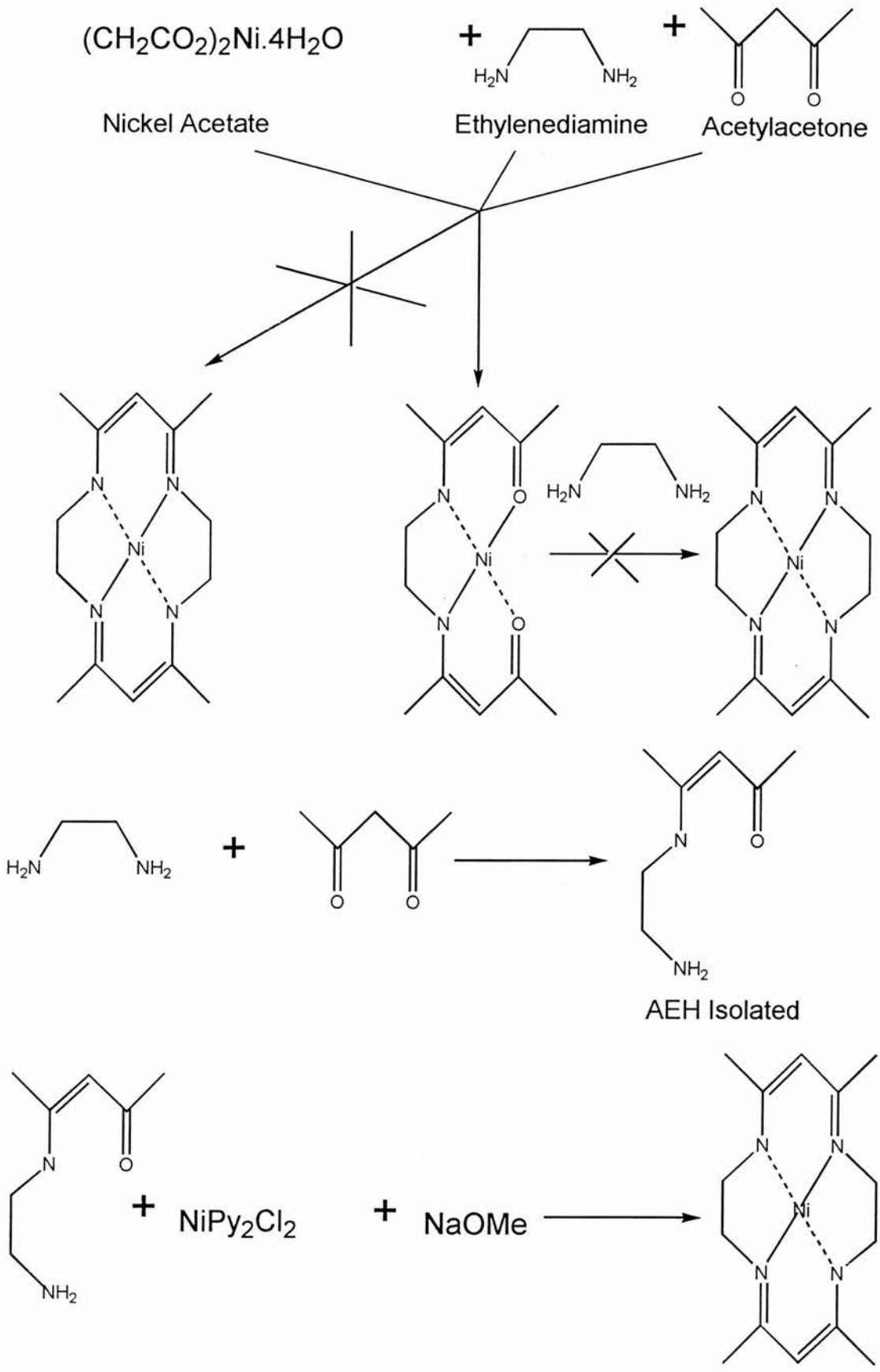
(CH2CO2)2Ni.4H2O
Nickel Acetate
Ethylenediamine
Acetylacetone
AEH Isolated
NiPy2Cl2
NaOMe

Scheme 3.8 **8**

3.8 Thermal properties of Azo derivatives of TMTAA

These compounds were sent to Prof. John Goodby at the Liquid Crystal and Advanced Organic Materials Research Group in Hull University as they have far greater experience in identifying Liquid crystalline phases by observation on a heated stage microscope. Compounds with chain length 12, 14 and 16 displayed smectic A liquid crystalline behaviour (Table 3.3).

Table 3.2 *DSC data for macrocycles Ni(8)*

Sample		Transitions Temperature °C (ΔH kJ mol^{-1})			
8a	Heat 1	239.43 (37.25)			
	Cool 1	203.39 (-31.22)			
8b	Heat 1	81.72 (13.98)	218.41 (31.45)		
	Cool 1	127.29 (-4.58)			
	Heat 2	161.85 (5.03)			
	Cool 2	No peaks			
8c	Heat 1	81.13 (26.26)	164.12 (3.66)	168.65 (2.97)(16.76)	216.61 (25.53)
	Cool 1	54.46 (-18.34)	154.33 (-9.38)	168.89 (-12.29)	
	Heat 2	85.33 (16.73)	163.06 (10.08)	191.36 (8.63)	
	Cool 2	No peaks			
8d	Heat 1	91.72 (32.09)	137.81 (5.23)	143.44 (4.45)	217.03 (22.24)
	Cool 1	66.59 (-25.03)	126.22 (-2.99)	129.59 (-1.4)(-14.35)	175.27 (-13.48)
	Heat 2	93.66 (25.75)	135.8 (1.62)	139.2 (0.23)(15.21)	197.26 (13.64)
	Cool 2	70.19 (-4.45)	110.33 (-9.76)		
8e	Heat 1	94.47 (32.22)	130.24 (7.90)	135.26 (2.49)	211.74 (23.75)
	Cool 1	No peaks			

Temperatures, and ΔH of the peaks found in DSC curves of ***8****. Numbers in brackets refer to absorption (+) or emission (-) of energy measured in kJ mol^{-1}.*

The observed transition temperatures correspond well with the transitions observed in DSC traces (Table 3.2). The lower transitions must correspond to crystalline phase transformations possibly associated with intramolecular motions, discussed in the next section.

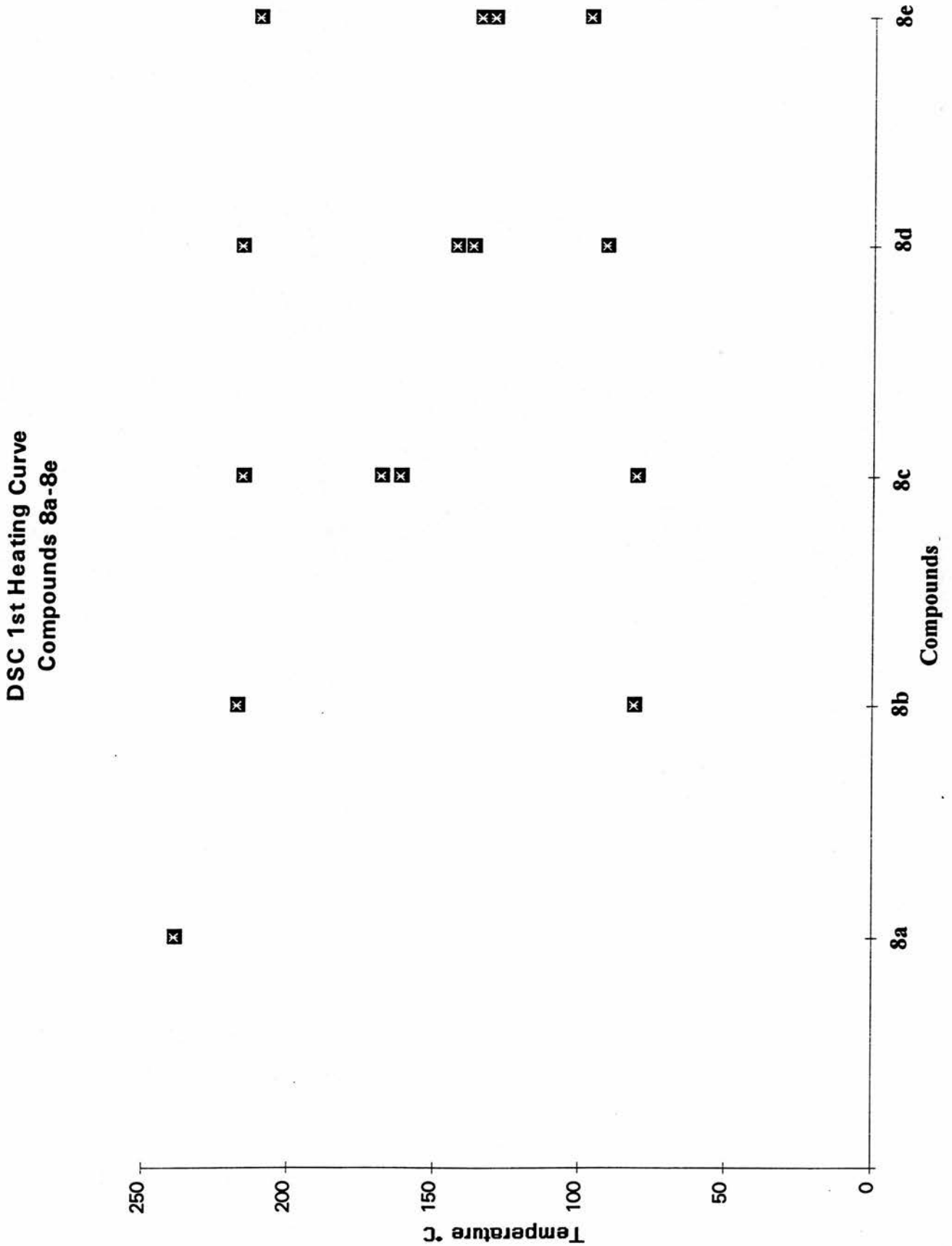

Figure 3.6 *Graph of the peaks from the first DSC heating cycle of compounds* ***8 a-e***

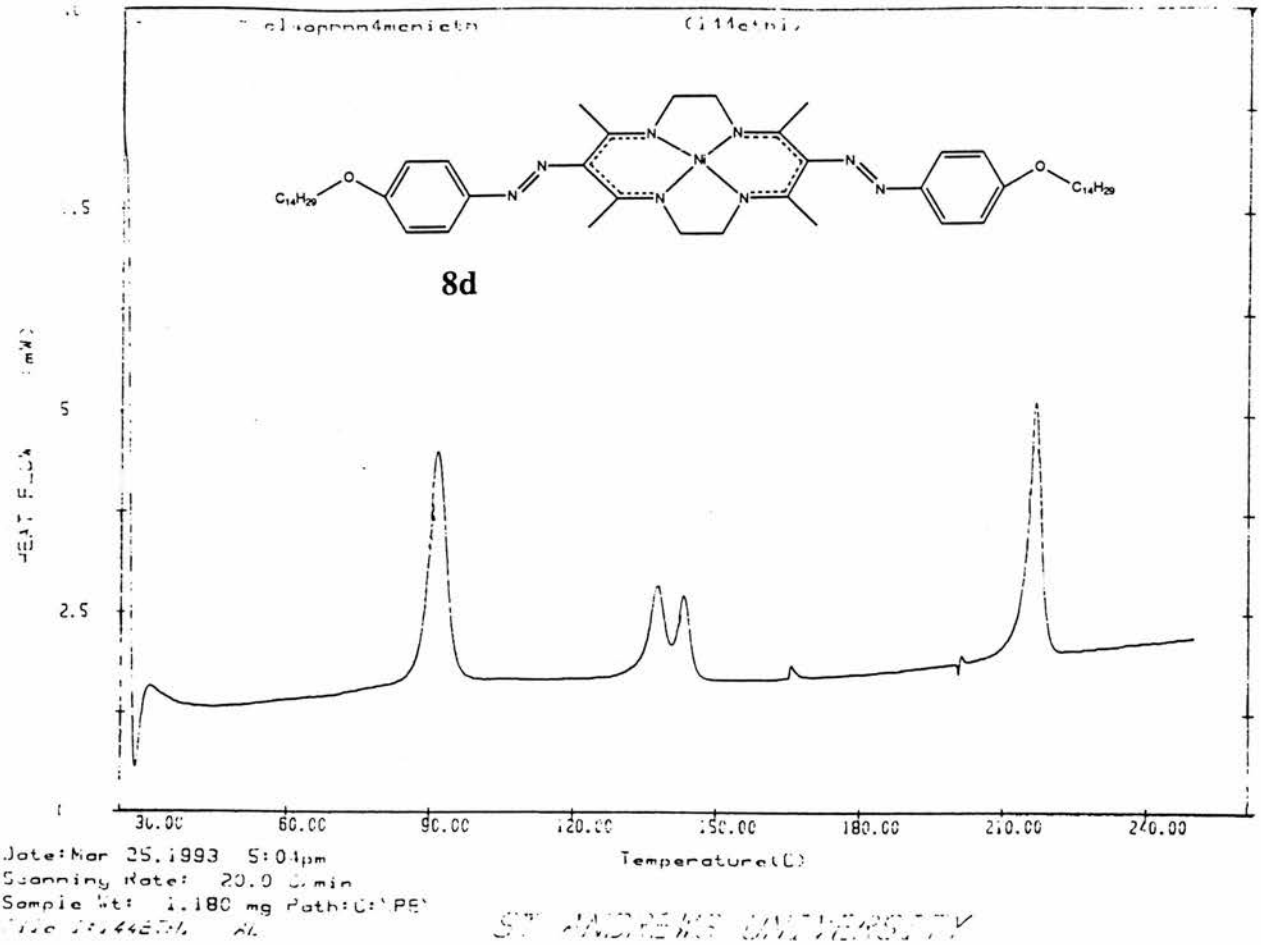

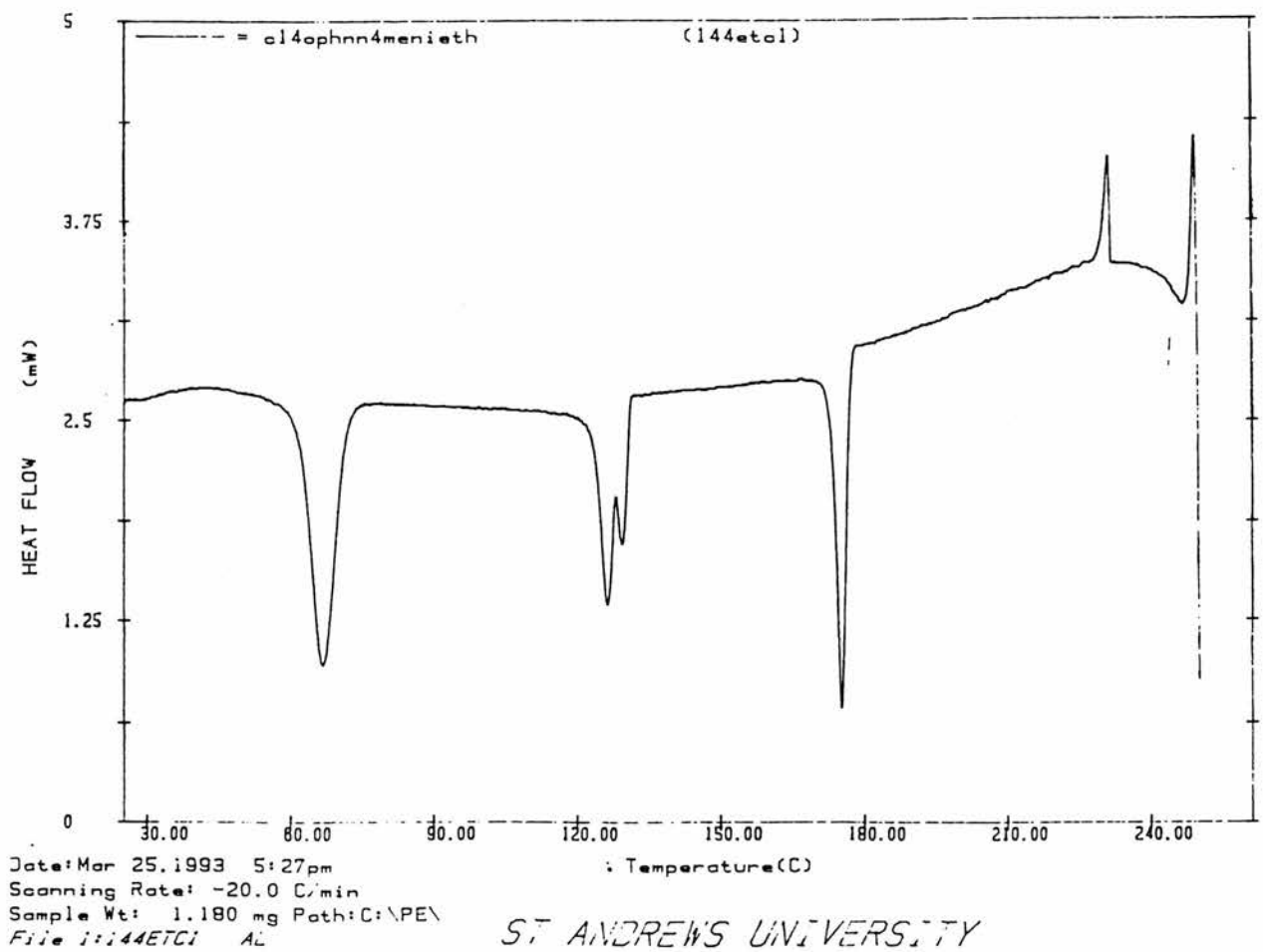

Figure 3.7 1st heating and cooling DSC curve of ***8d***

Table 3.3 Liquid crystalline behaviour observed by microscopy

8c	C_{12}	mp 219.7	S_A	242.8°C	Isotropic Liquid
			(Decomposition)		
8d	C_{14}	mp 217.2	S_A	254.4°C	Isotropic Liquid
			(Decomposition)		
8e	C_{16}	mp 214.7	S_A	239.6°C	Isotropic Liquid
			(Decomposition)		

3.9 Thermochromism

When viewed under a microscope during heating a reversible colour change could be seen for **(8 c-e)**. The crystals which are colourless/yellow at room temperature turn to red/orange colours after the first peak on the DSC trace. This is accompanied by a dancing of the crystals and it is possible to follow the wavefront with the naked eye as it passes through the crystal. A similar change was reported[47] by Bloomquist (Figure 3.8) where it was postulated that the thermochromic change was due to a sudden change in the in plane ligand field strength caused by conformational changes in the $Ni(en)_2$ ring system.[48]

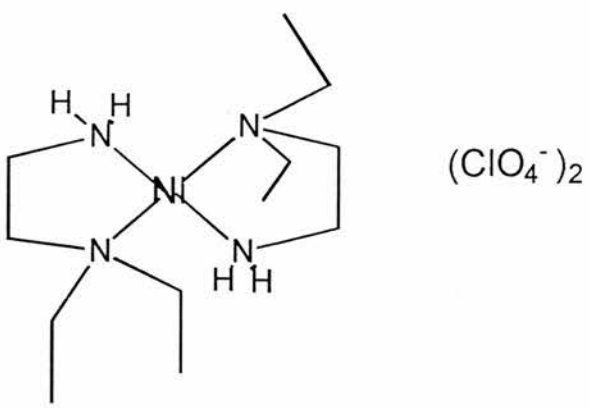

***Figure 3.8** Bis(NNdiethylethylenediamine) Nickel II Perchlorate*

At low temperature optimal overlap of the nitrogen lone pair with the metal d orbitals is established. At high temperature a point is reached where the energy of thermal motion is sufficient to weaken the hydrogen bonding network to allow the Ni diamine ring systems to begin rapid conformational interconversion. This weakens the overlap of the in-plane Ni d-orbitals with the N lone pairs causing a sudden decrease in the in-plane field strength and a resulting red shift (Figure 3.9).

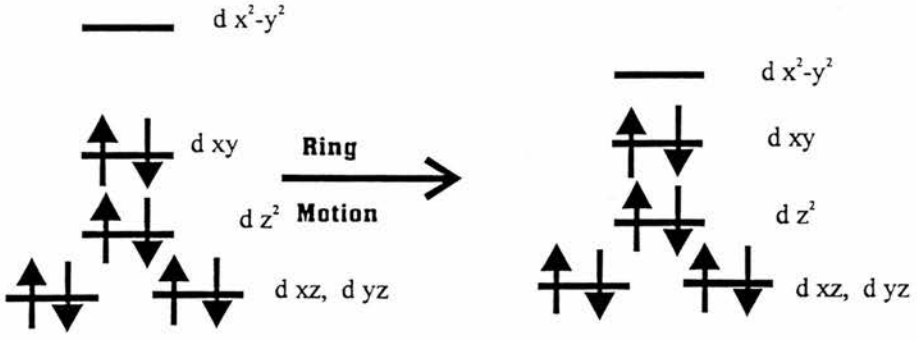

Figure 3.9

Other possibilities include two separate stable conformations in the solid state at different temperatures, perhaps the *cis* and *trans* molecules discussed above. To fully assign these solid state transformations a crystal structure would be required at both temperatures. However despite, our best efforts it proved impossible to grow a crystal large enough to do this type of study. An example of this possible explanation was given by J. Eilmes[49] regarding a compound based on an analogue of our larger Ni(TMTAA) compounds. It must be noted that our derivatives of Ni(TMTAA) showed no evidence of this thermochromic effect and the only difference in the structure is the exchange of benzene rings for ethylenediamine linkages. The evidence therefore leans heavily on the side of the rapid interconversion of the diamine ring system rather than a *cis / trans* conversion at the diazonium linkage.

3.10 Removal Of All Side Groups

The replacement of phenylenediamine groups with ethylenediamine groups made the molecules thinner and in doing so induced liquid crystalline behaviour. However, the range over which this state exists is at a very high temperature and decomposition occurs rapidly at the clearing temperature, neither of which are desirable qualities for a liquid crystal. If the molecule could be made even more slimline perhaps the properties would improve. The removal of the four methyl groups was the target set. To accomplish a molecule of this type the azo linkage had to be attached to an intermediate[35] before the template synthesis of the macrocycle. This was already tried on a macrocycle with benzene side groups which only obtained a three quarter closure. Exactly the same thing happened when ethylenediamine was used: indeed, prolonged refluxing using pure ethylenediamine as solvent had no discernible effect.

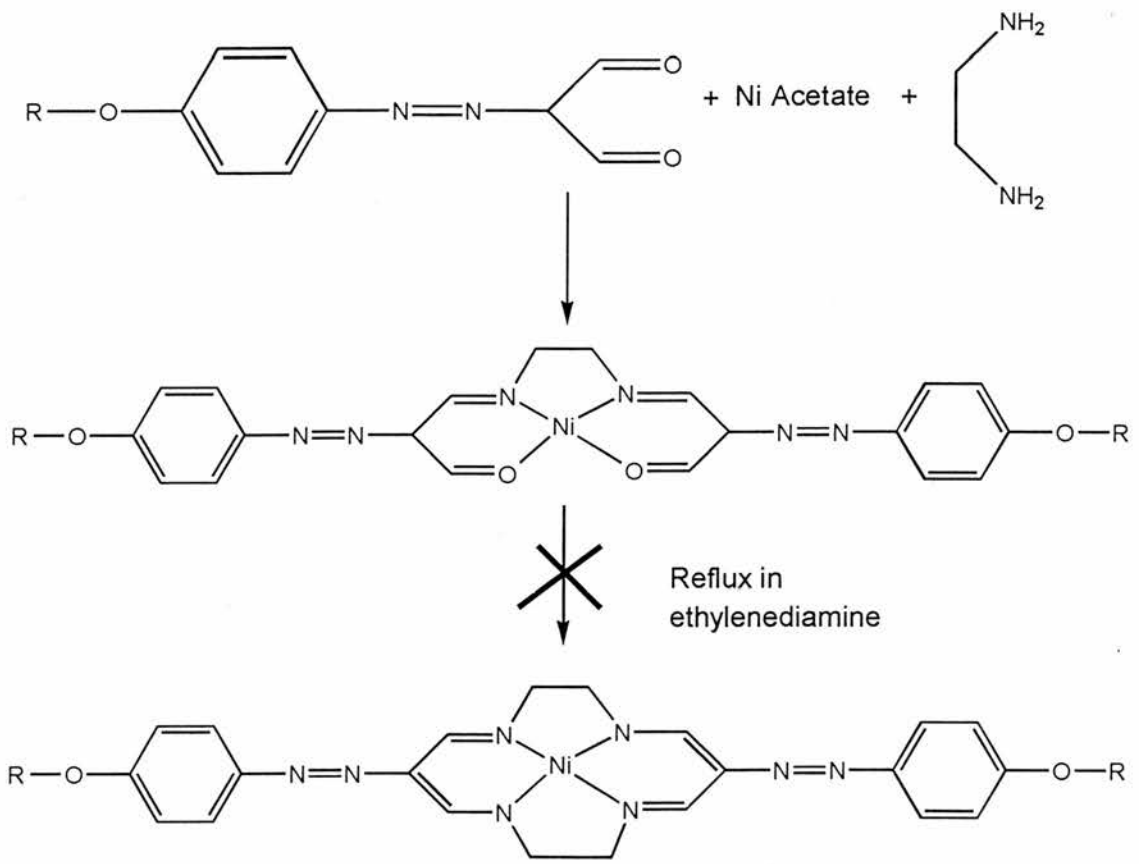

Scheme 3.9

Papers by Pugin and L'Eplattenier[36,50] proved very useful in preparing these compounds. By using 2-methoxyethanol the yield of the three-quarter macrocycle can be greatly enhanced. They had found that formation of the three-quarter macrocycle with *o*-phenylenediamine as the bridge was much more susceptible to ring closure by ethylenediamine. In fact, for their molecules it not only closed the macrocycle but also replaced the benzene bridge to form a molecule without bulky side groups:

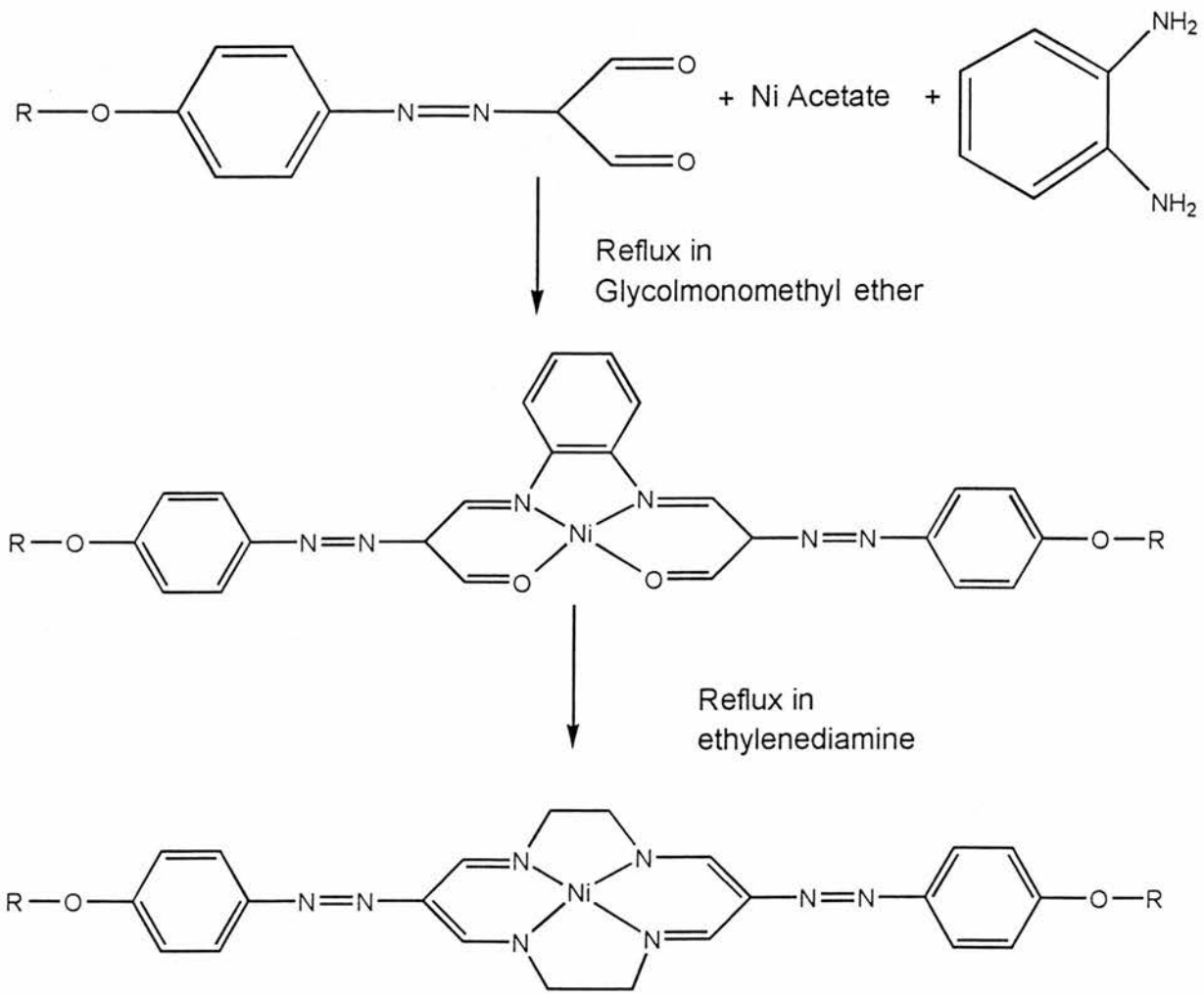

5

Scheme 3.10

The NMR and all the other spectroscopic data for the product molecule seemed in order and the series of molecules were synthesised. The FAB mass specrometry, however, returned from Swansea with a peak in addition to the M + H. This peak corresponds to a closed macrocycle **9** with one benzene and one ethylenediamine unit.

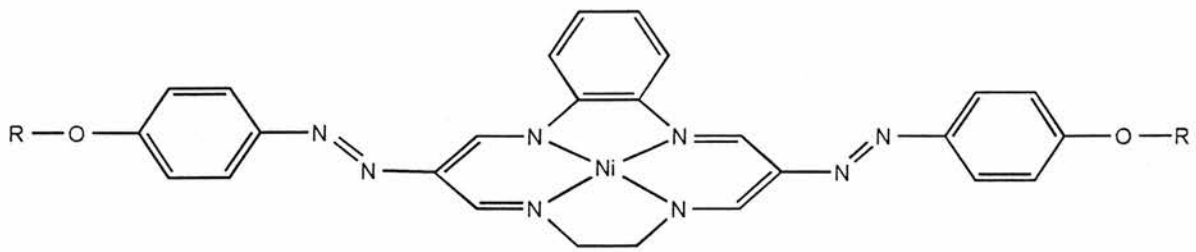

9

There were no peaks for the three-quarters closed macrocycle. The physical properties of the two molecules **5** and **9** are very similar, as are their spectroscopic properties. It is very difficult with such a large molecule of low solubility to determine relative amounts of **5** and **9**. Recrystallisation would not get rid of the unwanted mixed unit macrocycle **9** as the solubility properties were too much alike. .Column chromatography did not separate the molecules as the electric dipole moments are almost identical. Repeated refluxing in ethylenediamine surprisingly had no effect in removing the impurity. Although there are several peaks in the DSC trace (Table 3.3) little can be derived from these results because we cannot attribute the peaks to any one molecule and the mixture itself could have different properties to the molecules taken individually.

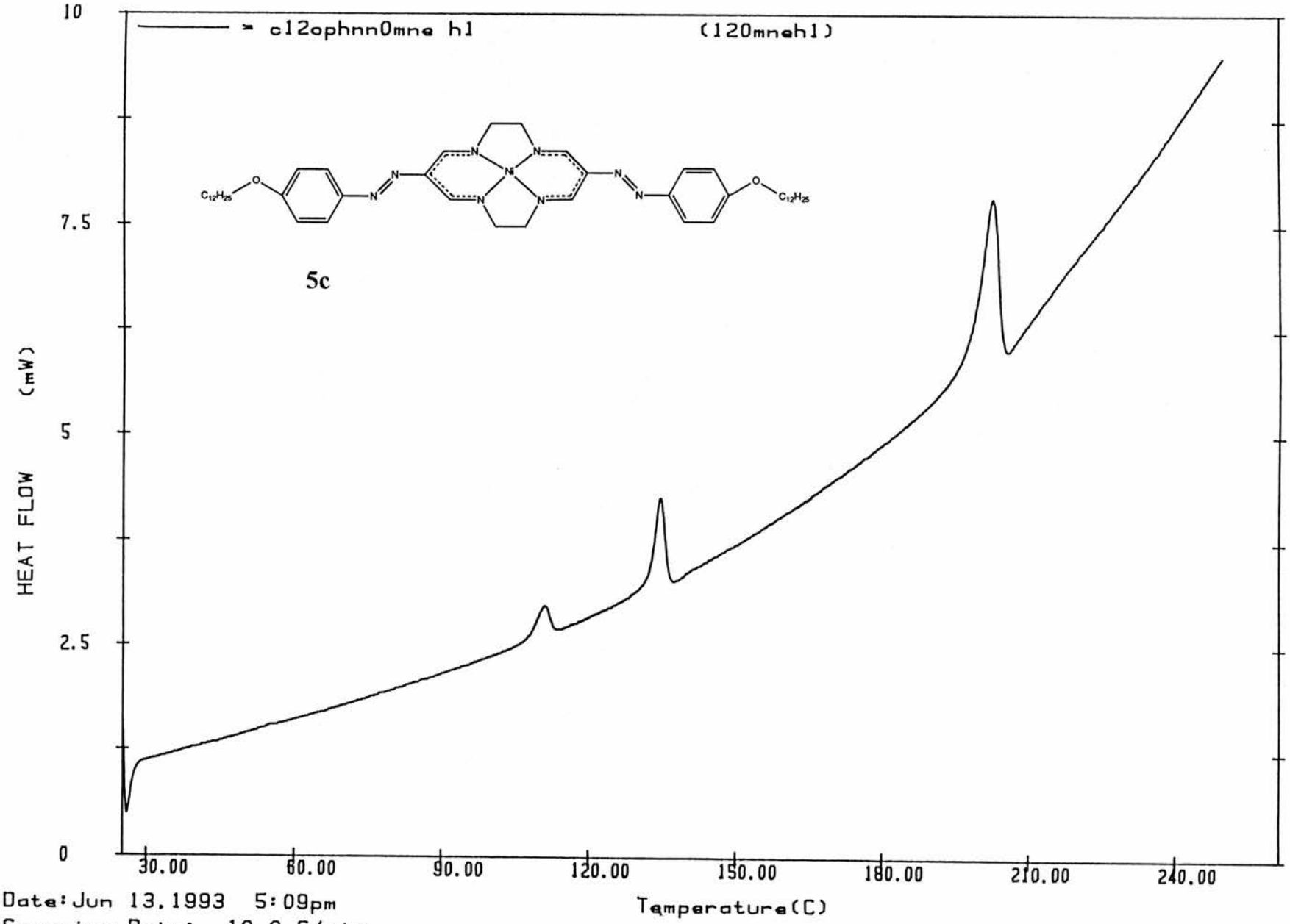

5c

Figure 3.10 1st DSC heating curve of **5c**

Table 3.4 DSC Results for (10)

Sample	Transitions Temperature °C (ΔH kJ mol-1)			
5a C8	131 °C (17.87)	212 °C (19.65)		
5b C10	112 °C (2.63)	130 °C (10.94)	203 °C (17.55)	
5c C12	110 °C (2.53)	134 °C (6.20)	202 °C (8.43)	
5d C14	62 °C (4.17)	104 °C (4.58)	127 °C (1.14)	186 °C (19.34)

Temperatures, and ΔH of the peaks found in DSC heating curves of ***5****. Numbers in brackets refer to absorption (+) or emission (-) of energy measured in kJ mol*$^{-1}$

3.11 Summary and conclusions

Phenylazo derivatives of the nickel tetraazaannulene complexes are readily prepared and have unusual thermal behaviour. Melting and cooling the crystals produces a glassy material which recrystallises on reheating. It is proposed that this behaviour is due to bulky side benzene groups which prevent efficient packing of the rod like molecules. Synthesis of a related class of macrocyclic complexes without benzene or methyl substituents was attempted, but it was difficult to obtain pure products. Similar macrocyclic complexes with methyl substituents were successful. These do indeed show liquid crystalline phases. They also display a number of other solid state transitions associated with thermochromism which are proposed to be caused by conformational changes in the ethylene side chains.

REFERENCES

1 A. M. Giroud-Godquin and P. M. Maitlis, *Angew. Chem. Int. Ed. Engl.*, 1991, **30**, 375.

2 F. Lely, G. Morelli, G. Ricciardi, A. Roviello and A. Sirigu, *Liquid Crystals*, 1992, **12**, 941.

3 C. Piechocki, J. Simon, A. Skoulios, D. Guillon, P. Weber, *J. Am. Chem. Soc.*, 1982, **104**, 5245.

4 I. Chambrier, M. J. Cook, M. Helliwell and A. K. Powell, *J. Chem. Soc. Chem. Commun.*, 1992, 444.

5 Y. Okuono, W. E. Ford and M. Calvin, *Synthesis*, 1980, 537.

6 M. Hanack, A. Beck and H. Lehmann, *Synthesis*, 1987, 703.

7 H. Schultz, H. Lehmann, M. Rein and M. Hanack, *Structure and Bonding 74*, Springer-Verlag: Heidelberg, 1991, 41.

8 F. Lelj, G. Morelli, G. Ricciardi and A. Rosa, *Polyhedron*, 1991, **10**, 523.

9 M. Hunziker, B. Hilti and G. Rihs, *Helv. Chim. Acta*, 1981, **64**, 82.

10 M. Hunziker and G. Rihs, *Inorg. Chim. Acta*, 1985, **102**, 39.

11 A. Wegmann, M. Hunziker and B. Tieke, *J. Chem. Soc. Chem. Commun.*, 1989, 1179.

12 F. Bonosi, F. Lely, G. Ricciardi, M. Romanelli and G. Martini, *Langmuir*, 1993, **9**, 268.

13 S. M. Critchley, M. R. Willis, M. J. Cook, J. McMurdo and Y Maruyama, *J. Mater. Chem.*, 1992, **2**, 157.

14 A. Wegmann, M. Hunziker and B. Tieke, *J. Chem. Soc. Chem. Commun.*, 1989, 1179.

15 J. A. Ouyang and A. B. P. Lever, *J. Phys. Chem.*, 1991, **95**, 2101.

16 P. J. Lukes, A. C. McGregor, T. Clifford and J. A. Crayston, *Inorg. Chem.*, 1992, **31,** 4697.

17 P. A. Forshey and T. Kuwana, *Inorg. Chem.*, 1983, **22**, 699.

18 C. L. Ni, C. K. Chang, I. Abdalmuhdi and F. C. Anson, *J. Phys. Chem.*, 1987, **91**, 1158.

19 M. J. S. Dewar and R. S. Goldberg, *Tetrahedron Lett.*, 1966, 2717.

20 P. Keller and L. Liebert, *Solid State Physics Supplement,* 1978, **14**, 19.

21 Vogel, *Textbook of Practical Organic Chemistry,* Longman, 4th edn., 712.

22 J. March, *Advanced Organic Chemistry*, J. Wiley and Sons, 1992.

23 D. P. Fisher, F. C. McElroy and D. J. Macero, J. C. Dabrowiak, *Inorg. Nucl. Chem. Lett.*, 1976, **12**, 435.

24 J. D. Goddard, *Inorg. Nucl. Chem. Lett.*, 1977, **13**, 555.

25 D. A. Place, G. P. Ferrara, J. J. Harland and J. C. Dabrowiak, *J. Heterocycl. Chem.*, 1980, **17**, 439.

26 M. C. Weiss and V. L. Goedken, *J. Am. Chem. Soc.*, 1976, **98**, 3389.

27 J. C. Dabrowiak, D. P. Fisher, F. C. McElroy and D. J. Macero, *Inorg. Chem.*, 1979, **18**, 2304.

28 J. Eilmes and E. Sledziewska, *Bull. Acad. Pol. Ser. Sci. Chim.*, 1978, **26**, 441.

29 W. Wedler, D, Demus, H. Zaschke, K. Mohre, W. Schafer and W. Weissflog, *J. Mater. Chem.*, 1991, **1**, 347.

30 P. J. Lukes, J. A. Crayston, D. J. Ando, M. E. Harman and M. B. Hursthouse, *J. Chem. Soc. Perkin 2*, 1991, 1845.

31 V. L. Goedken, J. J. Pluth, S.-M. Peng, and B. Burnsten, *J. Am. Chem. Soc.*, 1976, **96**, 8014.

32 V. L. Goedken and M. C. Weiss, *Inorg. Synth.*, 1980, **20**, 115.

33 T.S. Ma and R. C. Rittner, *Modern Organic Elemental Analysis*, Marcel Dekker, New York, 1979.

34 M. Wisniewski, *Polish Journal of Chemistry*, 1983, **57**, 593.

35 C. Reichardt and W. Grahm, *Chem. Ber.*, 1970, **103**, 1065.

36 F. A. L'Eplattenier and A. Pugin, *Helv. Chim. Acta*, 1975, **58**, 2283.

37 J. Eilmes, *Polyhedron*, 1991, **10**, 1779.

38 G. J. Lestina and T. H. Regan, *J. Org. Chem.*, 1969, **34**, 1685.

39 G. W. H. Holm, W. Hemminger, and H. J. Flammersheim, *Differential Scanning Calorimetry*, Springer Verlag, Berlin, 1996.

40 C. Pugh and V. Percec, *J. Mater. Chem.*, 1991, **1**, 765.

41 H. O. Finklea, S. Fedyk and J. Schwab, *A.C.S. Symp. Ser.*, 1988, **378**, 431.

42 M. D. Porter, J. B. Bright, D. L. Allara and C. E. D. Chidsey, *J. Am. Chem. Soc.*, 1987, **109**, 3559.

43 J. Rusling, *Acc. Chem. Res.*, 1991, **24**, 75.

44 D. A. Van Galen and M. Majda, *Anal. Chem.*, 1988, **60**, 1549.

45 J. P. Costes and G. Cros, *C. R. Acad. Sc. Paris Ser. B*, 1982, **294**, 173.

46 J.P. Costes, *Polyhedron*, 1987, **6**, 2169.

47 D. R. Bloomquist and R. D. Willett, *Coord. Chem. Rev.*, 1982, **47**, 125.

48 I. Grentre, P. Paoletti, M. Sandstrom and S. Glikberg, *Inorg. Chem.*, 1979 **18**, 2687.

49 J. Eilmes, S. A. Hodorowicz, B. J. Oleksyn, B. Panek and J. Sliwinski, *Acta Physica Polonica*, 1988, **A74**, 511.

50 F. A. L'Eplattenier and A. Pugin, *Helv. Chim. Acta,* 1975, **58**, 917.

50 D. M. L. Goodgame, M. Goodgame and M. J. Weeks, *J. Chem. Soc.*, 1964, 5199.

51 N. S. Gill and R. S. Nyholm, *J. Inorg. Nucl. Chem.*, 1961, **18**, 88.

52 N. P. Buu-Hoi, M. Gautier and N. Dat Xuong, *Bull. Soc. Chim. Fr.*, 1962, 2154.

Appendix 3.1

Synthesis

Dichlorodipyridinenickel(II)[51, 52] Py_2NiCl_2 - A solution of pyridine (Fischer) (13.68 g) in ethanol (56 ml) was added to a solution of nickel chloride hexahydrate (Aldrich) (41.12 g) in ethanol (231 ml). The greenish precipitate was filtered and washed with ethanol (with a small amount of pyridine added) and dried under vacuum. Yield 55 %.

Sodium methoxide NaMeO- Sodium (Fisons) (10 g) was cut into small pieces and placed in a dry three necked round bottomed flask. Methanol was added slowly but at a rate sufficient to maintain vigorous reaction. The resulting solution was evaporated to produce a dry white powder of NaMeO which was kept dry to prevent production of NaOH. Yield quantitative.

7-Amino-4-methyl-5-aza-3-hepten-2-one AEH intermediate[45]- Acetylacetone (Lancaster) (21.6g) in 200 ml of dichloromethane was slowly added to ethylenediamine (Aldrich) (13 g) in 200 ml of dichloromethane with vigorous stirring. The mixture was stirred overnight and the water layer which formed from the condensation reaction was separated before being evaporated down to pure AEH, an orange liquid. This was normally used immediately as over time it forms crystals of 3/4 macrocycle. Yield 100 %.

$\delta_H(CDCl_3)$ 1.5 (2 H, s, NH_2), 1.95 (3 H, s, CH_3), 2.0 (3 H, s, CH_3), 2.9 (2 H, m, CH_2N), 3.2 (2 H, m, CH_2N), 5.0 (1 H, s, CH), 10.9 (1 H, bs, OH). IR cm^{-1} (KBr) 3447,

2920, 2850, 2362, 2343, 1647, 1588, 1497, 1473, 1389, 1326, 1241, 1181, 1096, 1019, 965, 836, 814, 720, 669, 564, 534,

M/z 142 (M^+).

5, 7, 12, 14-Me_4[14] hexaenato(2-)N_4 Ni 4MeNiEth **(8)** [46]-

Dichlorodipyridinenickel(II), Py_2NiCl_2 (2 g), and sodium methoxide NaMeO (0.75 g) were added to AEH (2 g) in methanol (60 ml). The solution was refluxed for 24h, then cooled. The red solution precipitated crystals of **8** which were then recrystallised from toluene. Yield typically 5 %. $\delta_H(CDCl_3)$ 1.95 (6 H, s CH_3), 3.15 (4 H, s NCH_2), 4.6 (1 H, s, bri); $\delta_C(CDCl_3)$ 21.2, 53.4, 96.9, 158.4. IR cm^{-1} (KBr) 1576, 1570, 1554, 1542, 1529, 1474, 1437, 1412, 1364, 1354, 1130, 1041, 1011, 725, *M/z* 304 (M^+).

p-Hydroxyacetanilide (Acetamidophenol)- 24 ml of acetic anhydride (Aldrich) was added to 22 g of 4-aminophenol (Aldrich) suspended in 100 ml H_2O. This was heated on a water bath and more acetic anhydride was added (30 ml) until solid had dissolved. This was stirred for 10 minutes cooled, and filtered to yield a grey precipitate. Yield 100 %.

p-n-Alkoxyaniline *p*-Hydroxyacetanilide[20,53] (2 g) was dissolved in ethanol (10 ml) by gentle heating. Potassium hydroxide (Fisons) (0.93 g) dissolved in the minimum amount of H_2O was added dropwise to form the potassium salt. A stoichiometric amount of the long chain alkyl bromide in ethanol (20 ml) was added dropwise. The mixture was refluxed for 1 h, cooled and filtered. The grey/brown waxy solid *p-n*-alkoxyacetanilide was washed with water and can be recrystallised or used directly in the next stage (deprotection). Yield typically >83 %.

p-n-Octyloxyacetanilide $\delta_H(CDCl_3)$ 0.9 (3 H, t, CH_3) 1.2-1.55 (10 H, m, chain), 1.75 (2 H, m, C**H**$_2$ CH_2O), 2.15 (3 H, s, CH_3CO), 3.9 (2 H, t, CH_2O), 6.85 (2 H, d, ar) 7.35 (2 H, d, ar.)

p-n-Dodecyloxyacetanilide $\delta_H(CDCl_3)$ 1.0 (3 H, t, CH_3) 1.2-1.6 (18 H, m, chain), 1.85 (2 H, m, C**H**$_2$ CH_2O), 2.25 (3 H, s, CH_3CO), 4.0 (2 H, t, CH_2O), 6.9 (2 H, m, ar) 7.45 (2 H, m, ar). *M/z* 319 (M^+).

p-n-Tetradecyloxyacetanilide $\delta_H(CDCl_3)$ 0.9 (3 H, t, CH_3), 1.3-1.8 (22 H, m, chain), 2.2 (3 H, s, CH_3CO), 3.9 (2 H, t, CH_2O), 6.9 (2 H, m, ar) 7.45 (2 H, m, ar) 7.1 (1 H, sb, NH).

Deprotection of Alkoxyanilide

p-n-Alkoxyacetanilide (0.025 mole) in 25 ml ethanol was refluxed and 3.5 ml of 20 M solution of potassium hydroxide (Fisons) was added and solution refluxed for 6 h. The ethanol is removed and the product is cooled, filtered and washed with water until neutral (often dissolved in dichloromethane and washed with water). The crude product was recrystallised from an ethanol and 40-60 pet. ether mixture, the ratio depending on chain length.. Yield typically 78 %.

p-Octyloxyaniline $\delta_H(CDCl_3)$ 0.85 (3 H, t, CH_3),1.1-1.5 (10 H, m, chain), 1.75 (2 H, quintet, C**H**$_2$$CH_2O$), 3.3 (2 H, s, NH_2), 3.85 (2 H, t, CH_2O), 6.6-6.8 (4 H, dd, ar). *M/z* 221 (M^+).

p-Decyloxyaniline *M/z* 249 (M^+).

p-Dodecyloxyaniline $\delta_H(CDCl_3)$ 1.0 (3 H, tb, CH_3), 1.2-1.7 (18 H, m, chain), 1.85 (2 H, m, CH_2CH_2O), 3.1 (2 H, bs, NH_2), 4.0 (2 H, m, CH_2O), 6.6 -7.0 (4 H, m, ar). *M/z* 277 (M^+).

p-Tetradecyloxyaniline $\delta_H(CDCl_3)$ 0.85 (3 H, t, CH_3), 1.25 (22 H, s, chain), 1.8 (2 H, m, CH_2CH_2O), 3.4 (2 H, s, NH_2), 3.8 (2 H, t, CH_2O), 6.6 -6.8 (4 H, dd, ar). $\delta_C(CDCl_3)$ 14.02, 22.6, 25.98, 26.12, 29.28, 29.35, 29.52, 29.59, 31.84, 68.57, 114.58, 115.52, 116.29, 121.77, 139.72, 152.20. IR cm^{-1} (KBr) 3600, 3388, 2931, 2349, 2281, 1672, 1519, 1464, 1377, 1300, 1250, 1097, 1041, 1027, 878, 829, 816, 720. *M/z* 305 (M^+).

p-Hexadecyloxyaniline *M/z* 333 (M^+).

[5, 7, 12, 14-Me_4-2, 3: 9, 10-Bzo_2[14] hexaenato(2-)N_4] Ni(II)- Ni **4**[32]

Nickel acetate tetrahydrate (Aldrich) (50 g), *o*-phenylenediamine (Aldrich) (43.47 g) and 2,4-pentanedione (Lancaster) (40.3 g) in 500 ml of methanol was refluxed for 95 h. Product was cooled, filtered and recrystallised from toluene. Yield 42.4 % $\delta_H(CDCl_3)$ 2.05 (12 H, s, CH_3) 4.9 (2 H, s, bri), 6.3 (8 H, d, ar) . $\delta_C(CDCl_3)$ 22.6, 111.69, 121.40, 122.33, 147.86, 155.95 IR cm^{-1} (KBr) 3436, 1636, 1546, 1466, 1397, 1275, 1206, 1035, 752.

[5, 7, 12, 14-Me_4-2, 3: 9, 10-Bzo_2[14] hexaene N_4]ligand **2**

HCl (anhydrous) was bubbled through a suspension of the nickel complex in ethanol until the solution is acidic and a precipitate of blue green $[C_{22}H_{26}N_4]$ $[NiCl_4]$ was formed. This was cooled to 0°C for 1 hr, then filtered. This was changed to the hexafluorophosphate salt by dissolving in a small amount of water and adding a twofold

excess of ammonium hexafluorophosphate (Fluka) (or potassium hexafluorophosphate (Avocado)) in the minimum amount of water slowly. This was stirred for 30 minutes, filtered and washed with water. Green traces of unreacted material were removed with dichloromethane. The free ligand was obtained by neutralising a suspension of the hexafluorophosphate salt in methanol with triethylamine (Aldrich). The yellow product precipitate was washed with methanol and dried. The process was repeated to remove all traces of starting material. Yield 50.5 %.

$\delta_H(CDCl_3)$ 2.0 (12 H, s), 4.9 (2 H, s, bri), 7.0 (8 H, s, ar), 12.58 (bs, NH). IR cm^{-1} (KBr) 3436, 1619, 1554, 1510, 1463, 1382, 1365, 1295, 1276, 1188, 1028, 805, 745. Found: 76.09 %C 7.17 %H 15.78 %N, theoretical: 76.71 % C 7.02 % H 16.62 %N, $C_{22}H_{24}N_4$.

M/z 345 (M^+).

[6, 13 Alkoxphenyldiazo, 5, 7, 12, 14-Me_4-2, 3: 9, 10-Bzo_2[14] hexaenato(2-)N_4] M (M = Ni, H_2 or Co **6** A suspension of *p-n*-alkoxyaniline in an equal mixture of water and conc HCl was cooled in an ice bath and kept between 0 and 5 °C while a solution of sodium nitrite (Aldrich) was added slowly until starch iodide paper turned blue (indicating nitrous acid). Acetonitrile was added to the solution. The resulting liquid containing the diazonium salt was added simultaneously with triethylamine (Aldrich) to a large conical flask containing a suspension of **2** (M = Ni or H_2) in acetonitrile at 50 °C. This was left overnight filtered, and recrystallised from various solvents.

[6, 13, Phenyldiazo 5, 7, 12, 14-Me_4-2, 3: 9, 10-Bzo_2[14] hexaenato(2-)N_4] Ni(II) **6a** - A dark blue powder, Yield 80 % $\delta_H(CDCl_3)$ 2.65 (12 H, s, CH_3), 6.75 (4 H, m, ar mac) 6.9 (4 H, m, ar mac), 7.2 (s, ar chain) 7.4 (t, ar chain) 7.6 (d, ar chain).

M/z 609 (M^+).

6, 13, Butylphenyldiazo 5, 7, 12, 14-Me_4-2, 3: 9, 10-Bzo_2[14] hexaenato(2-)N_4] Ni(II) **6b** - A Blue / black microcrystalline, Yield 25 % $\delta_H(CDCl_3)$ 0.9 (3 H, t,), 1.2-1.7 (6 H, m, chain),2.6 (6 H, s, CH_3), 6.75 (2 H, m, ar mac) 6.9(2 H, m, ar mac), 7.2 (4 H, t, ar chain) 7.55 (4 H, d, ar chain).

M/z 721 (M^+).

6, 13, Octyloxyphenyldiazo 5, 7, 12, 14-Me_4-2, 3: 9, 10-Bzo_2[14] hexaenato(2-)N_4] Ni(II) **6c** -A green blue powder yield 75 % $\delta_H(CDCl_3)$ broad spectrum (paramagnetic),0.95 (s, CH_3), 1.3 (s, chain), 2.55 (s, CH_3), 6.5-7.1 (m, ar mac), 7.6 (d, ar chain). IR cm^{-1} (KBr) 3430, 2923, 2852. 1600, 1579, 1534, 1498, 1463, 1425, 1397, 1364, 1302, 1241, 1154, 1100, 1024, 832, 744.

6, 13, Octyloxyphenyldiazo 5, 7, 12, 14-Me_4-2, 3: 9, 10-Bzo_2[14] hexaenato(2-)N_4] Co(II) **6c** - Cobalt acetate tetrahydrate (B.D.H.) (0.125 g) in methanol (10 ml) was degassed with N_2 and added to ligand **6c** (0.1 g) dissolved in N_2 degassed acetonitrile (30 ml) excluding air. This mixture was refluxed for 10min and left for 1h. The product was filtered washed and dried under vacuum. Compound changed from bright yellow to dark green indicating complexation. NMR gave broad peaks because of the

paramagnetic nature. IR cm^{-1} (KBr) 3436, 2927, 2855, 2361, 2341, 1629, 1508, 1474, 1384, 1246, 753, 669, 403. Yield 37 %

6, 13, Octyloxyphenyldiazo 5, 7, 12, 14-Me_4-2, 3: 9, 10-Bzo_2[14] hexaenato(2-)N_4] Ligand- **6c** Yellow precipitate from red solution formed. Yield 66 % $\delta_H(CDCl_3)$ 0.9 (6 H, t, CH_3), 1.2-1.5 (20 H, s chain), 1.8 (4 H, m, C**H**$_2CH_2O$), 2.25 (6 H, s, CH_3 mac) 2.45 (6 H, s, CH_3 mac), 3.9 (4 H, m, CH_2O), 6.7-7.6 (16 H, m, ar), 10.9 (2 H, s, NH); $\delta_C(CDCl_3)$ 14.10, 14.51, 19.80, 22.66, 23.31, 26.07, 29.25, 29.39, 31.82, 68.52, 114.61, 114.76, 115.41, 119.81, 120.18, 122.41, 123.84, 124.46, 125.00, 137.30, 137.42, 138.09, 142.78, 154.40, 162.97, 164.59, 169.22

6, 13, Tetradecyloxyphenyldiazo 5, 7, 12, 14-Me_4-2, 3: 9, 10-Bzo_2[14] hexaenato(2-)N_4] Ni(II) **6d** -Dark green micro crystals. Yield 60 %. $\delta_H(CDCl_3)$ 0.9 (t) 3H CH_3, 1.1-1.6(24 H, m, chain), 2.55 (6 H, s, CH_3), 4.0 (2 H, t, CH_2O), 6.5-6.9 (m) 7.5δ (8 H, d, ar). IR cm^{-1} (KBr) 3430, 2919, 2850, 1597, 1546, 1491, 1467,1426, 1376, 1347, 1302, 1242, 1154, 1104, 1020, 843, 747, 527

Found: 71.27 %C, 8.34 %H, 10.62 %N, theoretical: 72.01 %C, 8.38 %H, 10.84 %N, $C_{62}H_{86}N_8O_2Ni_1$

FAB M+H 1034

6, 13 Alkoxyphenyldiazo 5, 7, 12, 14-Me_4[14] hexaenato(2-)N_4 **8a-e** were prepared in a manner analogous to **6** and in general gave the best crystals when recrystallised from DMF (dimethylformamide) (normally twice occasionally three times)

6, 13 Octyloxyphenyldiazo 5, 7, 12, 14-Me_4[14] hexaenato(2-)N_4 Ni(II) **8a**

Red/brown lustrous crystals (plates) Yield 33 % $\delta_H(CDCl_3)$ 0.9 (3 H, sb, CH_3), 1.2-1.6(12 H, m, chain), 2.45 (6 H, s, CH_3), 3.45 (4 H, s, CH_2N), 3.95 (2 H, t, CH_2O), 6.85 (4 H, d, ar) 7.5 (4 H, d, ar). $\delta_C(CDCl_3)$ 14.12, 20.95, 22.66, 26.01, 29.15, 29.23, 29.33, 31.80, 53.57, 68.20, 114.07, 131.81, 131.96, 134.35, 159.35, 162.66, 198.95 ppm. IR cm^{-1} (KBr) 3432 2921 1560 1378, 1290, 1230, 1191, 1011 .

Found: 64.72 %C, 7.97 %H, 14.34 %N, theoretical: 65.54 %C, 8.11 %H, 14.55 %N, $C_{42}H_{62}N_8O_2Ni_1$

FAB M+H = 769.5

6, 13 Decyloxyphenyldiazo 5, 7, 12, 14-Me_4[14] hexaenato(2-)N_4 Ni(II) **8b**

Red/orange lustrous crystals Yield 25 %. $\delta_H(CDCl_3)$ 0.9 (sb) 3H CH_3, 1.2-1.8 (16 H, m, chain), 2.45 (6 H, s, CH_3), 3.45 (4 H, s, CH_2N), 3.95 (2 H, t, CH_2O), 6.85 (2 H, d, ar), 7.5 (2 H, d, ar). IR cm^{-1} (KBr) 3442, 2921, 1560, 1492, 1458, 1425, 1379, 1347, 1291, 1237, 1192, 1105, 1010, 838, 474 .

Found: 66.02 %C, 8.44 %H, 13.33 %N, theoretical: 66.91 %C, 8.54 %H, 13.37 %N, $C_{46}H_{70}N_8O_2Ni_1$

FAB M+H 826

6, 13 Dodecyloxyphenyldiazo 5, 7, 12, 14-Me_4[14] hexaenato(2-)N_4 Ni(II) **8c**

Brown lustrous crystals. Yield 25 %. $\delta_H(CDCl_3)$ 0.9 (3 H, sb, CH_3), 1.2-1.6(20 H, m, chain), 2.45 (6 H, s, CH_3), 3.5 (4 H, s, CH_2N), 3.95 (2 H, t, CH_2O), 6.85 (4 H, d, ar) 7.5 (4 H, d, ar). IR cm^{-1} (KBr) 3448, 2921, 2851, 1598, 1560, 1492, 1453, 1425, 1401, 1378, 1347, 1311, 1291, 1230, 1218, 1192, 1010, 839, 809, 720, 550, 479.

Found: 65.31 %C, 8.71 %H, 12.30 %N, theoretical: 68.10 %C, 8.91 %H, 12.71 %N, $C_{50}H_{78}N_8O_2Ni_1$

FAB M+H 882

6, 13 Tetradecyloxyphenyldiazo 5, 7, 12, 14-Me_4[14] hexaenato(2-)N_4 Ni(II) **8d**.

Red microcrystals. Yield 30 % $\delta_H(CDCl_3)$ 0.9 (3 H, t, CH_3), 1.2-1.6 (24 H, m, chain), 2.45 (6 H, s, CH_3), 3.4 (4 H, s, CH_2N), 3.95 (2 H, t, CH_2O), 6.85 (4 H, d, ar) 7.5 (4 H, d, ar). $\delta_C(CDCl_3)$ 14.1, 22.7, 26.0, 29.3, 29.4, 29.6, 29.7, 31.9, 68.4, 114.45, 115.1, 126.5, 129.3. IR cm^{-1} (KBr) 3433, 2920, 1560, 1492, 1474, 1378, 1238, 1011, 474.

Found: 68.20 %C, 9.31 %H, 11.36 %N, theoretical: 69.13 %C, 9.24 %H, 11.95 %N, $C_{54}H_{86}N_8O_2Ni_1$

6, 13 Hexadecyloxyphenyldiazo 5, 7, 12, 14-Me_4[14] hexaenato(2-)N_4 Ni(II) **8e**

Red microcrystals Yield 7 % $\delta_H(CDCl_3)$ 0.9 (3 H, sb, CH_3), 1.1-2.0 (1 H, m, chain), 2.45 (6 H, s, CH_3), 3.45 (4 H, s, CH_2N), 3.95 (2 H, t, CH_2O), 6.95 (4 H, d, ar) 7.6 (4 H, d, ar). $\delta_C(CDCl_3)$ 14.64, 21.44, 23.19, 26.5, 29.64, 29.74, 29.86, 30.09, 30.18, 32.41, 54.06, 68.69, 110.94, 114.55, 132.3, 134.83, 159.82, 163.15, 177.56, 199.44. IR cm^{-1} (KBr) 3448, 2919, 2851, 1560, 1492, 1378, 1347, 1312, 1292, 1237, 1193, 1010, 839, 809 .

Found: 62.03 %C, 8.42 %H, 10.24 %N, theoretical: 70.08 %C, 9.53 %H, 11.27 %N, $C_{58}H_{94}N_8O_2Ni_1$

FAB M+H 994

6, 13 Methoxyphenyldiazo 5, 7, 12, 14-Me_4[14] hexaenato(2-)N_4 Ni(II) **8f**

$\delta_H(CDCl_3)$ 1.55 (12 H, s, CH_3), 2.5 (8 H, s, CH_2N), 3.6 (6 H, sb, CH_3O), 6.9 (4 H, d, ar), 7.6 (4 H, m, ar).

p-Alkoxyphenyldiazomalonaldehydes[35] **12** Malonaldehyde bisdimethylacetal (Fluka) (16.4 g) was stirred vigorously with 25 ml of 0.5 M HCl until a homogeneous liquid was formed (about half an hour). To this solution was added the diazonium salt of the alkoxyphenylamine prepared in a similar manner to the previous synthesis. Sodium acetate (Aldrich) was added to neutralise HCl . The highly coloured solid formed was filtered dissolved in dichloromethane, washed with water and dried with magnesium sulphate. The solvent was removed and the product was recrystallised (ethyl acetate). Yield typically 37 %. (The low yield is due to decomposition of diazonium salt and incomplete reaction of long chain amine and salt due to solubility problems).

p-Phenyldiazomalonaldehyde **12a** Red crystals Yield 70 %. $\delta_H(CDCl_3)$ 7.3-7.6 (5 H, m, ar) 9.65 (1 H, s) 10.0 (1 H, s). $\delta_C(CDCl_3)$(18.4, 58.36)EtOH, 116.86, 127.27, 129.81, 133.21, 140.52, 186.59, 189.79. IR cm^{-1} (KBr) 3436, 2852, 2361, 1670, 1636, 1593, 1531, 1489, 1461, 1409, 1352, 1320, 1304, 1250, 955, 762, 733. *M/z* 176 (M^+).

p-Methoxyphenyldiazomalonaldehyde **12b** Red powder Yield 65 %. $\delta_H(CDCl_3)$ 3.85 (3 H, s, CH_3O), 6.95 (2 H, d, ar) 7.45(2 H, d, ar), 9.6 (1 H, s, CHO) 9.9 (1 H, s, CHO). $\delta_C(CDCl_3)$ 55.64, 115.07, 118.42, 132.92, 134.02, 159.04, 186.08, 189.68. *M/z* 206 (M^+).

p-Octyloxyphenyldiazomalonaldehyde **12c** Red microcrystals Yield 77 %. $\delta_H(CDCl_3)$ 0.85 (3 H, sb, CH_3), 1.2-1.6(10 H, m, chain), 1.8 (2 H, m, C**H**$_2$$CH_2O$), 3.9 (2 H, t, CH_2O), 6.7-7.3 (4 H, m, ar) $\delta_C(CDCl_3)$ 14.12, 22.67, 26.07, 29.25, 29.37, 31.82, 36.12, 53.02, 53.44, 67.86, 68.26, 101.74, 114.46, 115.33, 120.42, 121.11, 129.38, 159.10.

p-Decyloxyphenyldiazomalonaldehyde **12d** Orange crystals Yield 75 %. $\delta_H(CDCl_3)$ 0.85 (3 H, t, CH_3), 1.2-1.6(14 H, m, chain), 1.8 (2 H, m, C**H**$_2$$CH_2O$), 3.95 (2 H, t, CH_2O), 6.7-7.3 (4 H, m, ar), 9.6 (1 H, s, CHO) 9.9 (1 H, s, CHO).

p-Dodecyloxyphenyldiazomalonaldehyde **12e** Orange/yellow lustrous crystals Yield 36 % $\delta_H(CDCl_3)$ 0.85 (3 H, t, CH_3), 1.2-1.6(18 H, m, chain), 1.8 (2 H, quint, C**H**$_2$$CH_2O$), 3.95 (2 H, t, CH_2O), 6.7-7.3 (4 H, m, ar), 9.6 (1 H, s, CHO) 9.9 (1 H, s, CHO). $\delta_C(CDCl_3)$ 14.15, 22.72, 26.03, 29.21, 29.39, 29.61, 31.94, 68.46, 68.54, 115.46, 118.42, 119.19, 121.44, 132.99, 133.67, 158.75, 189.11, 189.63.
M/z 361 (M^+).

p-Tetradecyloxyphenyldiazomalonaldehyde **12f** Orange crystals. Yield 50 %. $\delta_H(CDCl_3)$ 0.9 (3 H, sb, CH_3), 1.2-1.65 (22 H, m, chain), 1.8 (2 H, m, C**H**$_2$$CH_2O$), 4.0 (2 H, q, CH_2O), 6.9 (2 H, m, ar) 7.5 (4 H, m, ar); $\delta_C(CDCl_3)$ 14.65, 23.20, 26.53, 29.73, 29.87, 30.10, 30.17, 32.43, 68.88, 115.75, 115.88, 119.67,121.90, 144.10, 191.12. IR cm^{-1} (KBr) 3429, 2919, 2851, 1699, 1677, 1600, 1579, 1513, 1475, 1395, 1249, 1109, 1039, 830, 719, 506. *M/z* 389 (M^-).

p-Hexadecyloxyphenyldiazomalonaldehyde **12g** Orange microcrystals, used directly in the next stage.

7 3/4 formed macrocycle An intermediate in the formation of the ethylenediamine based macrocycles, this was isolated only a few times to ensure reaction was proceeding as expected, otherwise was used in the next stage as crude product.

The procedure was based on preparation of macrocycles without aliphatic tails by Pugin and L'Eplattenier[50]

7 *o*-phenylenediamine (Aldrich) (0.26 g) and nickel acetate tetrahydrate (Aldrich) (0.6 g) in glycolmonomethyl ether (2-methoxyethanol) (5 ml) was heated at 60 °C for 30 min under N_2. *p*-Alkoxyphenyldiazomalonaldehyde **12** (0.005 mol) was warmed in glycolmonomethylether (15 ml) and added to the reaction. The mixture was heated at 60 °C-17 °C for 2 h under N_2. This was then cooled filtered and washed with ethanol and acetone and dried under vac. Black sticky tar. Yield 38 %.

Crude product from **7** was used directly to produce the complexes **5**. Complex **7** (0.5 g) was placed in a vast excess of ethylenediamine (Aldrich) (10 ml) and refluxed for two hours. The mixture was cooled, filtered, washed with ethanol and dried under vac. Yield 75.6 %, overall 30.8 %.

6, 13 Methoxyphenyldiazo [14] hexaenato(2-)N_4 Ni(II) **5a** Brown / red powder Yield 30 %

Found: 54.86 %C, 4.34 %H, 21.32 %N, theoretical: 55.73 %C, 5.07 %H, 21.66 %N, $C_{24}H_{26}N_8O_2Ni_1$

FAB MS M+H 517

6, 13 Octyloxyphenyldiazo [14] hexaenato(2-)N_4 Ni(II) **5a** Purple lustrous crystals $\delta_H(CDCl_3)$ 0.85 (3H t) CH_3, 1.1-1.8 (12 H, m, chain), 3.5 (8 H, s, CH_2N), 3.95 (4 H, t, CH_2O), 6.9 (4 H, d, ar)7.5 (4 H, d, ar), 7.7 (4 H, s, CHN) $\delta_C(CDCl_3)$ 14.12, 22.67, 26.06, 29.26, 29.31, 29.4, 31.83, 58.75, 68.28, 114.74, 122.18, 158.61.

Found: 63.49 %C, 7.28 %H, 15.48 %N, theoretical: 63.96 %C, 7.63 %H, 15.7 %N, $C_{38}H_{54}N_8O_2Ni_1$

6, 13 Decyloxyphenyldiazo [14] hexaenato(2-)N_4 Ni(II) **5b** Purple lustrous crystals $\delta_H(CDCl_3)$ 0.9 (6H t) CH_3), 1.1-1.8 (32 H, m, chain), 3.5 (8 H, s, CH_2N), 3.95 (4 H, t, CH_2O), 6.9 (4 H, d, ar) 7.6 (4 H, d, ar), 8.0 (4 H, sb, CHN)

Found: 57.8 %C, 7.56 %H, 15.85 %N, theoretical: 65.64 %C, 8.12 %H, 14.56 %N, $C_{42}H_{62}N_8O_2Ni_1$

6, 13 Dodecyloxyphenyldiazo [14] hexaenato(2-)N_4 Ni(II) **5c** Purple lustrous crystals. Yield 36 %. $\delta_H(CDCl_3)$ 0.9 (t) 6H CH_3, 1.1-1.6 (36 H, m, chain), 1.8 (4 H, t, C**H**$_2CH_2O$), 3.5 (8 H, s, CH_2N), 3.95 (4 H, t, CH_2O), 6.9 (4 H, d, ar) 7.6 (4H d, ar), 8.0 (4 H, sb, CHN); $\delta_C(CDCl_3)$ 14.14, 22.70, 26.06, 29.36, 29.44, 29.61, 29.65, 31.93, 58.79, 68.24, 114.66, 122.11, 122.70, 132.07, 147.49, 158.54. IR cm^{-1} (KBr) 3448, 2921, 1597, 1523, 1497, 1389, 1240, 1090.

Found: 66.99 %C, 8.16 %H, 13.5 %N, theoretical: 66.9 %C, 8.54 %H, 13.57 %N, $C_{46}H_{70}N_8O_2Ni_1$

6, 13 Tetradecyloxyphenyldiazo [14] hexaenato(2-)N_4 Ni(II) **5d** Red lustrous crystals Yield 46 % $\delta_H(CDCl_3)$ 0.9 (t) 6H CH_3, 1.1-1.6 (44 H, m, chain), 1.75 (4 H, m, CH_2CH_2O), 2.7 (8 H, t, CH_2N) 4 (4 H, t, CH_2O), 6.9 (4 H, d, ar), 7.55 (4 H, d, ar), 7.75 (4 H, s, CHN). IR cm^{-1} (KBr) 3435, 2920, 2851, 1604, 1499, 1392, 1241,. Found: 68.12 %C, 9.14 %H, 12.27 %N, theoretical: 61.8 %C, 8.91 %H, 12.71 %N, $C_{50}H_{78}N_8O_2Ni_1$

FAB MS peak 882 but also a peak at 929 corresponding to one phenyl one ethane group rather than two ethane groups.

6, 13 Hexadecyloxyphenyldiazo [14] hexaenato(2-)N_4 Ni(II) **5e** Low yield red powder. FAB 910 indicating 3/4 cyclised Schiff base complex with only one ethylenediamine.

CHAPTER 4

Benzoylation of Tetraazaannulenes

4.0 Introduction

In the production of LC materials the aggregate packing effects are the source of the unusual properties and the packing formation is derived from the structural and electronic properties of individual molecules. The previous chapter indicated that certain tetraazaannulenes are susceptible to electrophilic attack.[1-7] By altering the bulky side groups on the substituted macrocycle while retaining every other characteristic, over a range of chain lengths, we were able to attribute the changes in the properties to changes in the steric bulk of the macrocycle.[8] By changing the diazo coupling to a carboxyl linkage while retaining every other characteristic of the liquid crystalline molecules it is possible to isolate the effect of the different conformational characteristics of the linkage.

It has been found experimentally that catalytically active species exhibiting functions similar to that of a biological enzyme can be generated *in situ* by Fe^{III},[9,10] Mn^{III}[11] and Cr^{III}[12] porphyrins. In an effort to, ultimately, produce complex biological macrocycles Julita Eilmes[13-20] demonstrated a method of constructing peripherally substituted macrocycles based on the reaction between acid chlorides and Ni(TMTAA) **4**. The demetallisation, a procedure using harsh conditions has been reported to lead to the destruction of the macrocycle[21,22] or loss of substituents.[23] The method of Eilmes[13] based on the demetallation of the unsubstituted macrocycle using anhydrous HCl[24] was

more successful and has been adopted as the standard method for such reactions. Although limited to benzoyl chloride this work presented an avenue towards synthesising the type of liquid crystal molecules required.

The demetallated benzoyl compound exhibits two peaks on a DSC trace corresponding to two crystalline solid phases.[25] The material is actually a mixture of two crystal forms, orange and green of which the orange turns completely to green at 419K. An X-ray crystallography study reveals that the difference lies in the position of the benzoyl groups in a similar fashion to the *cis* and *trans* of the diazo groups of the previous chapter.

The long chain alkoxybenzoic acids needed for the synthesis of the disubstituted macrocycles have been reported previously and show remarkable liquid crystalline properties[26]. *p-n*-Octyloxybenzoic acid shows four transition on heating. A solid state transition at 75 °C solid to smectic at 101 °C, smectic to nematic at 108 °C and nematic to isotropic at 146 °C. The acids are probably present in the form of dimers through H-bonding at the acid head groups. Nevertheless, the joining of compounds with such striking LC properties at low temperatures suggested that the resulting metal containing compounds would also display such properties.

In this chapter the synthesis of a further range of compounds with a carbonyl linkage will be described and their properties compared with their diazo counterparts.

4.1 **Results : synthesis**

The bridgehead position of the TAA macrocycle is again the point of attack for the pendant arm substituents. The attacking substituents are, in this case, acyl chlorides. The first attempts using long chain carboxylic acids were not very successful. A small amount of product was obtained but the yield was negligible. It was reported by Bonosi

et al[27] that the yield for the hexadecanoyl substituted compound (the only one prepared) was 20 % but in our hands only 1 % of mixed mono and di-substituted product was obtained (Figure 4.1).

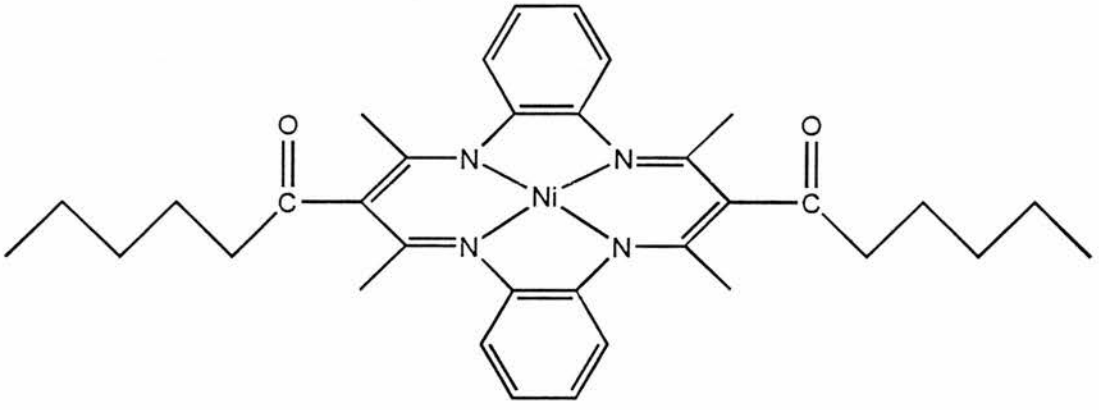

Figure 4.1

As with the diazo linkage it was found that there had to be a benzene group adjacent for the reaction to proceed at a reasonable rate. Reaction of commercially available molecules such as benzoic acid proved the reaction was viable. Although a mixture of products (mono and disubstituted) was formed, they were easily separated by column chromatography. The synthesis of the acids which would mimic the amines used in the last chapter proved more difficult. The synthesis was traced to a paper by Brynmor Jones[28] and it seemed that subsequent workers[26] who used these long chain *p*-alkoxybenzoic acids also used this method. It involved the reflux of the alkyl iodide, sodium hydroxide and *p*-hyroxybenzoic acid in an ethanol-water mixture. Isolation of the acid was achieved by addition of warm sulphuric acid after a few hours reflux. However, this apparently simple reaction gave negligible yields. Changing the solvents, the number of hours refluxed, using NaOH instead of KOH, and even a two phase reaction with benzyltributylammonium chloride as the transfer agent all failed to promote the reaction. After discussions with the organic chemistry colleagues a successful preparation was devised. Very small amounts of solvent were used and the *p*-

hydroxybenzoic acid was converted to the salt in pure methanol before the acyl halide in acetone was added dropwise and refluxed for an hour. This altered preparation is simple and gives good yields (Scheme 4.1).

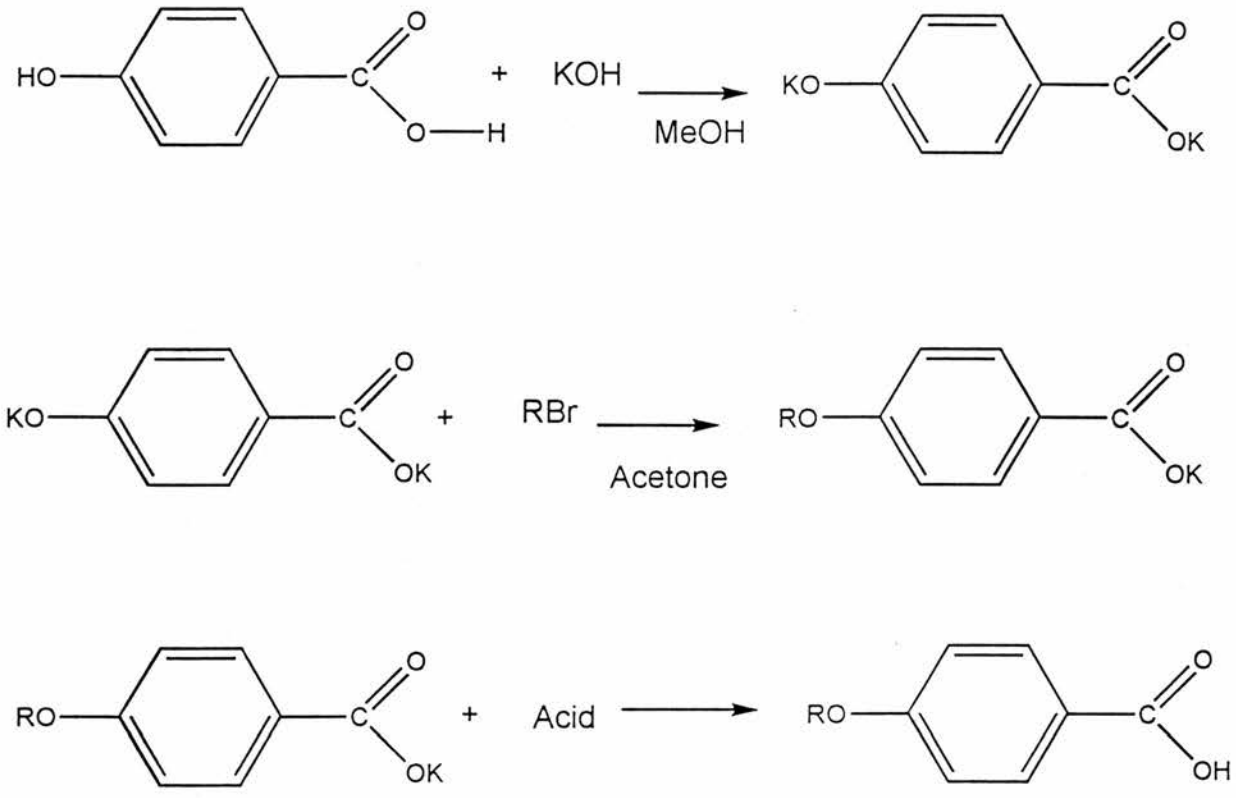

Scheme 4.1

Once a reliable preparation for *p*-alkoxybenzoic acids was found the conversion into acyl halides by refluxing in thionyl chloride was quite straightforward (Scheme 4.2). After the thionyl chloride was distilled off the acid chloride was purified by distillation under high vacuum in a kugelrohre apparatus.

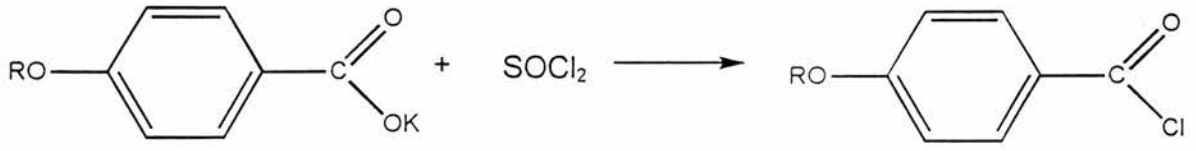

Scheme 4.2

The kugelrohre apparatus needed to be kept at its maximum operating temperature (250 °C) to distil the higher molecular weight compounds. The product was very pure and had the benefit of remaining stable, if dry, until needed, unlike the diazo salts which are explosive when solid and decompose more rapidly than the acid chlorides.

By the time a reliable method had been found to produce these compounds it was found that the bulky core of **4** was detrimental to the formation of LC phases. Therefore a complete series of compound **10** was not prepared only a selection were synthesised to screen their thermal behaviour.

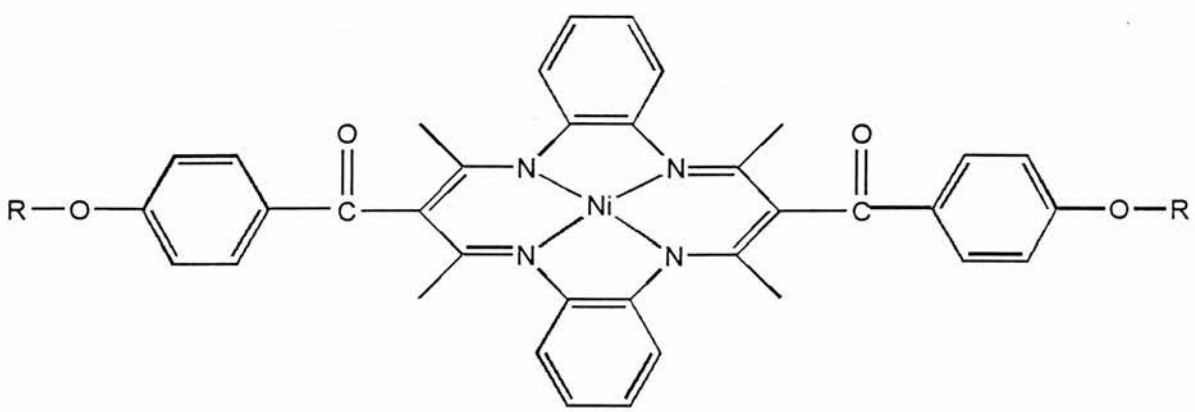

10

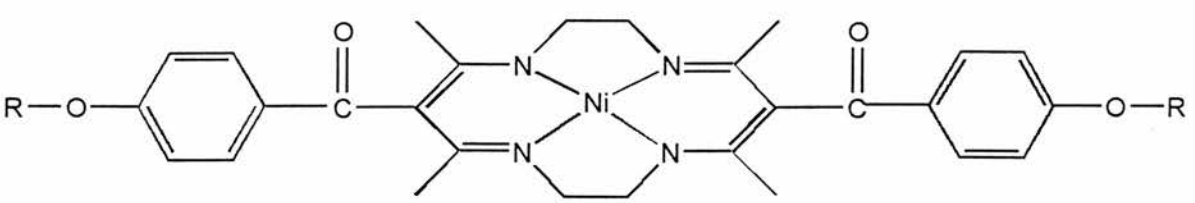

11

11a R = C_8H_{17}; **11b** R = $C_{10}H_{21}$; **11c** R = $C_{12}H_{25}$; **11d** R = $C_{14}H_{29}$ **11e** R = $C_{16}H_{33}$

Reactivity

^{1}H NMR is very useful in determining the extent of the reaction. If only one bridgehead C has a chain attached, the remaining proton, on the other bridgehead C, shows up clearly at 4.6-4.8δ. It was found that reactions involving **4** produced almost equal quantities of mono and di-substituted product which were readily separated by column chromatography. Reactions involving **8**, however produced only disubstituted product. Chromatography was used if needed to remove unreacted **8** in some preparations but in most it was sufficient to use an excess of acid chloride and recrystallise from acetone. The more reactive nature of **8** is put down to the absence of the benzene rings which act to remove electron density from the reactive bridgehead carbon.

4.2 DSC results

The first heating curve (Table 4.1) took the compounds to just over their melting points as determined previously on a conventional melting point apparatus. All transitions observed are solid state transitions occurring in the crystal lattice structure. The compounds appear to have fewer transitions as the chain length increases. It seems that the greater the aliphatic nature of the compounds the more suppressed or stabilised the transitions become.

Table 4.1 1st heating curves of 11

Sample	Transitions Temperature °C (ΔH kJ mol-1)			
11a (C8)	**79.95 (1.80)**	**94.97 (5.74)**	**208.01 (5.36)**	**244-250**
11b (C10)	**70.92 (5.61)**	**84.83 (12.22)**	**205.53 (12.11)**	**239.17 (43.53)**
11c (C12)	**108.31 (26.52)**	**230.15 (37.22)**		
11d (C14)	**90.66 (29.44)**	**233.19 (19.07)**		

Temperatures, and ΔH of the peaks found in DSC heating curves of ***11****. Numbers in brackets refer to absorption (+) or emission (-) of energy measured in kJ mol*$^{-1}$

Subsequent cooling and heating curves

11a cool 1 no peaks; heat 2 peak 238; cool 2 peak 205.94(-10.47)

11b cool 1 peak 184.82 (-12.77), 130.2 (-3.76), glass trans Tg 76.2; heat 2 decomposed,

11c cool 1 peak 153.49 (-4.59), 146.49 (-2.76); heat 2 decomposed

11d cool 1 peak 181.82 (-11.95), 125.32 (-3.64), glass trans Tg 75; heat 2 decomposed.

Little can be derived from the subsequent heating and cooling cycles because although the substitution of the diazo linkage with benzoyl linkage has added to the chemical stability of the compounds the high temperatures of the melting points continue to degrade the compounds. Two of the compounds did seem to display curves which relate to glass transitions on the first cooling cycle.

= c10co4mne h1

(10coh1)

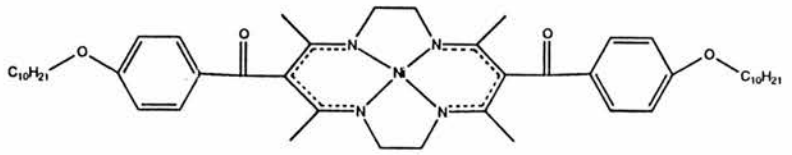

11b

Peak from: 63.12
to: 76.78
Onset= 69.11
J/g = 6.79

Peak from: 78.21
to: 91.15
Onset= 82.91
J/g = 14.80

Peak from: 196.81
to: 213.34
Onset= 202.12
J/g = 14.67

Peak from: 222.68
to: 245.32
Onset= 236.44
J/g = 52.71

Peak= 84.83

Peak= 70.92

Peak= 205.53

Peak= 239.77

HEAT FLOW (mW)

11.25
7.5
3.75
0

30.00 60.00 90.00 120.00 150.00 180.00 210.00 240.00

Temperature (C)

Date: Jan 12, 1994 6:48pm
Scanning Rate: 10.0 C/min
Sample Wt: 2.400 mg Path: C:\PE\
File 1: 10COH1 AM

ST ANDREWS UNIVERSITY

All samples were sealed in aluminium pans which had been heated in an oven 300 °C for at least 24 hours then washed with ether and dichloromethane to remove any grease.

4.3 Thermochromism

When viewed through a microscope fitted with a heated stage one of the phase changes associated with the peaks on the DSC can easily be detected. The phase change on the first heating curve at about 84 °C for **11b** can be seen without the need of cross polarisers, as the individual crystals almost jump up or dance as the temperature passes the transition range. This would seem to indicate that a massive internal rearrangement was occurring in the crystal and as the transition is reversible, at these relatively low temperatures, there are no changes to the chemical structure taking place. This can be seen in all the long chain examples correlating to the peak at about 90 °C. The distortion of the crystal is more pronounced than the corresponding diazo but takes place at roughly the same temperature. As before we have the possibility of conformational changes in the $Ni(en)_2$ ring system[29,30] but we also have the possibility of *cis-trans* isomerisation which was demonstrated by Eilmes.[25] Although the compound used by Eilmes is demetallated, based on **4** and without an aliphatic chain, the linkage of the benzoyl moiety is the same. She believes that the benzoyl linkage is the origin of the thermotropic phase changes.

The long chain itself could be the origin of some of the phase changes: it may not necessarily be completely *trans* as would be expected, or at a certain temperature it could begin to rotate accounting for the peaks in the DSC. However , the diazo linked dibenzo macrocycles with long chains do not have any phase changes below 100 °C the thermochromic effect is therefore unlikely to be due to the motions of the long chain.

It is not possible to assign the large number of solid state phase changes without more structural information. X ray crystallography at different temperatures would be one way to identify what each peak meant, however, the crystal size which could be obtained was simply not big enough or the correct shape. Powder diffraction X ray crystallography is not really practical with molecules of such a large and complex size with present methods.

Liquid crystalline properties

To test for liquid crystalline properties compounds **11** were placed under a crossed polariser microscope and subjected to a heating and cooling cycle. They were also sent to Prof. John Goodby at Hull University who has greater experience in detecting LC phase changes.

No liquid crystalline phase changes were detected. As described in Chapter 3 compounds **8** with a diazo linkage show smectic A mesophases; however, compounds **11,** which only differ in the linkage, do not show any LC phases.

The ether linkage on the chain is bent but is the same for both molecules. The *cis* and *trans* possibilities with the carbonyl linkage and the diazo linkage offer differences in overall shape. Even if the *cis trans* effect was not a factor the shape of carbonyl compound is not as linear.

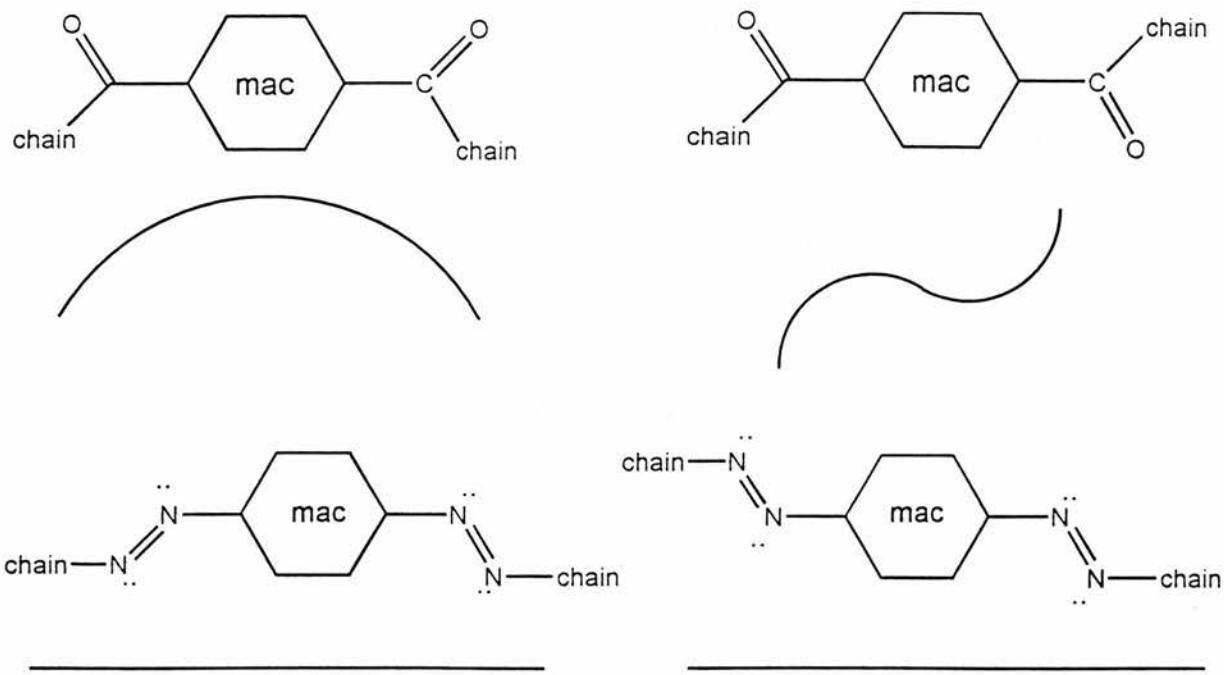

Figure 4.2

It was thought that the long chain length and hence the high length to width ratio would out weigh the effects of the unusual shape. The long chain was expected to dominate this condition by virtue of its great lability which would compensate for them starting at slightly different angles. The structures are now chemically more stable and less likely to decompose in the sample pan when subjected to heat; however, the melting point has not really been reduced by the changes. At such high temperatures, even if there was LC behaviour, there could only be limited use for such compounds.

4.5 Conclusions

An entirely new series of compounds have been synthesised. They are highly coloured and have several distinct solid state transitions.

The experiments conducted demonstrate the effect of replacing one particular part of a molecule on the overall physical properties. It was found that the LC properties found on the diazo linked molecules were not present on the carbonyl linked molecules.

The crystal solid phase conformational changes remain and indeed become more pronounced. The accompanying colour changes remain indicating that the linkage is not involved in this phase change and lending weight to the contribution of the enamine rings.

There is the possibility of changing the metal centre and increasing the chain length, and type, to determine more about how liquid crystalline properties are established.

Experimental: APPENDIX 4.1

References Chapter 4

1 D. P. Fisher, F. C. McElroy, D. J. Macero and J. C. Dabrowiak, *Inorg. Nucl. Chem. Lett.*, 1976, **12**, 435.

2 J. D. Goddard, *Inorg. Nucl. Chem. Lett.*, 1977, **13**, 555.

3 D. A. Place, G. P. Ferrara, J. J. Harland and J. C. Dabrowiak, *J. Heterocycl. Chem.*, 1980, **17**, 439.

4 M. C. Weiss and V. L. Goedken, *J. Am. Chem. Soc.*, 1976, **98**, 3389.

5 J. C. Dabrowiak, D. P. Fisher, F. C. McElroy and D. J. Macero, *Inorg. Chem.*, 1979, **18**, 2304.

6 J. Eilmes and E. Sledziewska, *Bull. Acad. Pol. Ser. Sci. Chim.*, 1978, **26**, 441.

7 M. Basato, G. Valle and J. Eilmes, *Inorg. Chim. Acta*, 1991, **190**, 19.

8 W. Wedler, D. Demus, H. Zaschke, K. Mohr, W. Schäfer and W. Weissflog, *J. Mater. Chem.*, 1991, **1**, 347.

9 J. T. Groves, T. E. Nemo and R. S. Myers, *J. Am. Chem. Soc.*, 1979, **101**, 1032.

10 J. T. Groves and T. E. Nemo, *J. Am. Chem. Soc.*, 1983, **105**, 5786.

11 J. T. Groves, W. J. Kruper and R. C. Haushalter, *J. Am. Chem. Soc.*, 1980, **102**, 6375.

12 J. T. Groves and W. J. Kruper, *J. Am. Chem. Soc.*, 1979, **101**, 7613.

13 J. Eilmes, *Polyhedron*, 1985, **4**, 943.

14 J. Eilmes, *Polyhedron*, 1988, **7**, 2197.

15 J. Eilmes, *Polyhedron*, 1991, **10**, 1779.

16 J. Eilmes, *Polyhedron*, 1987, **6**, 423.

17 J. Eilmes, *Pol. J. Chem.*, 1987, **61**, 405.

18 J. Eilmes, *Polyhedron*, 1989, **8**, 1243.

19 J. C. Dabrowiak, D. P. Fisher, F. C. McElroy and D. J. Macero, *Inorg. Chem.*, 1976, **18**, 2304.

20 S. J. Dzugan and D. H. Bush, *Inorg. Chem.*, 1990, **29**, 2528.

21 E. G. Jäger, *Z. Anorg. Allg. Chem.*, 1969, **364**, 177.

22 E. G. Jäger, *Z. Chem.*, 1968, **8**, 30.

23 V. L. Goedken and M. C. Weiss, *Inorg. Synth.* 1980, **20**, 115.

24 D. P. Riley and D. H. Busch, *Inorg. Synth.*, 1978, **18**, 41.

25 J. Eilmes, S. A. Hodorowicz, B. J. Oleksyn, B. Panek and J. Sliwinski, *Acta Physica Polonica*, 1988, **74**, 511.

26 A. J. Herbert, *J. Chem. Soc. Faraday Trans.*, 1967, **63**, 555.

27 F. Bonosi, F. Lely, G. Ricciardi, M. Romanelli and G. Martini, *Langmuir*, 1993, **9**, 268.

28 B. Jones, *J. Chem. Soc.*, 1935, 1874.

29 D. R. Bloomquist and R. D. Willett, *Coord. Chem. Rev.*, 1982, **47**, 125.

30 I. Grenthe, P. Paoletti, M. Sandstrom and S. Glikberg, *Inorg. Chem.*, 1979, **18**, 2687.

Appendix 4.1

Synthesis

p-n-Alkoxybenzoic acid To KOH (Fisons) (1.34 g) in MeOH (4 ml) was added *p*-hydroxybenzoic acid (BDH) (1.38 g) in MeOH (2 ml). Bromoalkane (slight molar excess) in acetone (8 ml) was added dropwise and the mixture refluxed for 1 h with overhead stirring. Addition of acetone and MeOH was required as reaction proceeded due to frothing of product. The mixture was cooled, water was added and alkyl bromide was removed by extraction with ether. The water layer was acidified and the precipitate filtered and recrystallised from glacial acetic acid and EtOH. Recrystallisation from EtOH provides product with high purity.

p-n-Alkoxybenzoyl chloride The *p-n*-alkoxybenzoic acid was refluxed in a large excess of thionlyl chloride (Fluka) for 1 h using dry glassware and calcium chloride dry traps. The excess thionyl chloride was removed by vacuum distillation (water tap vacuum). *p-n*-Alkoxybenzoyl chloride was purified by distillation under oil pump vacuum on a kugelrohre apparatus. Longer chain lengths were distilled at the highest temp (250 °C).

11 6, 13 bis (*p*-alkoxybenzoyl) 5, 7, 12, 14-Me_4[14] hexaenato(2-)N_4 Ni

Two molar equivalents of *p* alkoxybenzoyl chloride in dichloromethane were added to **8** (5, 7, 12, 14-Me_4[14] hexaenato(2-)N_4 Ni) in dichloromethane while simultaneously adding triethylamine (Aldrich) (2 molar equivalents) in dichloromethane. The precipitate formed was filtered and recrystallised from toluene / pet. ether, then again from acetone (analar grade).

p-Hydroxybenzoic acid δ_H(DMSO) 6.85 (2 H, d, ar), 7.85 (2 H, d, ar), 10.25 (1 H, bs, OH). δ_C(DMSO) 115.4, 121.63, 131.86, 161.87, 167.52.

p-n-Methoxybenzoic acid δ_H($CDCl_3$) 3.85 (3 H, s CH_3O), 6.95 (2 H, d, ar) 8.05 (2 H, d, ar). δ_C($CDCl_3$) 55.49, 113.72, 121.57, 132.34, 164.01, 171.63.

p-n-Hexyloxybenzoic acid δ_H($CDCl_3$) 0.9 (3 H, t, CH_3 ter), 1.3-1.55 (6 H, m, chain), 1.8 (2 H, quin, C**H**$_2$$CH_2O$), 4.0 (2 H, t, CH_2O), 6.9 (2 H, d, ar), 8.05 (2 H, d, ar).

p-n- Octyloxybenzoic acid δ_H($CDCl_3$) 1.9 (3 H, t, CH_3 ter), 1.4 (10 H, bs, chain), 1.8 (2 H, q, C**H**$_2$$CH_2O$), 4.0 (2 H, t, CH_2O), 7.95 (2 H, d, ar), 8.05 (2 H, d, ar). δ_C($CDCl_3$) 14.59, 23.15, 23.27, 26.47, 29.26, 29.45, 29.57, 29.71, 29.81, 30.00, 32.29, 68.78, 114.67, 121.87, 132.82, 164.17, 172.48. *M/z* 250 (M^-)

p-n-Decyloxybenzoic acid δ_H($CDCl_3$) 1.9 (3 H, tb, CH_3 ter), 1.3 (14 H, bs, chain), 1.8 (2 H, m, C**H**$_2$$CH_2O$), 4.0 (2 H, m, CH_2O), 7.95 (2 H m, ar), 8.05 (2 H, m, ar).

p-n- Dodecyloxybenzoic acid δ_H($CDCl_3$) 0.9 (3 H, tb, CH_3 ter), 1.35 (18 H, bs, chain), 1.85 (2 H, m, C**H**$_2$$CH_2O$), 4.0 (2 H, t, CH_2O), 6.9 (2 H, d, ar), 8.05 (2 H, d, ar).

p-n-Tetradecyloxybenzoic acid δ_H($CDCl_3$) 0.9 (3 H, t, CH_3), 1.25 (22 H, s, chain), 1.8 (2 H, quin, C**H**$_2$$CH_2O$), 4.0 (2 H, t, CH_2O), 6.95 (2 H, d, ar), 8.05 (2 H, d, ar). δ_C($CDCl_3$) 26.47, 29.58, 29.86, 30.08, 30.16, 30.29, 32.42, 68.78, 114.67, 132.80

(small peaks at 164 and 184). IR cm^{-1} (KBr) 2899, 1670, 1607, 1466, 1377, 1259, 846, 772.

p-n-Hexadecyloxybenzoic acid $\delta_H(CDCl_3)$ 0.9 (3 H, t, CH_3), 1.15 (26 H, s, chain), 1.8 (2 H, m, $C\mathbf{H}_2CH_2O$), 4.0 (2 H, t, CH_2O), 6.95 (2 H, d, ar), 8.05 (2 H, d, ar).

Alkoxybenzoyl chlorides although stable thermally are susceptible to attack by water vapour in the air. To reduce the amount of carboxylic acid present the alkoxybenzoyl chloride was normally used immediately in the next stage of preparation of the disubstituted macrocycle. Alkyl = CH_3, C_8H_{17}, $C_{10}H_{21}$, $C_{12}H_{25}$, $C_{14}H_{29}$ and $C_{16}H_{33}$ were prepared. Two were isolated as shown below.

p-n-methoxybenzoyl chloride Yield 92.6 %. *M/z* 170 (M^+).

p-n-octyloxybenzoyl chloride Yield 83 %. $\delta_H(CDCl_3)$ 0.85 (3 H, t, CH_3 ter), 1.3 (10 H, bs, chain), 1.8 (2 H, quin, $C\mathbf{H}_2CH_2O$), 4.0 (2 H, t, CH_3O), 6.9 (2 H, d, ar) 8.05 (2 H, d, ar).

6, 13 bis (*p*-methoxybenzoyl) 5,7,12,14-Me_4[14] hexaenato(2-)N_4 Ni(II) Red lustrous crystals. Yield 92.6 %. $\delta_H(CDCl_3)$ 0.85 (12 H, s, CH_3), 3.2 (8 H, s, CH_2N en), 3.85 (6 H, s, CH_3O), 6.9 (4 H, d, ar) 7.9 (4 H, d, ar). $\delta_C(CDCl_3)$ 21.01, 53.47, 53.59, 55.47, 110.47, 113.64, 131.82, 134.65, 159.43, 163.00, 198.93

6, 13 bis (*p*-octyloxybenzoyl) 5,7,12,14-Me_4[14] hexaenato(2-)N_4 Ni(II) **11a** Bronze lustrous crystals. Yield 83 %. $\delta_H(CDCl_3)$ 0.9δ (3 H, t, CH_3 ter), 1.2-1.6 (10 H, s, chain), 1.8 (2 H, b, C**H**$_2CH_2O$), 1.85 (6 H, s, CH_3 mac), 3.2 (4 H, s, CH_2N en), 4.0 (2 H, t, CH_2O), 6.9 (2 H, d, ar), 7.9 (2 H, d, ar). IR cm^{-1} (KBr) 3745, 2922, 2855, 1643, 1601, 1576, 1548, 1474, 1399, 1346, 1251, 1156. M.p. 242-254 °C (decomp)

Found: C 68.48 % H 7.14 % N 7.12 %, theoretical: C 68.66 %, H 8.12 %, N 7.28 %, $C_{44}H_{62}N_4O_4Ni_1$

FAB M + H 769

6, 13 bis (*p*-decyloxybenzoyl) 5,7,12,14-Me_4[14] hexaenato(2-)N_4 Ni(II) **11b** Orange waxy powder. Yield 22 % $\delta_H(CDCl_3)$ 0.85 (3 H, t, CH_3 ter), 1.2-1.45 (14 H, s, chain), 1.6 (2 H, s, C**H**$_2CH_2O$) 1.8 (6 H, s, CH_3 mac), 3.2 (4 H, s, CH_2N en), 4.0 (2 H, t, CH_2O), 6.9 (2 H, d, ar), 7.9 (2 H, d, ar). $\delta_C(CDCl_3)$ 14.12, 20.88, 22.69, 26.03, 29.18, 29.33, 29.37, 31.90, 53.59, 68.25, 110.49, 114.11, 131.82, 134.42, 159.30, 162.70, 198.93. M.p. 244 °C (decomp) IR cm^{-1} (KBr) 3433, 2922, 2851, 1617, 1599, 1570, 1546, 1465, 1407, 1343, 1313, 1252.

Found: C 69.03 % H 8.50 % N 6.72 %, theoretical: C 69.81 %, H 8.54 %, N 6.78 %, $C_{48}H_{70}N_4O_4Ni_1$

6, 13 bis (*p*-dodecyloxybenzoyl) 5,7,12,14-Me_4[14] hexaenato(2-)N_4 Ni(II) **11c** Yellow / Gold lustrous micro crystals. Yield 70 %. $\delta_H(CDCl_3)$ 0.9 (3 H, t, CH_3 ter), 1.3 (18 H, s, chain), 1.6 (2 H, s, C**H**$_2CH_2O$), 1.8 (6 H, s, CH_3 mac), 3.2 (4 H, s, CH_2N en), 4.0 (2 H, t, CH_2O), 6.9 (2 H, d, ar), 7.9 (2 H, d, ar). $\delta_C(CDCl_3)$ 14.12, 20.87, 22.69, 26.03, 29.18, 29.36, 29.60, 29.65, 31.93, 53.60, 68.25, 110.51, 114.12, 131.82, 134.43,

159.29, 162.70, 198.93 . IR cm^{-1} (KBr) 2920, 2852, 1643, 1601, 1576, 1548, 1474, 1399, 1346, 1251, 1156. M.p. 247 °C

Found: C 70.94 % H 9.27 % N 6.45 %, theoretical: C 70.82 %, H 8.91 %, N 6.35 %, $C_{52}H_{78}N_4O_4Ni_1$

6, 13 bis (*p*-tetradecyloxybenzoyl) 5,7,12,14-Me_4[14] hexaenato(2-)N_4 Ni(II). **11d**

Yellow / Gold lustrous micro crystals. Yield 55 %. $\delta_H(CDCl_3)$ 0.85 (3 H, t, CH_3 ter), 1.0-1.5 (22 H, bs, chain), 1.55 (2 H, s, C**H**$_2CH_2O$), 1.8 (6 H, s, CH_3 mac), 3.2 (4 H, s, CH_2N en), 4.0 (2 H, t, CH_2O), 6.9 (2 H, d, ar), 7.9 (2 H, d, ar). $\delta_C(CDCl_3)$ 14.12, 20.87, 22.70, 26.03, 29.18, 29.37, 29.60, 29.67, 31.93, 53.59, 68.26, 110.51, 114.12, 131.82, 134.43, 159.29, 162.70, 198.92. IR cm^{-1} (KBr) 3433, 2919, 2851, 1653, 1646, 1643, 1601, 1576, 1545, 1474, 1399, 1346, 1252, 1156. M.p. 237°C.

Found: C 71.54 % H 9.49 % N 5.81 %, theoretical: C 71.71 %, H 9.24 %, N 5.97 %, $C_{56}H_{86}N_4O_4Ni_1$

6, 13 bis (*p*-hexadecyloxybenzoyl) 5,7,12,14-Me_4[14] hexaenato(2-)N_4 Ni(II) **11e**

Bronze lustrous micro crystals Yield 60.6 %. $\delta_H(CDCl_3)$ 0.9 (3 H, t, CH_3 ter), 1.3 (28 H, s, chain), 1.9 (6 H, s, CH_3 mac), 3.2 (4 H, s, CH_2N en), 4.0 (2 H, t, CH_2O), 6.9 (2 H, d, ar), 7.9 (2 H, d, ar). $\delta_C(CDCl_3)$ 14.16, 20.99, 22.70, 26.00, 29.14, 29.37, 29.60, 29.68, 31.92, 53.56, 68.19, 110.43s, 114.04, 131.80, 134.30s, 159.35, 162.64s, 198.96 . IR cm^{-1} (KBr) 3433, 2918, 2851, 1653, 16411599, 1570, 1548, 1472, 1437, 1408, 1344, 1252, 1155, 845. M.p. 240 °C

Found: C 71.81 % H 8.52 % N 5.52 %, theoretical: C 72.49 %, H 9.53 %, N 5.64 %, $C_{60}H_{94}N_4O_4Ni_1$

6, 13 bis (benzoyl) 5,7,12,14-Me_4[14]Bzo hexaenato(2-)N_4 Ni(II) $\delta_H(CDCl_3)$ 0.9 (12 H, s, CH_3 mac), 6.7 (8 H, bs, ar mac), 7.6 (6 H, m, ar benzoyl), 8.25 (4 H, bd, ar benzoyl). *M/z* 609 (M^+).

6, 13 bis (p methoxybenzoyl) 5,7,12,14-Me_4[14]Bzo hexaenato(2-)N_4 Ni(II) $\delta_H(CDCl_3)$ 1.9 (6 H, s, CH_3 mac), 3.9 (3 H, s, CH_3O), 6.6 (4 H, m, ar mac), 7.05 (2 H, d, ar) 8.25 (2 H, d, ar).

mono shows bridgehead H at 4.85δ and two environments for CH_3 mac at 1.9δ and 2.1δ

CHAPTER 5

Solid State NMR Of Tetraazaannulenes

5.1 Introduction

The previous chapters have shown that tetraazaannulenes display interesting phase transitions in the solid state which are related to dynamic processes within the molecule. It should be possible to draw general mechanistic conclusions about dynamic processes using both solid state NMR and X-ray results. Many cases have been reported in which solid state NMR detects the presence of motion in what X-ray presents as a motionless crystalline solid.[1]

High resolution ^{13}C NMR studies have conveyed much information about structural and electronic properties of organic molecules in solution.[2] The cross polarization (CP), high power decoupling, magic angle spinning (MAS) experiment offers a continuation into the solid state.[1] The spectrum obtained may differ from the solution spectrum in both the number of resonances and their chemical shifts. Interpretation of these differences may give important information about the solid phase. A number of difficulties are intrinsically present with CPMAS NMR of the solid state, primarily the much lower resolution when compared to solution NMR, and also factors such as crystal packing effects where nuclei which are chemically equivalent in solution may become non-equivalent in the solid phase. These same crystal packing

effects may also significantly alter any dynamic process which takes place freely in the solution and so modify the CPMAS spectra.

The tautomeric behaviour of malonaldehyde, tetraazaannulenes[3] and porphyrins[4] has been the focus of much theoretical and experimental study. Porphyrins have perhaps been the most actively studied partly because of the biological relevance of these naturally occurring compounds but also because of their peculiar electronic structure[2] and the wide range of derivatives that can be prepared to investigate the physiochemical properties. A large number of NMR studies in solution[5-12] have shown that in symmetrically substituted free base porphyrins the central hydrogens can migrate from one pair of nitrogens to another giving rise to two tautomers a and b (Figure 5.1)

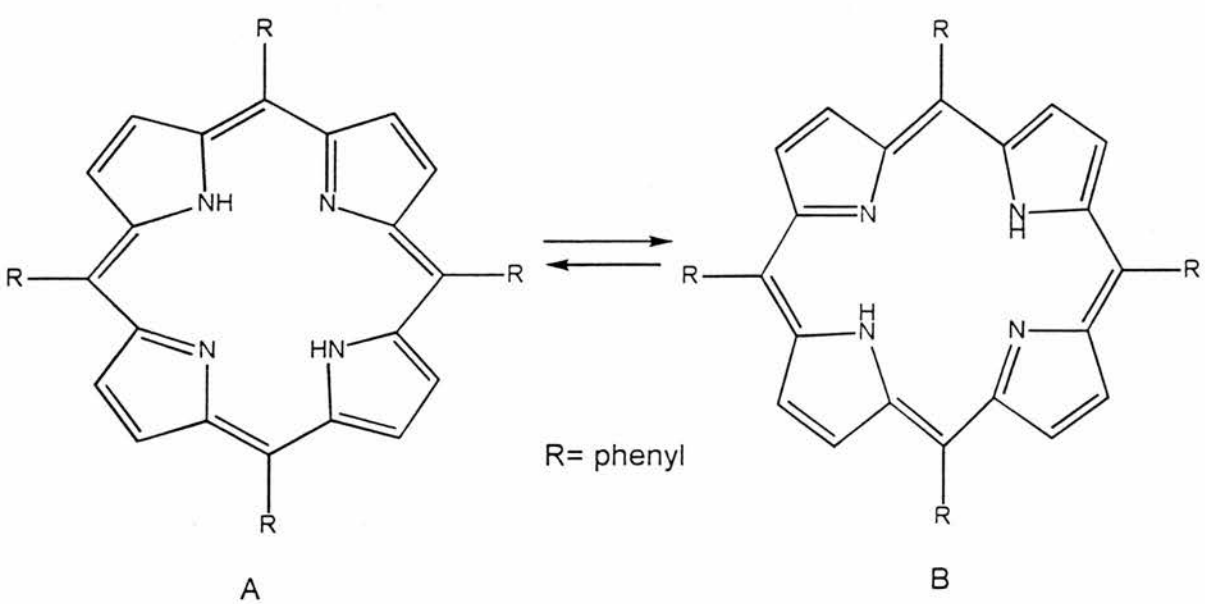

Figure 5.1 Tautomeric behavior of symmetrically substituted free base porphrins

This same tautomeric behaviour has also been studied in the solid state and put forward as a possible data storage medium if the two states corresponding to the two proton positions could be switched by an external method.[13] Free-base phthalocyanine, porphine and chlorin are potential systems for performing data storage in the frequency domain[2] by means of photochemical hole burning (PHB). This phenomenon is related to

the phototautomerisation that central hydrogens undergo between two tautomers of unequal energies when they are placed in an inert matrix at cryogenic temperatures and are irradiated at a specific laser frequency. It has been shown that if appropriate systems are found, the presence or absence of a spectral hole at a specific frequency could be utilised to encode as many as 1000 or more bits in the frequency domain within a single focused laser spot.[14]

The TAAs have many features in common with porphyrins including intramolecular proton transfer between the nitrogens in the core of the macrocycle. The diversity of the derivatives of TAA lead to several different tautomeric processes occurring in the solid state which can be studied by solid state NMR and X-ray crystallography. TAAs were also proposed as a model for malonaldehyde and its derivatives because the proton motion in the gaseous state is so fast that rate constants could not be obtained by NMR or any other method. As we had based most of our work on liquid crystalline derivatives of TAA, and we had a synthetic and spectroscopic database of a wide selection of TAAs, we decided to investigate the double proton motion in the core using ^{13}C CPMAS variable temperature experiments. Until now these molecules had only been examined by ^{15}N-CPMAS-NMR spectroscopy of ^{15}N enriched compounds. Isotopically enriching the sample with the less abundant spin 1/2 isotope ^{15}N because of the quadrupole moment of the ^{14}N nucleus is expensive and time consuming. It was proposed that the α-carbon next to the N on the propane-1,3-diiminato chelate ring (Fig 5.2) could be used as an indicator eliminating the need for isotope enrichment.

The α-carbon undergoes exchange between C=Cα-N and C-Cα=N which come at different chemical shifts. If the exchange of protons could be completely stopped by reducing the temperature sufficiently one peak will be seen for each carbon environment

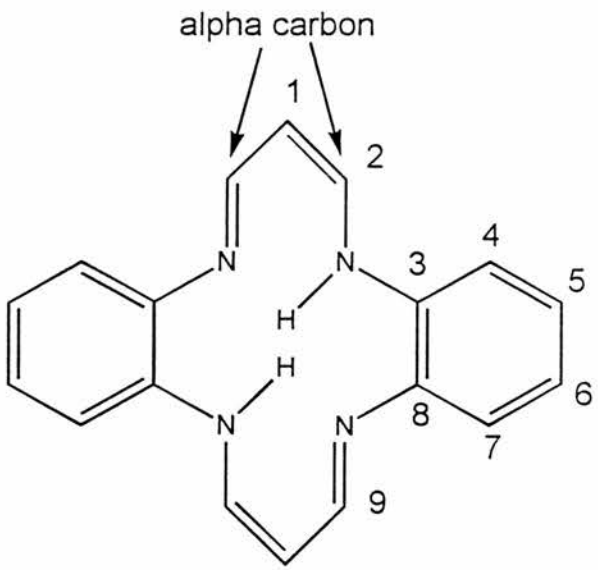

Fig 5.2 Alpha carbon position

As the temperature is raised the peaks will move together as the α-carbon environments take on a more mixed character:

C=====Cα======N

The amount that the α-carbon chemical shift moves towards the average is dependent on the probability that the N atom is protonated, taking into account all of the tautomers. In solution the populations of the tautomers are very unlikely to be different and so move from two peaks when tautomerisation is quenched (or slow on the NMR timescale) to one peak as fast proton transfer takes place. However in the solid state crystal packing forces may lift the degeneracy and so favour one tautomer over the other even at fast proton exchange rates. This would prevent the spectra ever showing only one line for α-carbons.

However there are problems involved with using the α-carbon as an indicator of proton transfer pathways. Unlike for example, hydride transfer in carbonium ions[15] the carbon atoms are not directly involved in the proton transfer so their NMR lines may not always be sensitive to these processes. The dipolar coupling ^{13}C-^{14}N cannot be completely removed by MAS because the eigenstates of the ^{14}N nuclei are not in general eigenstates of the Zeeman Hamiltonian so the ^{13}C resonances may appear broad or split into asymmetric doublets.[16]

To test the validity of this system with these types of compound it was necessary to compare our results to those obtained in recent studies of ^{15}N enriched compounds before branching out into compounds never before studied in the solid state.

5.2 Experimental

5.2.1 Physical Measurements

^{13}C CP/MAS NMR spectra were measured at 125.758 Mhz on a Bruker MSL 500 spectrometer at 296 K. High power ^{1}H decoupling and magic angle spinning were employed; the magic angle is set from time to time using KBr. Ground samples were packed into rotors (ZrO_2, 4 mm o.d) used at a spinning speed of 5-9 kHz. At least two spinning speeds were used for the ambient-temperature spectra of each sample in order to identify spinning sidebands. Contact times for cross-polarization were typically 1 ms and recycle delays of 5-15 s, sufficient to ensure almost total ^{1}H relaxation were employed. The number of scans typically vary from about 80 to over 800 depending on the resolution. Chemical shifts are referenced relative to the CH_2 in adamantane at 38.56 ppm.

5.2.2 Synthesis And Characterisation

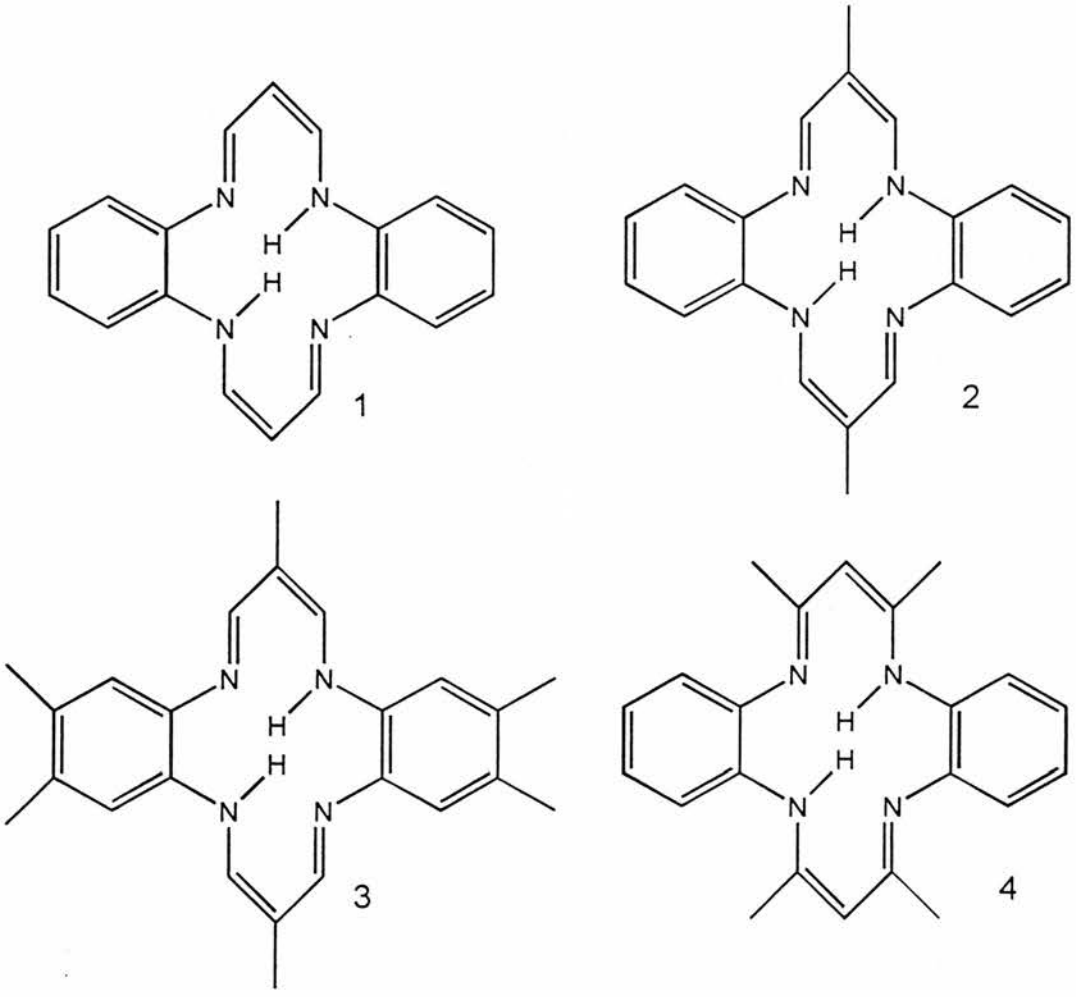

Figure 5.3 *Tetraazaannulene molecules.*

5.2.2.1 TAA 1,8-dihydro-dibenzo[b,i]-1,4,8,11-tetraazacyclotetradeca-4,6,11,13-tetraene = H_2[dibenzo[14]tetraene]N_4 **1**

This was prepared according to the method of Hiller[17]. Propargylaldehyde (prepared by adding chromic acid to propargyl alcohol (Aldrich)[18]) o-phenylenediamine (Aldrich) in a 1:1 ratio underwent a cyclisation reaction upon heating at 96 °C in DMF

(dimethylformamide) under nitrogen for 2 h. The reaction mixture was cooled and filtered to obtain red crystals. The ligand proved to be too insoluble for solution NMR. *M/z* 288 (M^+).

5.2.2.2 DMTAA 1,8-dihydro-6,13,-dimethyldibenzo[b,i]-1,4,8,11 tetraazacyclotetradeca-4,6,11,13-tetraene = H_2[Me2dibenzo[14]tetraene]N_4 **2**

This was prepared by the condensation reaction of a 1:1 mixture of 1.9 ml 2-methyl-3-ethoxyacrolein (Aldrich) and 2 g o-phenylenediamine (Aldrich) in 4 ml of refluxing DMF under N_2 for 12 h. The precipitate was recrystallised from DMF. Larger crystals can be obtained by dissolving in hot CH_2Cl_2 and adding pet. ether when cold. Yield 5.13 % Literature yield[19] 16-23 %. $\delta_H(CDCl_3)$ 1.95 (6 H, s, Me), 6.9 (4 H, m, ar), 7.05 (4 H, m, ar), 7.6 (4 H, s, methine), 13.3 (2 H, t, NH). $\delta_C(CDCl_3)$ 18.442 Me, 113.329 ar, 124.035 ar, 146.935 methine. Quaternary C did not show up. *M/z* 316 (M^+).

Found: 75.62 % C 5.42 % H 17.78 % N, theoretical: 75.92 % C 6.37 % H 17.71 % N, $C_{20}H_{20}N_4$

5.2.2.3 DMTAAxy 1,8-dihydro-6,13,-dimethyldixyly[b,i]-1,4,8,11-tetraazacyclotetradeca-4,6,11,13-tetraene = H_2[Me_2dixylyl[14]tetraene]N_4 **3**

This was prepared in an analogous method to 2 substituting 4,5-dimethyl-1,2-phenylenediamine (Aldrich) for o-phenylenediamine. $\delta_H(CDCl_3)$ 1.95 (6 H, s, CH_3), 6.85 (4 H, m, ar), 7.0 (4 H, m, ar), 7.6 (4 H, s, NCH). $\delta_C(CDCl_3)$ 18.44, 113.33, 124.04, 146.94. 2 quaternary peaks did not show up. *M/z* 372 (M^+).

Found: 76.92 % C 7.69 % H 15.09 % N, theoretical: 76.61 % C 8.50 % H 14.88 % N, $C_{24}H_{28}N_4$

5.2.2.4 TMTAA 1,8-dihydro-5,7,12,14-tetramethyldibenzo[b,i]1,4,8,11-tetraazacyclotetradeca-4,6,11,13-tetraene = H_2[Me_4dibenzo[14]tetraene]N_4 **4**

This was prepared by demetallating the nickel complex Ni^{II}(TMTAA) using a reported procedure.[20] This involves refluxing nickel acetate tetrahydrate, *o*-phenylenediamine and 2,4-pentanedione in methanol under N_2 for 48 h. The product obtained from this, Ni^{II}(TMTAA), is suspended in methanol and anhydrous HCl is bubbled through until the tetrachloronickelate(II) salt of the ligand is formed. The anion of the salt is changed to remove all Ni from the compound by dissolving in H_2O and adding ammonium hexafluorophosphate (Fluka) to form a precipitate of the hexafluorophosphate ligand salt. The yellow crystals of the pure ligand are isolated from this salt, dissolved in methanol, by addition of a slight excess of triethylamine (Aldrich). $\delta_H(CDCl_3)$ 2.0 (12 H, s CH_3), 4.9 (2 H, s, bri), 7.0 (8 H s, ar), 12.58 (2 H, bs, NH) *M/z* 345 (M^+).

Found: 76.09 % C 7.17 % H 15.78 % N, theoretical: 76.71 % C 7.02 % H 16.62 % N, $C_{22}H_{24}N_4$.

5.3 Results

Well-resolved CP/MAS spectra were obtained for all the free macrocycles, though many of the peaks can be attributed to spinning side bands (SSB) which complicate the spectra. The large number of SSBs are due to the high field and the large

chemical shift anisotropy found in rigid planar aromatic molecules. Fortunately, SSBs can be readily identified, as spinning the sample at a different rates moves them to a different chemical shift given by ν_{spin} / ν_L where ν_{spin} is the spinning frequency (Hz), and ν_L is the Larmor frequency (MHz). Thus, a rotation rate of 5 kHz will produce SSBs at *ca.* ± 40 ppm. for a Larmor frequency of 125 MHz. All samples were spun at two different frequencies at room temperature to identify which peaks are exclusively due to the sample. The frequency which gives the clearest representation was chosen for the printed spectra as the rate of spinning has no effect on the positions of sample shifts.

Non Quaternary Suppression (NQS) is a pulse sequence developed by Opella and co-workers[21] which includes a delay *ca.* 50 s before acquisition where a break in the proton decoupling sequence allows the decay of signals from carbons which have strong dipolar coupling to protons (CH and CH_2). The broad bands resulting from strong H C interactions lead to rapid decay of the transverse magnetisation. Quaternary carbons have relatively narrow coupled spectra so there is little decay of magnetisation during the delay and so a large signal can still be obtained. Methyl carbons, due to rapid internal rotations also give narrow bands and so these environments show up as large peaks in the NQS spectra. The net result is that only signals for quaternary carbons and methyl groups show up greatly aiding the assignment of the spectral features.

The ^{13}C CP/MAS spectra of a series of TAA derivatives were readily assigned (table 5.1) by both the use of this non-quaternary suppression (NQS) pulse sequence and by comparison with the solution spectra. The assignments are consistent along the series, and the number of carbon environments are generally in accord with the crystal structures.[22,24]

Table 5.1 *^{13}C Chemical shifts of TAA Compounds*

	Bridgehead	*C-NH*	*C=N*	*Phenyl*		
	C1	*C2*	*C9*	*C3/8**	*C4/7*	*C5/6*
1 TAA	97.5	145.0		137.2, 138.0	113.1, 114.1, 115.0b	122.3, 124.2
2 Me2TAA d	103.4*	140.0	153.0	136.8, 137.7	113.2, 116.6	122.5, 124.7
3 Me2dixyl d	104.9*	140.3	152.3	134.9	113.5, 116.9	131.0*, 135.9*
4 TMTAA c,d	99.8	154.2, 157.5 161.1, 161.8		135.9, 138.0, 139.9, 141.5	122.1	125.4
TMTAA d,e	98.5	159.5		139.0	123.4	123.6

* Quaternary (demonstrated by NQS)

a Overlapping

b There are more than two peaks here, perhaps because this compound has a different crystal structure with Z=4 and molecule not lying on a centre of symmetry

c Molecule does not lie on a centre of symmetry; there may be twice the number of resonances

d The number and positions of the methyl resonances were as expected

e Solution ($CDCl_3$)

5.3.2TAA (1)

The TAA ligand **1** exhibits only one resonance in the region occupied by C2 (C-NH) and C9 (C=N)at 145.0 ppm. This is despite the fact that the crystal structure does not demand a centre of inversion for TAA and so in principle there ought to be a slight splitting of each peak, since the two halves of the molecules are no longer related by

symmetry. Peak splitting is indeed observed but only for carbons on the phenyl ring. Examination of the crystal structure reveals only slight differences in the geometry of each half of the molecule, and thus the splittings of all the peaks may not be resolved.

The single peak at 145.0 ppm is mid-way between the separate C=N and C-NH chemical shifts observed for DMTAA **2** and hence is assigned as a carbon adjacent to a nitrogen atom which is bonded to a proton for 50 % of the time. On cooling (Figure 5.4), this peak is observed to broaden significantly. This is attributed to the fast proton transfer process interfering with the proton dipolar decoupling, which has a frequency of ca 60 kHz.[32]

5.3.3 DMTAAxy (3)

DMTAAxy **3** shows clearly a split in the resonance for the carbons adjacent to N on the propane-1,3-diiminato chelate ring. These resonances which do not show up in the NQS and which are not spinning side bands add credence to the slightly less clear picture in DMTAA and leads us to an unambiguous labelling of the peaks for **2.**

5.3.4 DMTAA (2)

The spectra of DMTAA **2** has two observable peaks in the C=N and C-NH region at 288 K which are not attributed to spinning side bands. These two peaks at 140.0 and 153.0 ppm (Figure 5.5) move apart on cooling, the one at 140.0 ppm apparently moving more rapidly to higher field. All the other peaks were readily assigned using NQS and solution spectra. There is only one peak for the methyl carbon and one for the bridgehead C1 but the carbons on the phenyl ring are split into individual resonances and have six peaks in the aromatic region as C3 + C8, C4 + C7 and C5 + C6

The crystal structures of the free macrocycles DMTAA **2**, and its dixylyl derivative **3**, show that these macrocycles are situated on special positions and inversion centres, and thus only nine unique ring carbon and benzene carbon environments are expected. This is confirmed by the solid state NMR spectrum. The most significant observation is that two resonances are observed for the methine carbons C2 (C-NH) and C9 (C=N) of the C_3N_2 unit. A similar assignment is arrived at for the structurally similar compound **3**.

5.3.5 TMTAA (4)

In the spectra of TMTAA **4** the region for C=N and C-NH resonances has a cluster of four peaks between 161.7 to 154.1 ppm at room temperature which are not due to spinning side bands. At room temperature the peak at 161.7 is clearly split into two peaks, particularly in spectra where more transients and hence better resolution is obtained. The range of chemical shifts, 154.1-161.7 seems to span the averaged chemical shift, 159.5, observed for the C2/C9 carbons in solution. Similarly the C3/8 resonances appear as a group of four resonances. The benzene carbons C4-C7 are all similar in chemical shift, in contrast to those of planar macrocycles which divide up into two groups (C4/7 and C5/6); this reflects the lower interaction between the benzene rings and the C_3N_2 group in TMTAA. Upon cooling (Figure 5.6), the far right 154.1 ppm peak shifts upfield, as does the central peak with loss of intensity. The 161.7 ppm doublet collapses to a singlet at 162.5 ppm.

Figure 5.4 ^{13}C SSNMR of TAA, 1

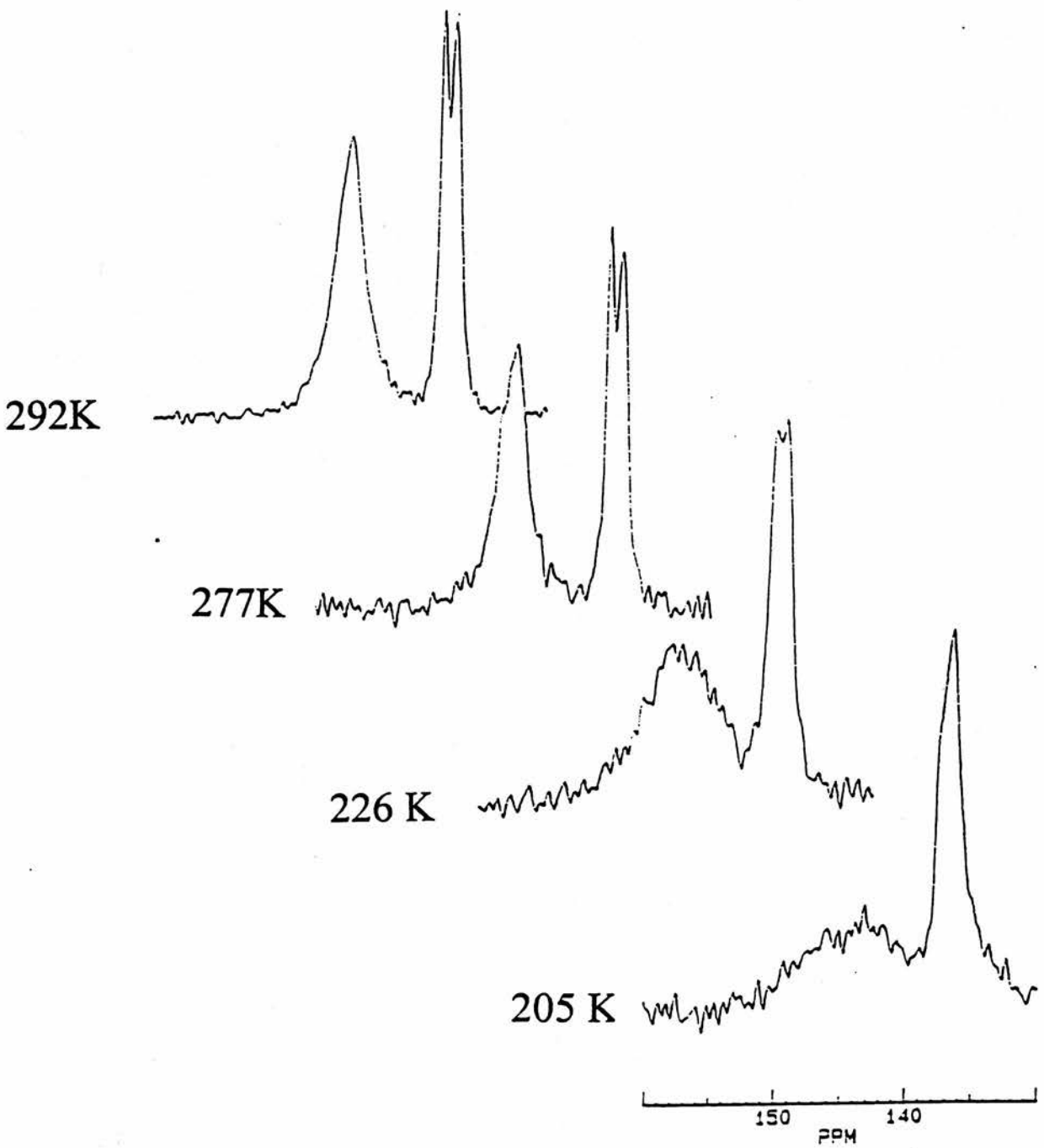

Figure 5.5 ^{13}C SSNMR of DMTAA, 2

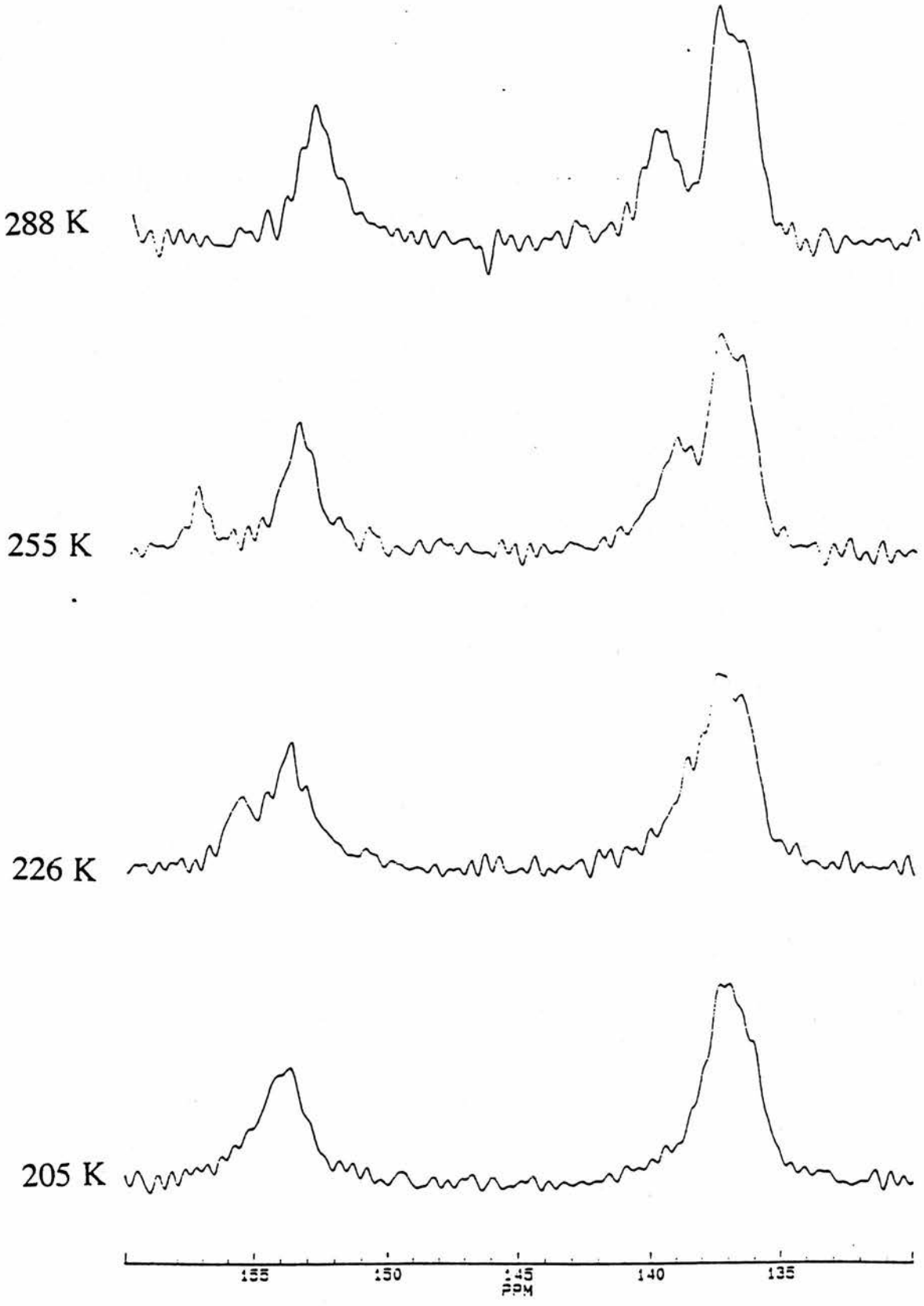

Figure 5.6 ^{13}C SSNMR of TMTAA, 3 (expanded)

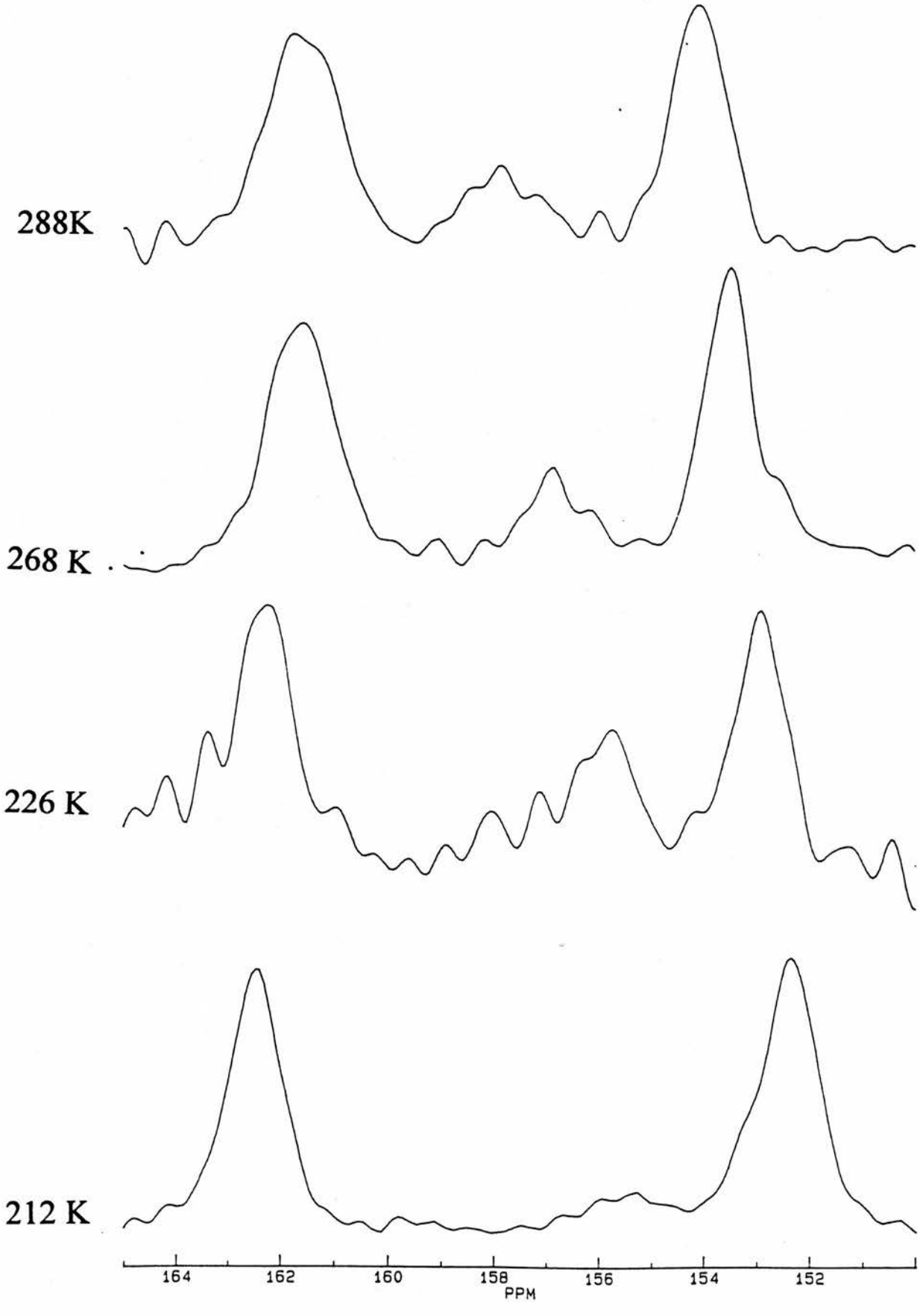

Figure 5.6 ^{13}C SSNMR of TMTAA, 3

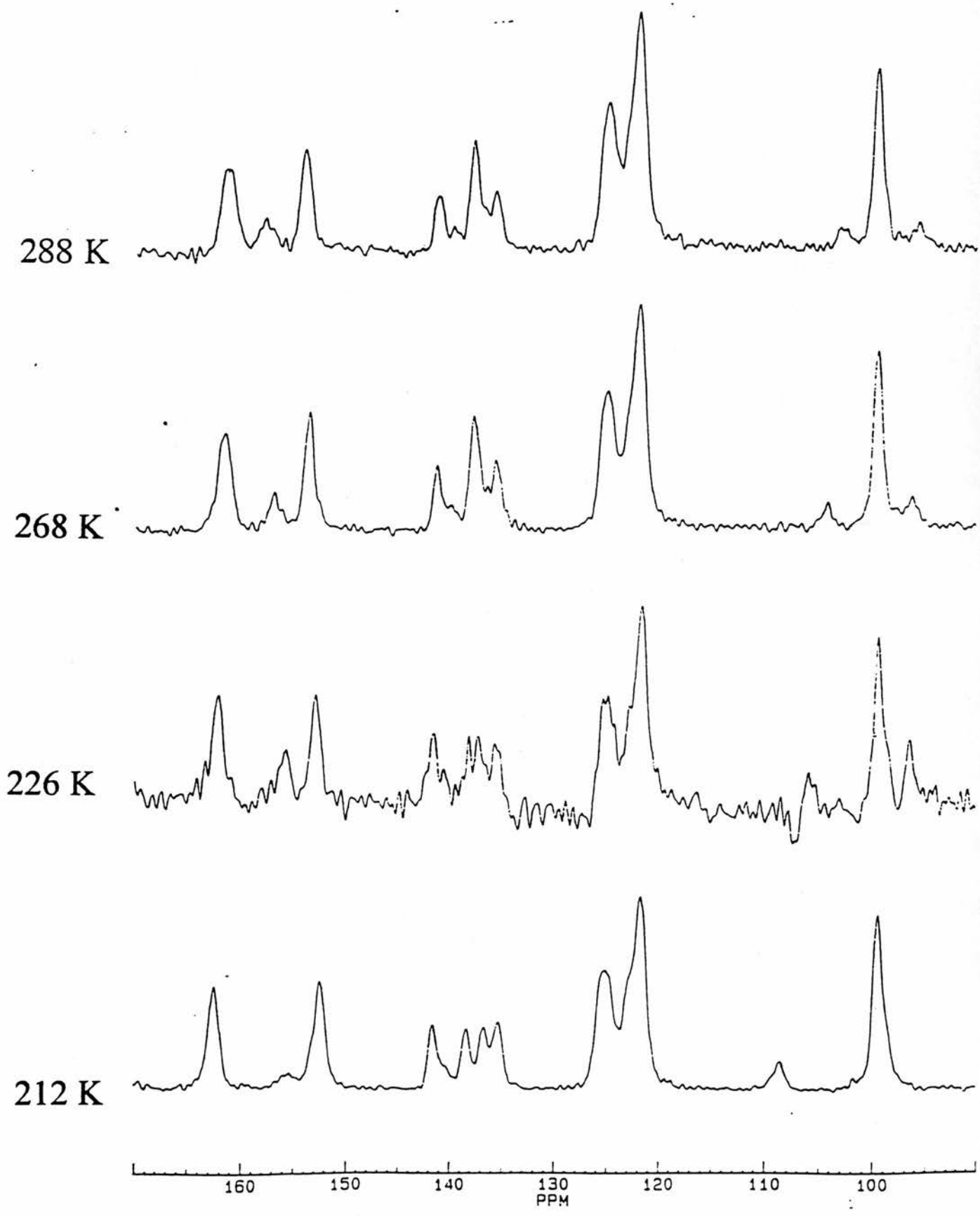

5.4 Discussion

Much work has been done in the area of proton transfer in tetraaza systems such as porphine, tetraalkyl porphyrins, phthalocyanine and recently tetraazaannulenes. Some unusual features and incongruities have come to light in the solid state when the crystal studies were compared to SSNMR studies of tautomerism. What was relatively straightforward in solution becomes much more complex, and kinetic solid state effects have to be taken into consideration to account for the observed results. The original purpose of these experiments was to find out the type of proton motion present during tautomerism. Several theories have been put forward to explain the observed data. For example, in tetraalkyl porphyrins several different mechanisms have been proposed: (i) an asynchronous 1,5 sigmatropic rearrangement; (ii) a simultaneous movement of the two hydrogens through a symmetrical transition state and (iii) an incoherent migration of the hydrogens in a four-minima potential energy surface.[25]

In the solution state it has been shown that these proton transfers are intramolecular,[26] are independent of solvent and are not affected by electron donating or withdrawing properties of the meso substituents[27]. Many of the changes can therefore be directly attributed to the crystal lattice and the nature of these changes may clarify some of the factors involved in the migration motion. The most obvious change in moving from solution to solid state is the loss of degeneracy of the tautomers in the solid state favouring one tautomer over another even during the fast exchange process. Therefore the rates of forward and back tautomerisation are no longer equal thus leaving one tautomer dominant. The crystal structure confirms this, with hydrogen electron density localised on opposite pairs of N atoms and not distributed in an average fashion over all four N atoms. It is understandable that the non-dominant tautomer was

not observed by X-ray crystallography due to its small population.[28,4] There are at least two molecules which do not fit in with this view of tautomerisation: porphine and meso-tetratolylporphyrin. In these compounds the kinetic behaviour of the central hydrogens in the solid state is similar to the one present in solution. For meso-tetratolylporphyrin this is consistent with the crystal structure which shows disordered protons. However, porphine displayed localised protons, in direct contradiction of the SSNMR results. It can be argued that it is difficult to detect a proton in a crystal structure especially when joined to an electronegative atom such as nitrogen, as hydrogen atoms are weak X-ray scatterers and in this case the electron density is distorted along the N-H bond. However the X-ray analysis of porphine also showed the heavier atoms distorted towards a D_{2h} -like configuration which should arise from static central hydrogens.[29]

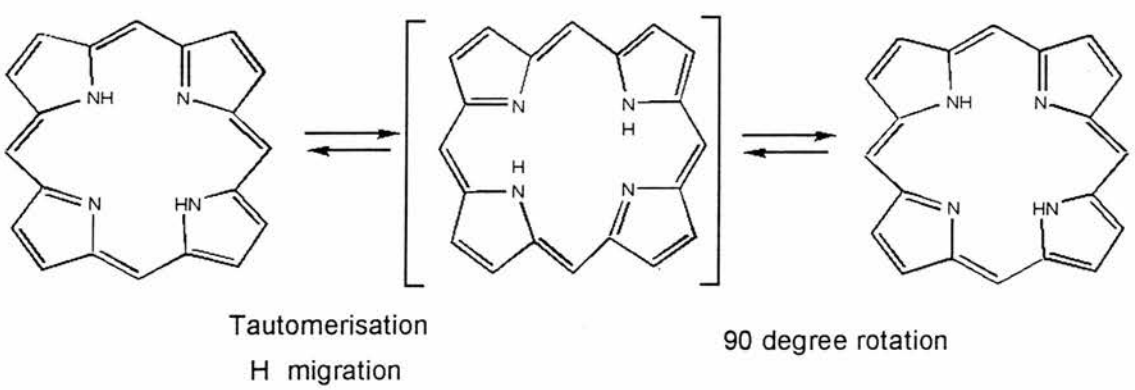

***Figure. 5.7** H migration coupled to molecular rotation*

The most recent explanation for this conflicting evidence was put forward by L. Frydman *et al.*[30,31] who suggested a molecular rotation of 90° about an axis perpendicular to the plane of the macrocycle in conjunction with the concerted proton exchange (Figure 5.7). In theory this would leave the crystal structure stationary, as

neither the hydrogen migration nor the macrocycles rotation would disturb the translational symmetry of the crystal.

5.4.1 Comparison With ^{15}N Studies

Having established that the processes involved are not always simple proton migrations we began by correlating our ^{13}C SSNMR data with previously reported ^{15}N SSNMR studies on **2** and **4**. Limbach *et al.* enriched the macrocycles **2**, DMTAA[3] and **4**, TMTAA[32] with ^{15}N in order to carry out a ^{15}N NMR study of the tautomerism.

5.4.2 DMTAA

For DMTAA **2** at low temperature two ^{15}N resonances m and n are observed in the sp^3 (high field) and sp^2 (low field) regions respectively. As the temperature is raised the separation between the lines decreases but reaches a limiting value rather than completely vanishing (coalescing) at room temperature. The limiting separation is characteristic of two unequally populated interconverting tautomeric states at room temperature. If the other tautomers, 2 and 4, were involved then four lines would have been observed in the low temperature spectrum. The implication is that concerted double proton transfer between 1 and 3 occurs in DMTAA (Fig. 5.8).

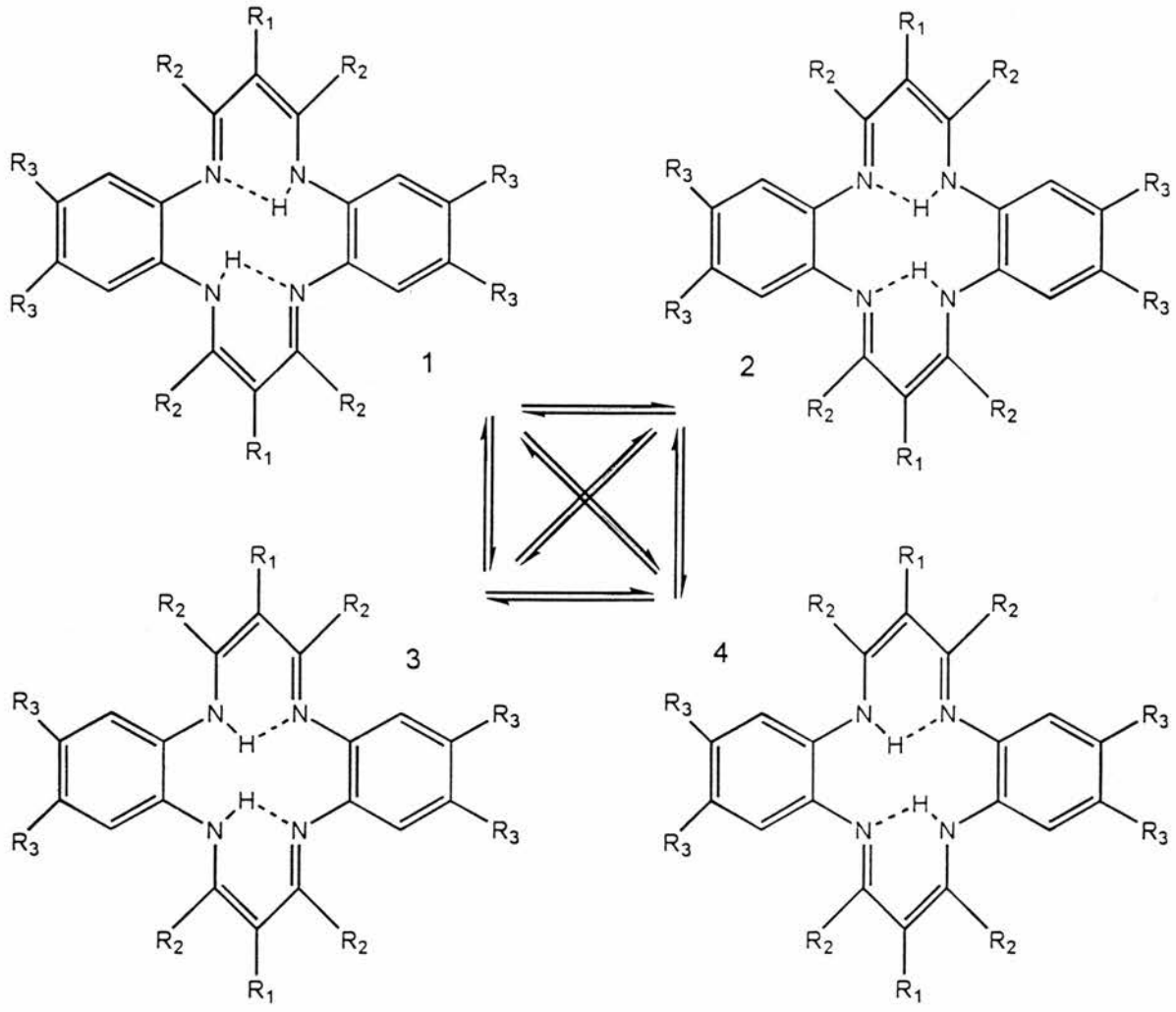

Figure 5.8 *Scheme of proton transfer*

We believe that the degeneracy of the two tautomers is lifted by a rhombic distortion of the N_4 plane induced by crystal packing effects. This distortion is clearly seen in the crystallographic data.[33] Table 5.2 shows the dimensions of the quadrangle, in which the exchanging hydrogens are enclosed, for the various macrocycles. This can be compared with crystal structures of related organic molecules[34] (Figure 5.9) which have similarities to the macrocycles yet do not undergo tautomerism.

Table 5.2 Dimensions of the macrocycle centres

	Lengths / A					
Name	N1N2	N2N3	N3N4	N4N1	N1N3	N2N4
TAA 1	2.788	2.674	2.795	2.67	3.791	3.936
DMTAA 2	2.753	2.675	2.753	2.675	3.766	3.91
DMXTAA 3	2.742	2.693	2.742	2.693	3.799	3.888
TMTAA 4 +	2.713	2.676	2.7	2.685	3.749	3.868

	Bond Lengths Iminato Ring			
	N1=C9	C9-C1	C1=C2	C2-N2(protonated)
TAA 1	1.299	1.402	1.363	1.331
DMTAA 2	1.300	1.417	1.368	1.343
DMXTAA 3	1.295	1.420	1.372	1.331
TMTAA 4 +	1.317	1.417	1.377	1.343

	Bond Angles			
	N1N2N3	N2N3N4	Torsion angle	REF
TAA 1	87.881	92.029	1.355	13
DMTAA 2	88	92	0	14
DMXTAA 3	89	91	0	14
TMTAA 4 +	88.172	91.54	1.354	15

+ = 75 % 25 % delocalised in X-ray

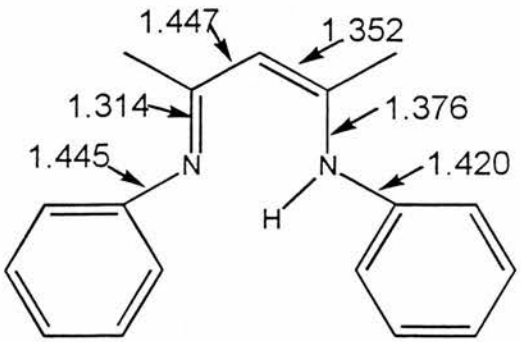

2N Phenylamino 4N Phenylimino 2 Pentene ref 40

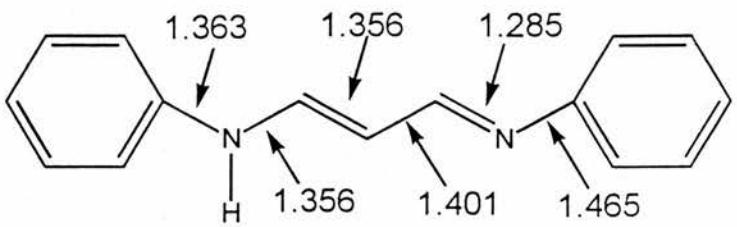

1- Anilino 3 phenylimino prop-1-ene ref 41

Figure 5.9 *X-Ray structures of similar molecules*

The crystal data for **2** was not available at the time of the ^{15}N studies and has only recently been solved by members of our group. However, Limbach reached the same conclusion based on the crystal structures of similar compounds.

In analysing the spectra Limbach *et al.* assumed that the chemical shifts of, for example, NH on one tautomer is the same as the chemical shift of NH on the other tautomer, and likewise for the non-protonated nitrogens. They also assumed that the actual chemical shifts are proportional to the probability that the N atom is protonated in the exchanging system, (Figure 5.10).

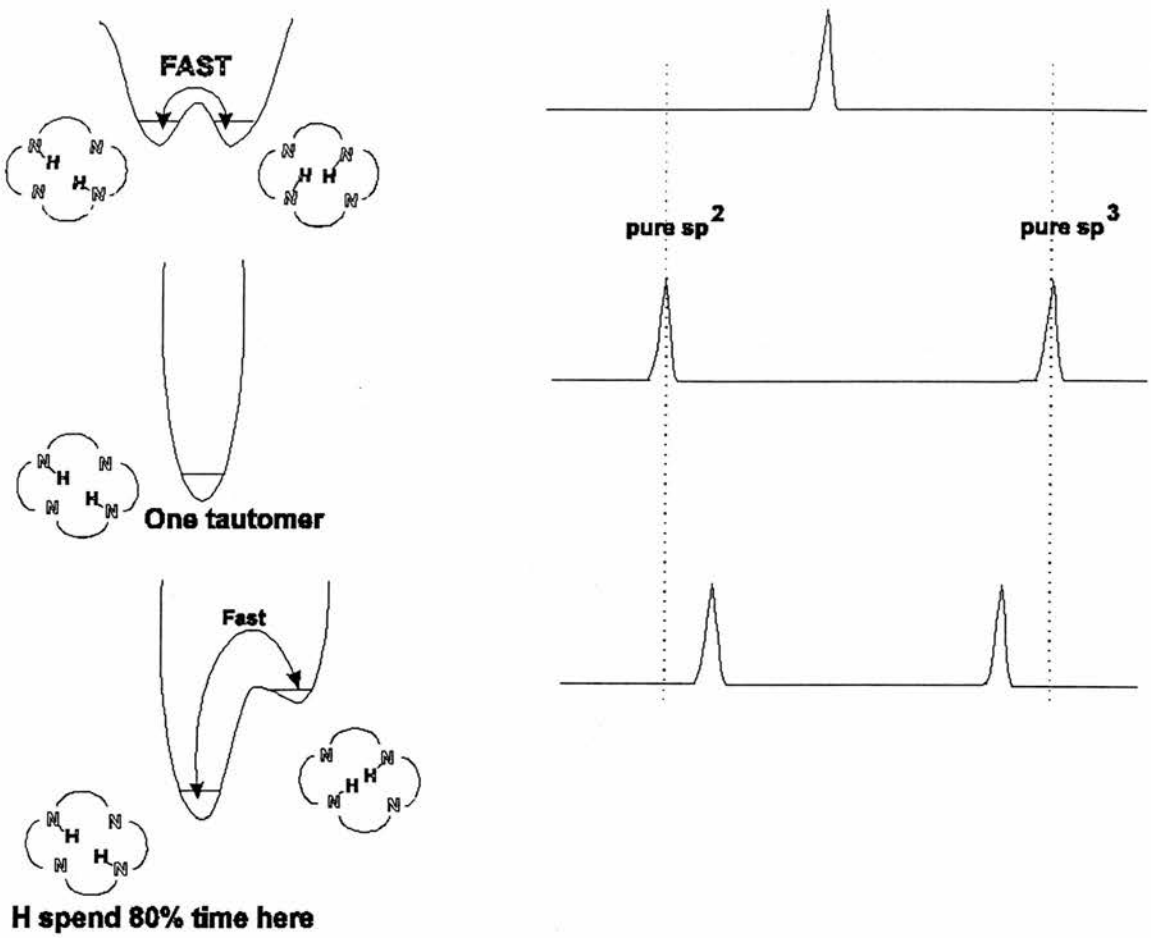

Figure 5.10 Energy diagram and ^{15}N NMR of macrocycle tautomerism

This can be shown for the carbon as

$$\delta_1 = p_a\ \delta C\alpha{=}N\text{-} + p_b\ \delta C\alpha\text{-}NH\text{-} \qquad (5.1)$$

$$\delta_2 = p_a\ \delta C\alpha\text{-}NH\text{-} + p_b\ \delta C\alpha{=}N\text{-} \qquad (5.2)$$

Where δ_1 and δ_2 are the observed chemical shifts, p_a and p_b are the probabilities of each tautomer and $\delta C\alpha{=}N$- and $\delta C\alpha$-NH- are the idealised chemical shifts for carbons adjacent to N with solely sp^2 or sp^3 character. The positions of the peaks at

very low temperatures where tautomerisation is frozen out is taken as a good approximation for the intrinsic δCα=N- and δCα-NH-.

If we take the line separation at low temperatures to be

$$\Delta_o = (\delta C\alpha{=}N\text{-}) - (\delta C\alpha\text{-}NH\text{-}) \qquad (5.3)$$

and

$$p_a + p_b = 1 \text{ and } p_a/p_b = K \therefore p_a = K/K{+}1 \text{ and } p_b = 1/K{+}1$$

where K is the equilibrium constant between the two tautomers A and D:

$$K = [D]/[A] \qquad (5.4)$$

The difference in chemical shift at any give temperature $\Delta T = \delta 1 - \delta 2$ is the relation:

$$\Delta_T = \Delta_o (1\text{-}K)/(1{+}K) \qquad (5.5)$$

From the ^{15}N data $\Delta_T/\Delta_o = 0.6$ and hence $K_{AD} = 0.25$. The reason for the unequal population is probably related to the rhombic distortion in DMTAA (Table 5.2) which favours protonation of the N atoms on the long diagonal.

Now this K_{AD} value (0.25 at room temperature) should be applicable to the ^{13}C NMR data for the carbons (C2 and C9) most affected by the protonation of the N atom. Thus our observed $\Delta_T^{mn} = \delta(C2) - \delta(C9) = 13$ ppm, at room temperature for DMTAA should be increased by a factor of $(0.6)^{-1}$ at low temperature to 22 ppm. We observe a separation of 17 ppm at the lowest temperature we could obtain (205 K). This is acceptable as the lowest peak recorded by Limbach was 122 K and there was certainly continuing movement down to 162 K.

In the ^{15}N experiment the two resonances not only moved apart upon cooling but also broadened and then regained sharpness. These line shape changes are typical for

the presence of two unequally populated interconverting tautomeric states. By spectral simulation of this data it was shown that one of the tautomers is favoured over the other by a reaction enthalpy of 3.8 ± 0.4 kJ mol^{-1} and negligible entropy.

The increased separation of the αC peaks as the temperature is lowered is consistent with a greater localisation of the protons to one particular pair (presumably opposite pair) of nitrogen atoms and a concerted jump of the protons between them. We cannot yet explain why the 140.0 ppm peak shifts more rapidly than the 153.0 ppm peak. We observe no exchange broadening even though this might be expected in the temperature range that we employed. However, broadening may not occur unless lower temperatures are encountered. For example, the chemical shift difference at 200 K (1600 Hz) would be comparable with the rate of proton transfer as measured by ^{15}N NMR (< 2 kHz at T < 200 K) as compared to $>10^5$ at room temperature. The lack of exchange broadening precludes the extraction of kinetic data on the proton transfer rate. The fact that the crystal structure shows protons localised on opposite pairs of N atoms but the SSNMR shows two tautomers interconverting at room temperature is probably explained by the non-dominant tautomer not showing up in the X-ray pattern because of its small population. Alternatively, it could be explained by a rotation coupled to a concerted proton transfer, analogous to porphyrin. To preserve translational symmetry a 180° rotation about a line parallel to the plane of the molecule is necessary.(Figure 5.11). The rates of the tautomerism and rotation need not be exactly the same as some of the minor tautomer can convert back to the major tautomer before rotation can take place. However, this seems highly unlikely given the constraints of the molecular packing.

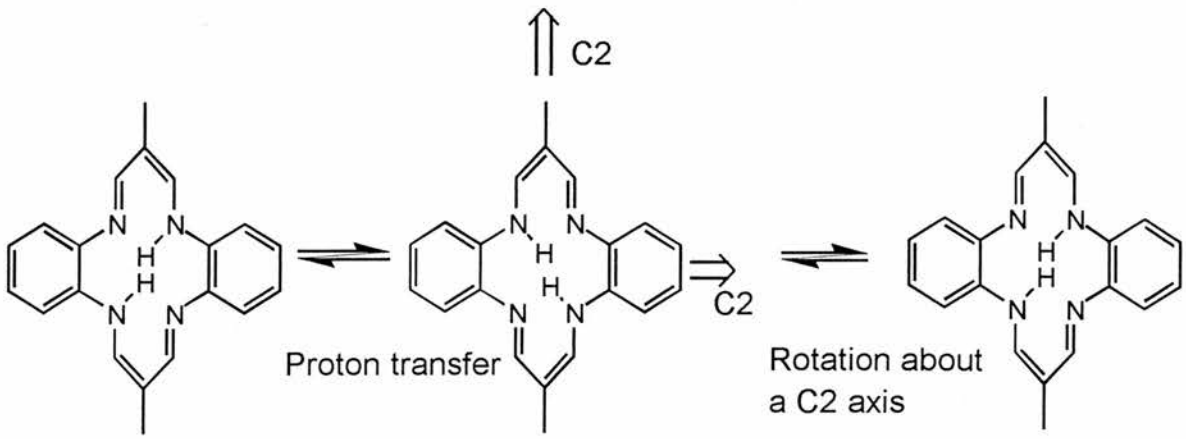

Figure 5.11 *Proton transfer coupled to molecular rotation in DMTAA*

5.4.3 TMTAA

Tetramethyltetraazaannulene **4** has also been studied by ^{15}N substitution SSNMR.[35] The four peaks we observed in the αcarbon region are consistent with the four resonances discovered in the ^{15}N spectra at room temperature.

The hydrogens can only move between nitrogens on the same imine ring and those nitrogens have resonances linked to the probability of finding a proton attached. At very low temperatures where exchange is "frozen" two discrete resonances appear, one for sp^2 and one for sp^3. As the temperature is increased the rate of exchange increases and therefore the probability of finding a proton attached on only one N decreases respectively. In solution the resonances, exhibiting a more mixed character as the temperature increases, move together until only one peak is observed indicating that both Ns have a 50 % probability of having a H attached. In the solid state the rhombic distortion makes one pair of tautomers more stable which alters the probabilities and favours finding a proton on one of the two N atoms. This is what prevents the two peaks coalescing. If the proton movement was not concerted *i.e.*, a proton can move between N_a and N_b independently of the proton on the other half of the molecule, then

the equilibrium constants of these transfers would be different and show a different dependence on temperature. This is what is believed to be happening in TMTAA where four peaks are found at room temperature (mnpq). Peaks m and n move apart on cooling as do peaks p and q but at a faster rate so that at low temperatures m and p coalesce and peaks n and q almost coalesce giving two resonances in the 'frozen' state. Since the proton motion is independent in each half of the molecule all four tautomeric states shown in Figure 5.8 are possible. The rhombic distortion lifts the degeneracy of states 2 and 4 as well as 1 and 3 and the equilibrium constant for proton movement between N_a and N_b can be expressed as mole fractions of tautomers;

$$K_{ab} = (x_1+x_2) / (x_3+x_4) \quad K_{dc} = (x_1+x_3) / (x_2+x_4) \qquad (5.6)$$

or as equilibrium constants between tautomers;

$$K_{ab} = K_{42}(1+K_{21}) / (1+K_{43}) \quad K_{dc} = K_{43}(1+K_{31}) / (1+K_{42}) \qquad (5.7)$$

the chemical shift data can give values of K_{ab} and K_{dc} from;

$$\Delta_T^{ab} = \Delta_O^{ab} (1-K_{ab})/(1+K_{ab}) \qquad (5.8)$$

$$\Delta_T^{dc} = \Delta_o^{dc} (1-K_{dc})/(1+K_{dc}) \qquad (5.9)$$

The crystal structure has one molecule in the asymmetric unit and no centre of symmetry. The decoupling of the proton motion in each half of the molecule is not unexpected since it is non-planar (saddle-shaped) due to steric interactions of the methyl groups with the benzene rings. The two central hydrogens were detected by X-ray diffraction, but did not show either a totally delocalised structure or a completely localised structure. Instead the structure is described as one in which each H atom was occupying two positions, one assigned a multiplicity of 0.75 and the other 0.25. The

refined hydrogen atoms lie in the plane defined by the αC, the N bonded to it, and the C adjacent to this N on the benzene ring. Thus the bonding involving the N atoms is not sp^3 but rather sp^2 hybridised with the lone pair electrons occupying a p orbital perpendicular to the bonding plane, permitting extensive delocalisation throughout the five atom ring.

The reported ^{15}N spectra show that the two sets of resonances have different temperature dependencies: for mn: $\Delta_T^{mn}/\Delta_0^{mn} = 0.6$, while for pq $\Delta_T^{pq}/\Delta_0^{pq} = 0.325$ at 288 K. From this ^{15}N data we would predict a change in the ^{13}C spectrum at low temperature. From the outer peaks of the C grouping (161.7 and 154.2 ppm), we observe $\Delta_T^{mn} = 915$ Hz, and from the inner resonances (161.1 and 157.5) $\Delta_T^{pq} = 400$Hz leading to predictions of the low-temperature separations of $\Delta_0^{mn} = 1525$ Hz and $\Delta_0^{pq} =$ 1415 Hz. The peaks become almost equally separated at low temperature, which is consistent with the ^{15}N spectra. At the lowest temperature recorded we observed a peak separation of the two outer peaks of 10 ppm (1260 Hz). The reason why the C2/C9 group of resonances are not of equal intensity is not completely understood.

DMTAA and TMTAA can conveniently be compared with porphine and porphycene[36] with the former having a concerted proton transfer and the latter independent proton transfers in each half of the molecule.

5.4.4 TAA

No SSNMR data has been reported in the literature for TAA (**1**) and as the αC investigating method has proved to be reliable on the basis of TMTAA and DMTAA it was used to probe the system of tautomerism of TAA in the solid state.

The single resonance for C2 (C-NH) and C9(C=N) in TAA **1**, with a chemical shift midway between the separated chemical shifts for C2 and C9 in DMTAA **2**, suggests that the sites are exchanging rapidly on the NMR time-scale. We can see from equations 5.1 and 5.2 that if $p_a = p_b = 0.5$ then $\delta_1 = \delta_2$ (the average of the two resonances). Fast proton-transfer at room temperature causes the C-N and C=N sites to be averaged such that the C2 and C9 resonances are above the coalescence point. This indicates a C adjacent to a N which is bonded to a proton 50 % of the time. This is unexpected because the crystal structure shows that the rhombic distortion in the centre of the molecule is even greater than that exhibited by TMTAA or DMTAA. One would expect this to lift the degeneracy of the tautomers because when positioned on one set of opposite Ns the protons are further apart (less strain, lower energy) than on the other.

On cooling, this single peak goes from a very sharp peak to an extremely broad one without changing chemical shift. In principle, there are two well-established mechanisms through which molecular motion might affect a ^{13}C CPMAS NMR spectrum: either by interfering with the coherent motion of the sample introduced by the magic angle spinning process[37] or by interfering with the coherent motion of the spins introduced by the high-power proton decoupling.[38,39] Both mechanisms are thought to have a common origin, namely, that a stochastic (random) motion tends to interfere with a coherent motion when both have similar rates. They possess different NMR timescales; interference with MAS will be relevant when the rates of molecular motions are on the order of the chemical shift anisotropy (*ca.* 10^3) while high power decoupling will cause interference when the motions are in the order Larmor frequency which is associated with the rf irradiation (*ca.* 3×10^4 to 10^5 Hz).

In accord with theory,[38] a plot of the linewidth vs. T^{-1} is linear and regression analysis gives a best fit line with a slope of 1.048 and an intercept on the ln(linewidth) axis of -4.106, R^2 has a value of 0.993 (Figure 5.12). From the slope an activation energy for the proton transfer process of 8.4 kJ mol^{-1} (2.0 kcal mol^{-1}) was calculated. The temperature could not be brought down low enough for the peak to regain sharpness and so the full rate equation was not obtained.

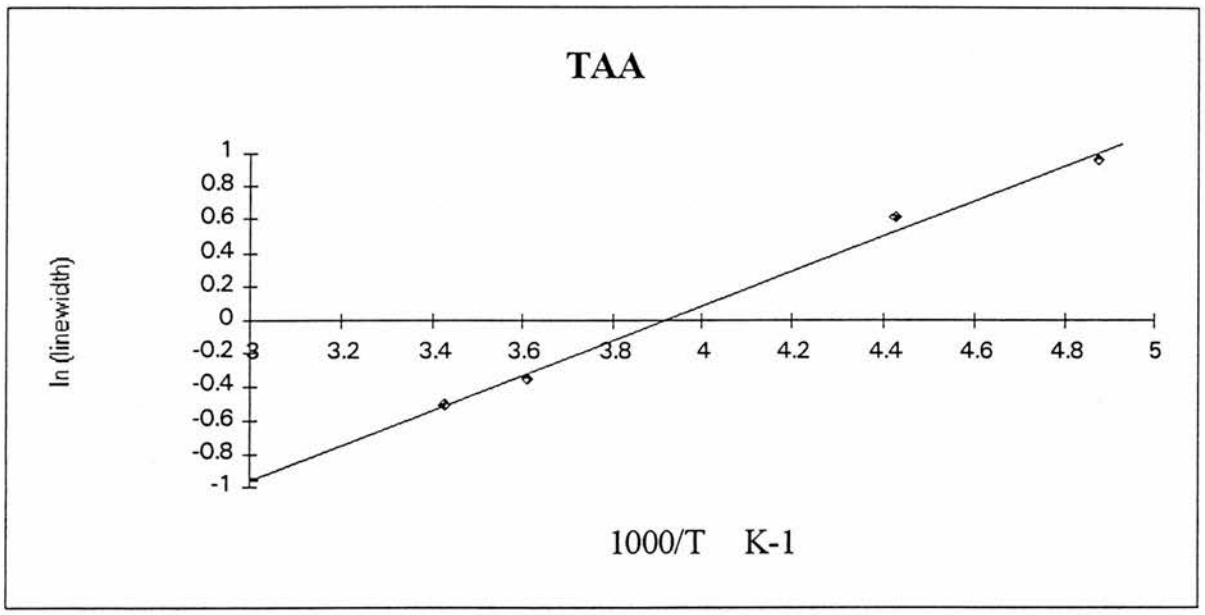

Figure 5.12 *Plot of ln linewidth vs. T^{-1} for TAA*

There is some ambiguity over the X-ray crystallography data[40] where examination of the last difference map suggests the hydrogens are distributed equally over all four N sites, other bond length measurements do not conform to this view. The αC to N bond distances are not all equal, which is unusual for equally distributed H, as we would expect to see a single average bond length between CN and C=N. The stereoscopic views presented show protons localised on opposite nitrogens N2 and N4 the data even goes so far as to give bond lengths for N2-H and N4-H, leading us to believe that the protons were totally localised on these two nitrogen atoms. Indeed, it was argued that the proton repulsion of these two hydrogens was responsible for slight

deviation from planarity in the molecule along a line drawn between the other two nitrogens, N1 and N3.

Goedken *et al.*[41] also had problems deciding on the position of protons in TMTAA and finally assigned two positions for each H one with a multiplicity of 0.75 and the other 0.25 after performing a difference fourier map through the plane of the four N atoms based on a structure factor calculation obtained by omitting the N-H hydrogen atoms. The four highest peaks remaining were due to the internal protons and indicated the ratio they were present in. The difference in position of the heavy atoms in the crystal structures different tautomers was very small and would easily be obscured by thermal motions.

The difficulties in accurately defining the position of the central hydrogens are highlighted in tetraphenyl porphyrin which in its triclinic phase has protons localised on opposite N atoms[42] and in its tetragonal phase has disordered protons.[43] Another example would be porphyrin itself which was first reported to have disordered protons[44] but this was found to be contaminated with Cu(II) and the subsequent report gave localised protons.[45] This highlights the problem of impurities, not only extraneous molecules but also different phases. Indeed other workers have pointed out the problems of crystal phase changes complicating the NMR data. If, for example, the compound crystallised into two distinct forms (phases) one of which was micro crystalline and the other formed large crystals, then the X-ray crystallography done on this large crystal would not be representative of the entire sample.

The derived activation energy for TAA indicates a very fast proton transfer at room temperature, and this obviously ties in with the NMR experiment. But it still does not explain the contribution of rhombic distortion which played such an important part

in DMTAA and TMTAA. Two peaks are expected because of the solid state effects removing the degeneracy of the tautomers. The absence of this is perhaps explained by the slight bend observed in the crystal structure which may have the effect of equalising the energy between the two tautomers by offsetting the rhombic distortion. This would have to be quite a coincidence to exactly equalise the energy difference between the two tautomers.

It is possible, as discussed earlier, that the crystal used for the X-ray crystallography was not representative of the bulk of the sample but merely a minority phase which forms large crystals

This was indeed proved to be the case when Sakata *et al.*[46] reported the crystal structure of TAA which had been recrystallised from xylene rather than vacuum sublimed at 250° as was prepared by Sister *et al.*.[22] The crystals formed had a different modification from Sister's crystal and possessed two independent molecules on the crystallographic centres of symmetry, each of which showed positional disorder at the amino hydrogen atoms. The alteration of bond lengths is not present either, indicating that our results for SSNMR studies of this compound are consistent with the new X-ray crystallographic data. Powder diffraction studies confirmed that our sample of TAA had Sakata's structure.

5.5 Summary And Conclusion

High resolution ^{13}C CP/MAS spectra of the DMTAA and TMTAA macrocycles are consistent with ^{15}N data concerning fast proton transfer, *i.e.* there are unequally populated tautomers whose energy difference is probably related to a lattice-induced rhombohedral distortion of the lattice. We also appear to reproduce in the ^{13}C spectra

evidence for participation of all four tautomers for TMTAA but only two tautomers for DMTAA. Our data concerning the simplest macrocycle, TAA, for which there is no corresponding ^{15}N data, suggests equal population of tautomers..

These set of experiments have proved that ^{13}C CPMAS NMR is a valid method for probing the tautomerisation process in tetraazaannulenes . It correlated very well with studies already performed and provided valuable information on untested compounds.

This work is expected to continue and investigate such compounds as PhCOTAA (as DMTAA but with benzoyl instead of methyl groups) which has disordered protons and no rhombic distortion so all four tautomers should be detected and PhTAA[47] (as DMTAA but with phenyl instead of methyl groups) which has localised protons and a pronounced rhombic distortion. A result similar to DMTAA is expected for PhTAA.

References for Chapter 5

1 C. A. Fyfe, *Solid State NMR for Chemists*, C. F. C. Press: Ontario Canada, 1983

2 R. J. Abraham, P. Loftus, *Proton and Carbon-13 NMR Spectroscopy*, Wiley: New York, 1985

3 H. H. Limbach, B. Wehrle, H. Zimmerman, R. D. Kendrick and C. S. Yannoni, *Angew. Chem. Int. Ed. Engl.*, 1987, **26**, 247.

4 H. H. Limbach, B. Wehrle, M. Schlabach, J. Braun, G. Scherer, Ber. Bunsenges and M. Rumpel, *Phys. Chem.*, 1992 **96**, 821.

5 D. Gerritzen anh H. H. Limbach, *J. Am. Chem. Soc.*, 1984, **106**, 869

6 C. B. Storm and Y. Teklu, *J. Am. Chem. Soc.*, 1972, **94**, 1745

7 L. Lunazzi and G. Panciera, *J. Chem. Soc. Perkin Trans. 2*, 1980, 52.

8 S. S. Eaton and G. R. Eaton, *J. Am. Chem. Soc.*, 1977, **99**, 1601

9 J. D. Haliday, E. A. Symons and P. E. Binder, *Can. J. Chem.*, 1978, **56**, 1470

10 D. Gust and J. D. Roberts, *J. Am. Chem. Soc.*, 1977, **99**, 3637

11 W. Seiffert and H. H. Limbach, *J. Am. Chem. Soc.*, 1980, **102**, 538

12 D. Gerritzen and H. H. Limbach, *J. Phys. Chem.*, 1980, **84**, 799

13 D. Y. Curtin and I. C. Paul, *Chem. Rev.*, 1981, **81**, 525.

14 H. de Vries and D. A. Wiersma, *J. Chem. Phys.*, 1980, **72**, 1851

15 H. H. Limbach, P. C. Myrrhe, J. D. Kruger, B. L. Hammond, S. M. Lok, V. Macho and C. S. Yannoni, *J. Am. Chem. Soc.*, 1984, **106**, 6079.

16 M. H. Frey and S. J. Opella, *J. Chem. Soc. Chem. Commun.*, 1980, 479.

17 H. Hiller, P. Dimroth and H. Pifitzner, *Justus Liebigs Ann. Chemie.*, 1968, **717**, 137.

18 J. C. Sauer, *Organic Syntheis*, 1956, **36**, 67.

19 E. Lorch and E. Breitmaier, *Chem. Ztg.*, 1975, **99**, 87 13

20 V. L. Goedken and M. C. Weiss, *Inorg. Synth.*, **20**, 115 (1980).

21 S. Opella and M. H. Frey, *J. Am. Chem. Soc.*, 1979, **101**, 5854.

22 E. Sister, V. Gottfried, M. Kapon, M. Kafory, Z. Dori, and H. B. Grey, *Inorg. Chem.*, 1988, **27**, 600.

23 P. J. Lukes, J. A. Crayston, D. J. Ando, M. E. Harman and M. B. Hursthouse, *J. Chem. Soc. Perkin 2*, 1991, 1845.

24 V. L. Goedken, J. J. Pluth, S.-M. Peng, and B. Burnsten, *J. Am. Chem. Soc.*, 1976, **98**, 8014

25 L. Frydman, A. C. Olivieri, L. E. Diaz, F. G. Morin, C. L. Mayne, D. M. Grant, A. D. Alder and B. Frydman, *J. Am. Chem. Soc.*, 1988, **110**, 336.

26 H. H. Limbach and J. Hennig, *J. Chem. Soc. Faraday Trans.2*, 1979, **75**, 752.

27 S. S. Eaton and G. R. Eaton, *J. Am. Chem. Soc.*, 1977, **99**, 1601.

28 S. J. Silvers and A. Tulinsky, *J. Am. Chem. Soc.*, 1967, **89**, 3331.

29 B. M. Chen and A. Tulinsky, *J. Am. Chem. Soc.*, 1972, **94**, 4144.

30 L. Frydman, A. C. Olivieri, L. E. Diaz, B. Frydman, I. Kustanovich and S. Vega, *J. Am. Chem. Soc.*, 1989, **111**, 7001.

31 L. Frydman, P. C. Rossomando, L. Sambrotta and B. Frydman, *J. Phys. Chem.*, 1992, **96**, 4753.

32 H. H. Limbach, B. Wehrle, H. Zimmerman, R. D. Kendrick and C. S. Yannoni, *J. Am. Chem. Soc.*, 1987, **109**, 929.

33 P. J. Lukes, J. A. Crayston, D. J. Ando, M. E. Harman and M. B. Hursthouse, *J. Chem. Soc. Perkin 2,* 1991, 1845.

34 F. H. Allen, O. Kennard, L. Brammer, R. Taylor, D. G. Watson, L. Brammer, and R. Taylor, *J. Chem. Soc. Perkin Trans. 2*, 1987, S1

35 H. H. Limbach, B. Wehrle, H. Zimmerman, R. D. Kendrick and C. S. Yannoni, *J. Am. Chem. Soc.*, 1987, **109**, 929.

36 H. H. Limbach, B. Wehrle, M. Kocher, O. Ermer and E. Vogel, *Angew. Chem. Int. Ed. Engl.*, 1987, **26**, 934.

37 W. P. Rothwell, D. Suwelack and J. S. Waugh, *J. Chem. Phys.*, 1980, **73**, 2559.

38 W. P. Rothwell and J. S. Waugh, *J. Chem. Phys.*,1981, **74**, 2721.

39 D. L. VanderHart and A. N. Garroway, *J. Chem. Phys.*, 1979, **71,** 2773.

40 E. Sister, V. Gottfried, M. Kapon, M. Kafory, Z. Dori, and H. B. Gray, *Inorg. Chem.*, 1988, **27**, 600.

41 V. L. Goedken, J. J. Pluth, S.-M. Peng, and B. Burnsten, *J. Am. Chem. Soc.*, 1976, **96**, 8014.

42 S. J. Silvers and A. Tulinsky, *J. Am. Chem. Soc.*, 1967, **89**, 3331.

43 M. J. Hamor, T. A. Hamor and J. L. Hoard, *J. Am. Chem. Soc.*, 1964, **86**, 1938.

44 L. E. Webb and E. B. Fleischer, *J. Chem. Phys.*, 1965, **43**, 3100.

45 B. M. L. Chen and A. Tulinsky, *J. Am. Chem. Soc.*, 1972, **94**, 4144.

46 N. Azuma, H. Tani, T. Ozawa, H. Niida, K. Tajima and K. Sakata, *J. Chem. Soc. Perkin Trans 2*, 1995, 343,

47 J. Jubb, L. F. Larkworthy, D. C. Povey and G. W. Smith, *Polyhedron*, 1993 **12** 1179